NISTIR 6893

Bridging the Gap between Structure and Properties in Nano-Particle Filled Polymers

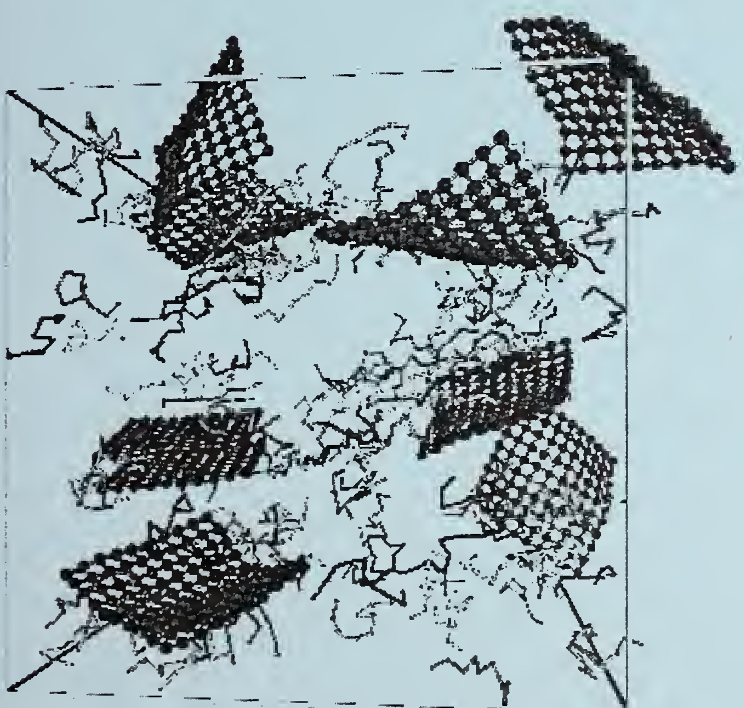

Erik Hobbie
Jack Douglas
Francis Starr
Charles Han

U.S. DEPARTMENT OF COMMERCE
Technology Administration
National Institute of Standards
and Technology
Gaithersburg, MD 20899-8910

NIST
National Institute of Standards and Technology
Technology Administration
U.S. Department of Commerce

NISTIR 6893

Bridging the Gap between Structure and Properties in Nano-Particle Filled Polymers

Erik Hobbie
Jack Douglas
Francis Starr
Charles Han

U.S. DEPARTMENT OF COMMERCE
Technology Administration
National Institute of Standards
and Technology
Gaithersburg, MD 20899-8910

July 2002

U.S. DEPARTMENT OF COMMERCE
Donald L. Evans, Secretary

TECHNOLOGY ADMINISTRATION
Phillip J. Bond, Under Secretary for Technology

NATIONAL INSTITUTE OF STANDARDS
AND TECHNOLOGY
Arden L. Bement, Jr., Director

Bridging the Gap Between Structure and Properties in Nanoparticle-Filled Polymers

May 29-30, 2002

National Institute of Standards and Technology
Gaithersburg, MD

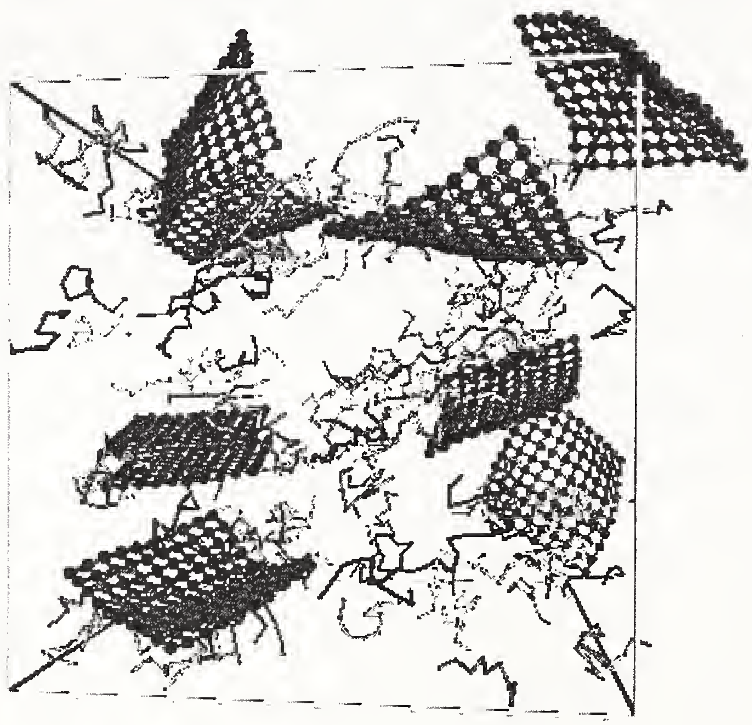

Organizers: Erik Hobbie
Jack Douglas
Francis Starr
Charles Han

I. Nanotechnology Workshop

On May 29-30 of 2002, a workshop on polymer nanocomposites was held at NIST in Gaithersburg, Maryland. The workshop was entitled **Bridging the Gap Between Structure and Properties in Nanoparticle-Filled Polymers** and focused primarily on the interrelation between particle dispersion and the properties of polymers filled with clay and nanotube fillers. The purpose of the workshop was to identify research topics for NIST research and to initiate research collaboration with industrial and academic researchers in this important technological area. The workshop participants included a diverse mix of industrial, government and academic researchers.

This document reproduces the slides presented by the speakers of this workshop along with a few introductory remarks about each contribution. We would like to thank the contributors for providing the presentations that made the workshop a success.

1) Douglas Hunter, **"The Effect of Extruder Processing on the Extent of Exfoliation in Clay-Polymer Nanocomposites"**
2) Jeff Gilman, **"Flame Retardant Polymer-Clay Nanocomposites"**
3) Ramanan Krishnamoorti, **"Melt Rheology of Polymer Nanocomposites"**
4) Satish Kumar, **"Processing, Structure, and Properties of Nano-Composite Fibers and Films"**
5) Alex Morgan, **"Polypropylene Nanocomposites: Clay Organic Treatment Concentration Effects on Mechanical Properties, Flammability Properties and Clay Dispersion"**

6) Atsushi Takahara, **"Structure and Mechanical Properties of Natural Inorganic Nanofiller / Polymer Hybrid"**

7) R. A. Vaia, **"Impact and Control of Ultrastructure (Meso) in Polymer Nanocomposites"**

8) Francis W. Starr, **"Probing Nanocomposite Structure and Properties Using Computer Simulations"**

9) Juan J. de Pablo, **"Molecular Simulation and Characterization of Ultrathin Films and Nanoscopic Polymeric Structures: Departures from Bulk Behavior"**

10) Guoqiang Qian, **"Applications of Plastic Nanocomposites"**

11) Eric A. Grulke, **"Production, Dispersion and Applications of Multiwalled Carbon Nanotubes"**

12) Ken McElrath and Tom Tiano, **"Achieving Conductive Polycarbonate with Single Wall Carbon Nanotubes"**

II. U.S. Government and Nanotechnology

Nanotechnology holds the promise to dramatically change many aspects of the world in which we live. The range and scope of the potential economic and societal benefits from nanotechnologies is so staggering it has been called the “Next Industrial Revolution”. Recognizing the large potential for nanotechnologies, the FY2001 Federal Budget included support for a major new initiative on nanotechnology. The National Nanotechnology Initiative (NNI) was established by the U.S. Government to promote long-term nanoscale research and development leading to potential breakthroughs in areas ranging from materials and manufacturing to biotechnology and agriculture to national security and Defense, and many others. The NNI creates a research infrastructure by coordinating activities such as fundamental research, Grand Challenges (which will be described later), and centers and networks of excellence, activities that are all potentially high payoff and broadly enabling. The NNI evolved from publications authored by the Interagency Working Group on Nanoscience, Engineering and Technology (IWGN), and is currently supported and monitored by the IWGN's successor, the Subcommittee on Nanoscale Science, Engineering, and Technology (NSET). In FY 2001, the total investment by the NSET agencies in nanotechnology was estimated to be $422million, of which NIST has invested approximately $13.5 million.

The NNI exemplifies the government's critical role in promoting the development of new science and technology. For clarity's sake, we should first consider what types of things we define as nanotechnology. Ask any scientist, engineer, or layperson for a definition of nanotechnology, and you will most likely receive a very different answer. In many cases, it is

considered hard to define; like good art, most people "know it when they see it" but have difficulty explaining it in general. Thus, we use the definition of nanotechnology given by the NSET:

Nanotechnology is defined as the ability to work at the atomic, molecular or macromolecular levels, in the length scale of approximately 1 - 100 nm range, in order to create, manipulate and use structures, devices and systems that have novel properties and functions because of the small size. The novel and differentiating properties and functions are developed at a critical length scale of matter typically under 100 nm. Nanotechnology includes integration of nanoscale structures into larger material components, systems and architectures that are used in most industries, health care systems, environment and national security. Within these larger scale devices, the control and construction of the devices remains at the nanoscale. In some particular cases, the critical length scale for novel properties and phenomena may be under 1nm (e.g., manipulation of atoms at ~0.1nm) or be larger than 100nm (e.g., nanoparticle reinforced polymers have the unique feature at ~200/300nm as a function of the local bridges or bonds between the nanoparticles and the polymer).

It is critical that the Federal government is involved at this stage in the development of nanotechnology, since "the necessary fundamental nanotechnology research and development is too broad, complex, expensive, long-term, and risky for industry to undertake." Industry is unable to fund or is under-funding critical areas of long-term fundamental research and development and is not developing the necessary nanoscience technologies needed to realize nanotechnology's potential.

In supporting the NNI, the participating agencies fund the NNI recommended R&D priorities as a function of their mission, contingent on

available resources. The stated goals of the NSET involve developing a…

...coherent approach for funding the critical areas of nanoscience and engineering, establishing a balanced and flexible infrastructure, educating and training the necessary workforce, and promoting partnerships to ensure that these collective research activities provide a sound and balanced national research portfolio. By facilitating coordination and collaboration among agencies, the NNI will maximize the productivity and utility of the Federal government's investment in nanotechnology and avoid unnecessary duplication of efforts.

III. Nanotechnology and NIST Polymers Division

Exfoliated clay and carbon nanotube materials can be considered to be two-dimensional polymeric materials, and the Polymers Division at NIST is in a good position to provide essential characterization information and to study the essential physics of this important class of materials, building on former work on conventional polymeric materials.

Similarly to high molecular weight blends, it is difficult to form stable dispersions of clay and nanotubes in polymer matrices. Dispersion is usually a matter of degree and this has a tremendous impact on the properties of polymeric materials filled with these additives. These materials raise many measurement challenges since the dimensions of these particles bridge molecular and colloidal particle scales so that characterization requires an array of techniques. Characterization is also made difficult by the complexity of the materials that depend on their source and processing history. It is clearly important to identify model systems allowing reproducible and meaningful measurement and measurement methods addressing more general questions (dispersion, interparticle interaction) and processes (phase separation, particle clustering). Simulation must play an important role in understanding these systems and the multi-scale physics involved. The workshop was intended to help focus these efforts.

IV. Workshop Presentations

1) Douglas Hunter, **"The Effect of Extruder Processing on the Extent of Exfoliation in Clay-Polymer Nanocomposites"** [PowerPoint] [PDF]

Dr. Hunter emphasized the importance of process conditions on the properties of exfoliated clay materials. Several screw extruders were investigated and the influence of residence time and position of the clay-polymer extrudate was considered in relation to the extent of clay exfoliation. The processing history and screw geometry was shown to have a pronounced effect on the state of dispersion and a hierchical dispersion model was introduced to rationalize these results. The importance of combining chemical treatment with processing to achieve good dispersion was emphasized. High shear intensity was found to be not necessarily beneficial for dispersion, but long residence times in the extruder normally has a positive effect on the relative dispersion. One of the general philosophical questions raised by this talk is the need for a better understanding of the role of shear on mixing processes and clustering in colloidal systems.

Extruder Processing of Nanocomposites - Agenda

- Overview of Presentation given at ANTEC
- University of Akron, Screw Pulling Results
- MXD6: Effect of Die
- Die study with PP

Note: Results Based on XRD, TEM. Properties Important to Market Applications not Determined

Processing Nanocomposites
Critical objectives of the presentation

- Process parameters as important as the choice of clay.
- Online monitoring of exfoliation can be deceptive – consideration needs to be given to the "die" effect.

The Processing Challenge

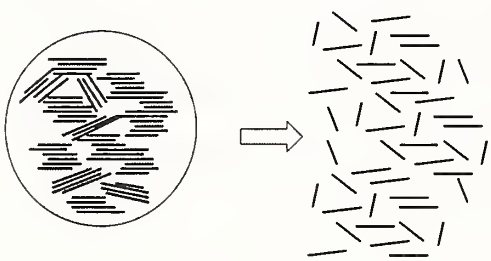

8μm Particle   >1 Million Platelets

Nanocomposite Processing
Antec

- Objective: establish the significance of processing.
- Multiple extruders and screw configurations.
- PA6 with Cloisite 15A, not exfoliate and Cloisite 30B, exfoliate.

Single and Co Rotating Screws

Killion Single Screw

Japan Steel Works Co Rotating Twin Screw

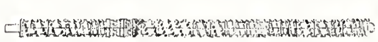

Low Shear

Medium Shear

Leistritz Counter Rotating Intermeshing

Low Shear

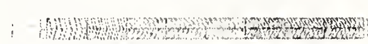

Medium Shear

High Shear

Leistritz Counter Rotating Non-Intermeshing

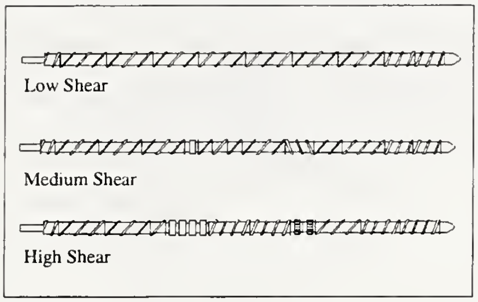

XRD Examples: 15A/PA6

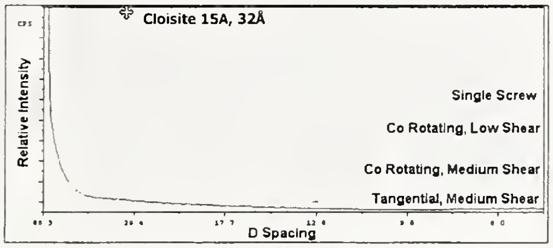

TEM Examples: 15A/PA6

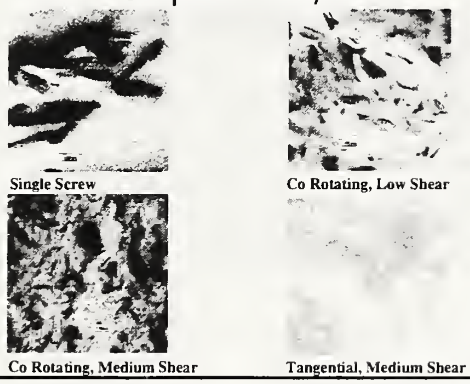

TEM Dispersion

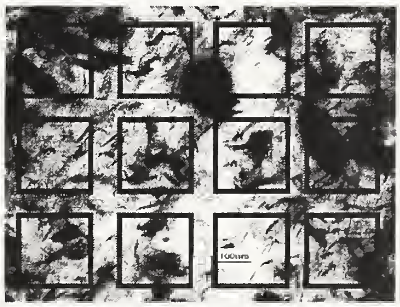

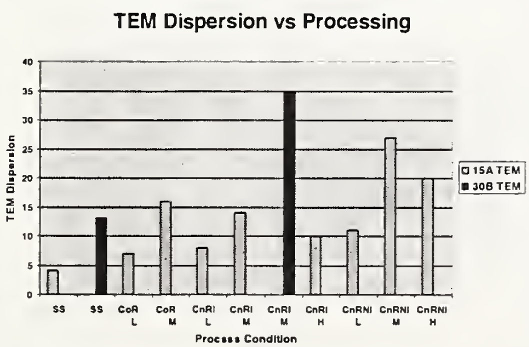

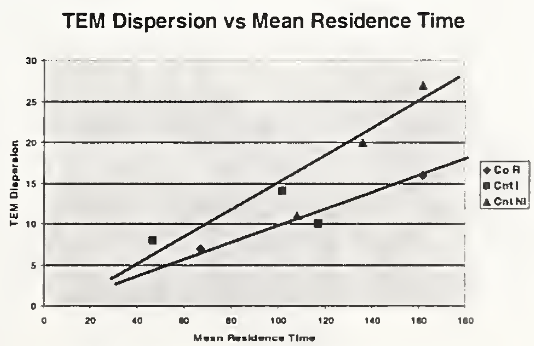

2

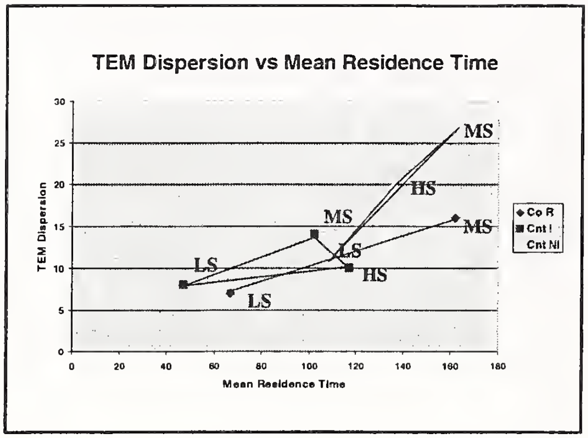
TEM Dispersion vs Mean Residence Time
TEM Dispersion
Mean Residence Time
LS
MS
HS
Co R
Cnt I
Cnt NI

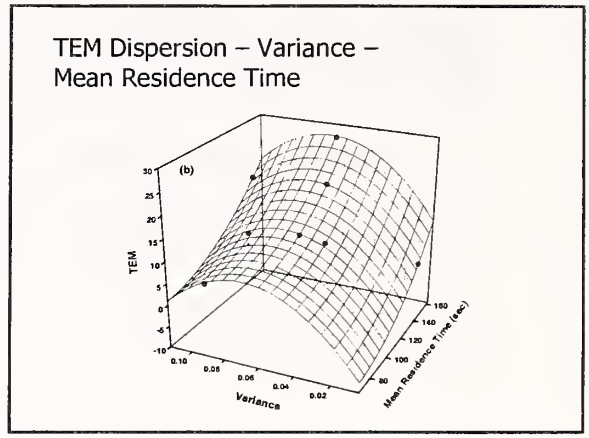
TEM Dispersion – Variance –
Mean Residence Time
(b)
TEM
Variance
Mean Residence Time (sec)

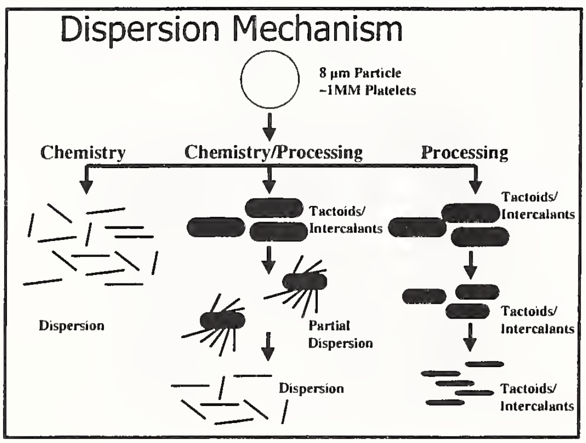
Dispersion Mechanism
8 μm Particle
~1MM Platelets
Chemistry
Chemistry/Processing
Processing
Tactoids/
Intercalants
Dispersion
Partial
Dispersion

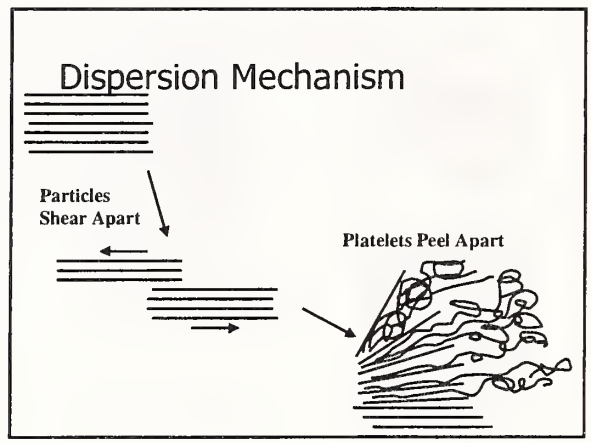
Dispersion Mechanism
Particles
Shear Apart
Platelets Peel Apart

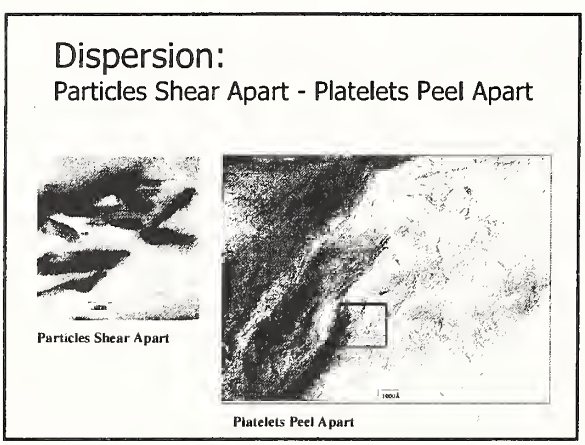
Dispersion:
Particles Shear Apart - Platelets Peel Apart
Particles Shear Apart
Platelets Peel Apart

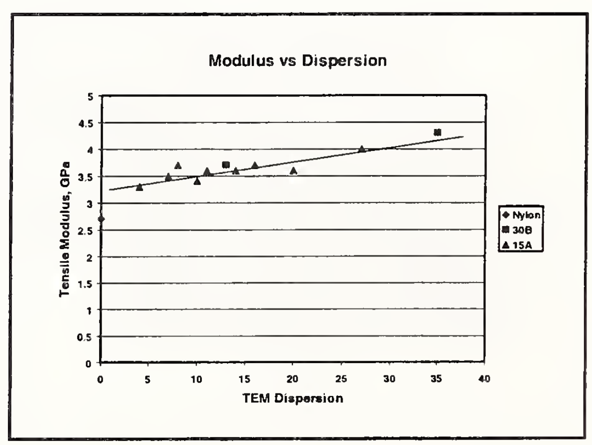
Modulus vs Dispersion
Tensile Modulus, GPa
TEM Dispersion
Nylon
30B
15A

3

Conclusions

- To Optimize Dispersion: Clay Treatment & Processing
- Longer Residence Time Important, Not only Variable
- Dispersion not Simply a Function of Shear Intensity
- Particles Shear Apart
- Platelets Peel Apart to Disperse

Exfoliation not limited to extruder processing

- Buss Kneader
- Brabender
- Banbury
- 2 Roll mill

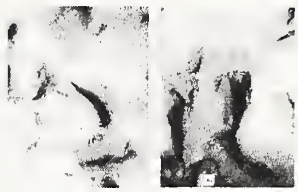

2 Roll Mill Extruder

Screw Pulling University of Akron

- Nanocomposites PA6/15A & PP/MAPP/15A
- Vary Screw Design
- Vary Process Conditions

Different Resin, JSW 5kg/hr/200rpm Alloy

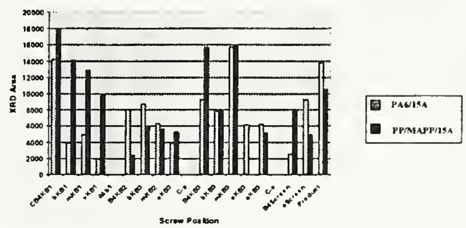

TEM Micrographs Pull Screw
PA6-Cloisite 15A -JSW Alloy

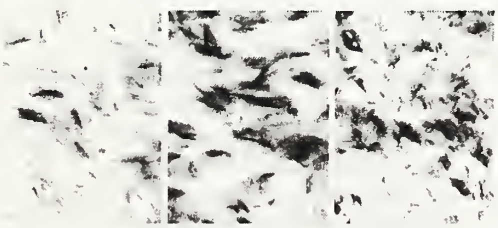

Beginning KB1 Middle KB1 End KB1

TEM Micrographs Pull Screw
PA6-Cloisite 15A -JSW Alloy

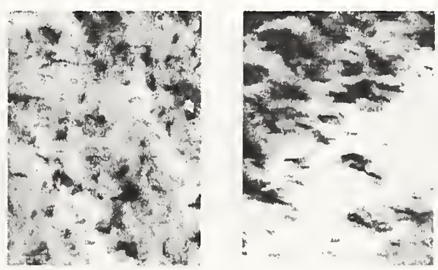

Before Die Product

Conclusions

- **Screw Design Important**
- **Process Conditions Important**
- **Possible to have the Optimum Design with Only Part of Screw**
- **What is the die effect?**

Effect of Die: MXD6 Study

•Two Organoclays, Cloisites 30B and 93A

•Clay Fed Downstream

•Multi-Kneading Block Screw

•Past Experience, Screw Should Work

MXD6 Nanocomposite XRD

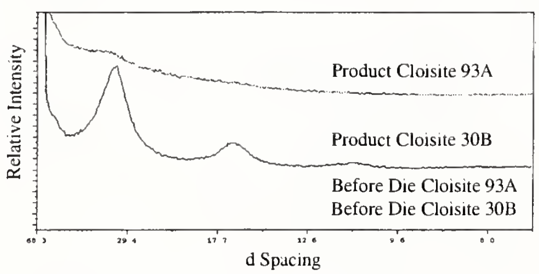

TEM MXD6 Nanocomposite

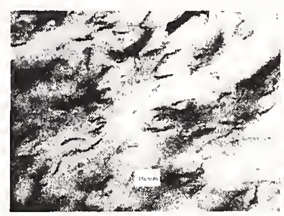

Cloisite 30B Before Die

Cloisite 30B Product

TEM MXD6 Nanocomposite

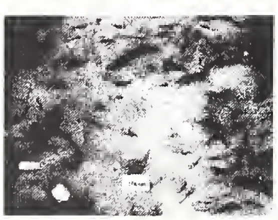

Cloisite 93A Before Die

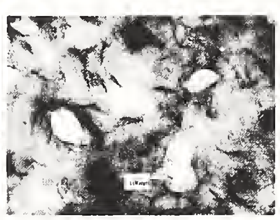

Cloisite 93A Product

Conclusions

- **Nanocomposite Sheared In Die**
- **Propose Results Controlled by Resin/Clay Treatment Compatibility**
- **Less Compatible Nanocomposite, Platelets Align - See in XRD and TEM**
- ***Die Hole Size Problem?***
- **Possible Solution: Larger Die Hole**

Vary the Die Hole Diameter
PP/MA-g-PP/Cloisite 20A

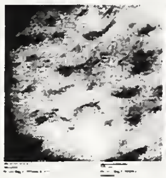
6 hole 1mm

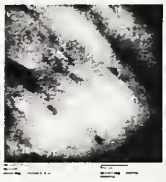
4 hole 2.1 mm


no die plate

Extruder Monitoring Exfoliation

- Assume slip stream to analysis tool
- Consider effect of shear in lines and analytical tool
- Platelet alignment during analysis alter results of the analysis

2) Jeff Gilman, **"Flame Retardant Polymer-Clay Nanocomposites"**
[PowerPoint] [PDF]

Dr. Gilman first stressed the human cost of home fires and the alternatives that exist for making flame retardent polymers. The challenge was indicated to be the development of environmentally friendly and economical approaches to reduce flammibility and the simultaneous improvement of the mechanical properties of the polymer-based materials. Clay nanocomposites were shown to be promising as fire suppressant agents due to the clay reinforcement of the char formed in the course of burning. Degradation issues of these materials under processing conditions were discussed and the advantages of combinatoric flammability tests were discussed in connection with optimizing and understanding the complex parameter space governing these complex materials.

Flame Retardant Polymer-Clay Nanocomposites

Jeffrey W. Gilman
Group Leader
Materials and Products Group
Fire Science Division

NIST Workshop on Polymer Nanocomposites and Multiphase Materials

NIST

Home Fires

- 4,000 Deaths/Year in US Home Fires - highest of Developed Countries
- 37 % from Upholstered Furniture Mattress and Bedding

Fire Statistics: National Fire Protection Assoc 1996

Also: carpet, wire and cable, aircraft, insulation, automotive, consumer electronics....

3 minutes to flashover !

NIST Bunk bed Study: www.fire.nist.gov

General Flame Retardant Approaches for Polymers

I- Gas Phase Flame Retardants
- Reduce Heat of Combustion (ΔH_c) resulting in incomplete combustion.
- Inherent Drawbacks: Negative Public Perception!

II- Endothermic Flame Retardants
- Function in Gas Phase and Condensed Phase
- Via endothermic release of H_2O, polymer cooled and gas phase diluted.
- Inherent Drawback: High loadings (30-50%) degrade mechanical properties.

III- Char Forming Flame Retardants
- Operate in Condensed Phase
- Provides thermal insulation for underlying polymer and a mass transport barrier, preventing or delaying escape of fuel into the gas phase.

Goal: develop environmentally friendly approaches to reduce flammability and improve physical properties

Polymer Flammability vs Cost

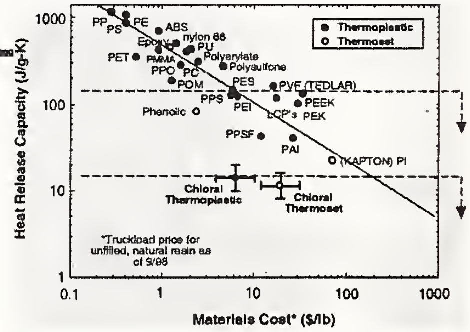

R. Lyon

PP-clay Nanocomposite: Cone Calorimetry

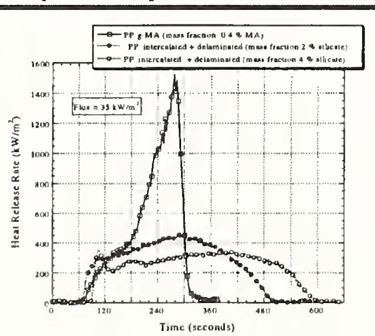

Gasification of Polystyrene Layered-silicate Nanocomposites

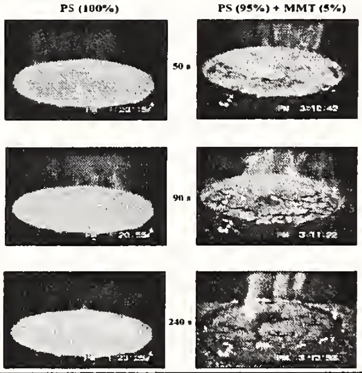

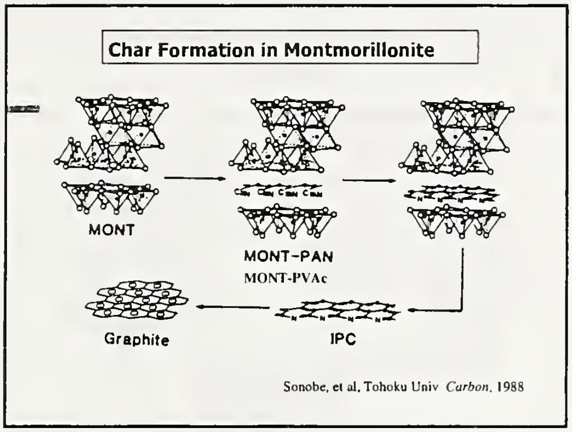
Char Formation in Montmorillonite
MONT
MONT-PAN
MONT-PVAc
Graphite
IPC
Sonobe, et al, Tohoku Univ Carbon, 1988

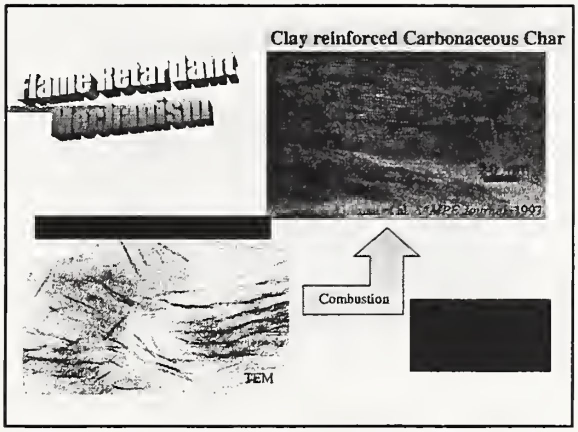
Clay reinforced Carbonaceous Char
[redacted]
Combustion
[redacted]
TEM

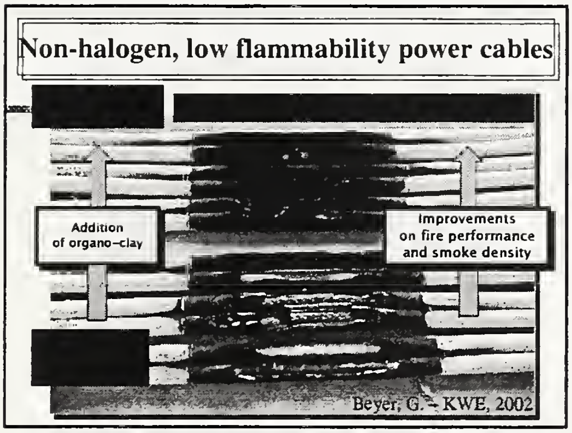
Non-halogen, low flammability power cables
[redacted]
Addition of organo-clay
Improvements on fire performance and smoke density
[redacted]
Beyer, G. - KWE, 2002

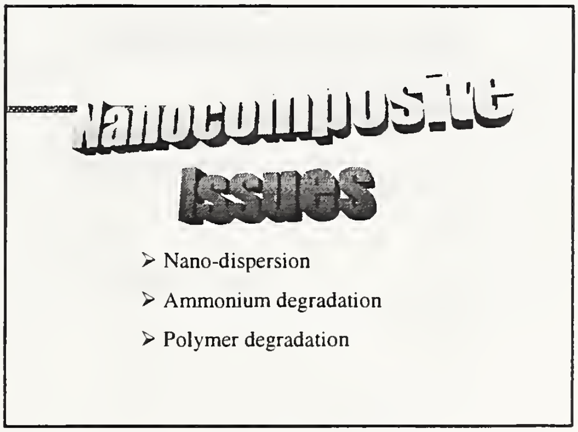
Nanocomposite Issues
➢ Nano-dispersion
➢ Ammonium degradation
➢ Polymer degradation

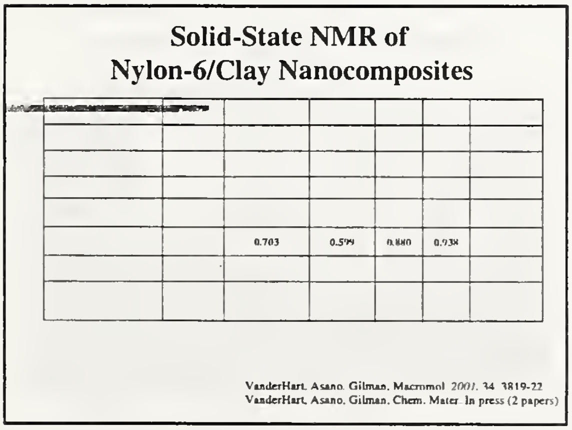
Solid-State NMR of
Nylon-6/Clay Nanocomposites
0.703
0.599
0.880
0.938
VanderHart, Asano, Gilman, Macromol 2001, 34, 3819-22
VanderHart, Asano, Gilman, Chem. Mater. In press (2 papers)

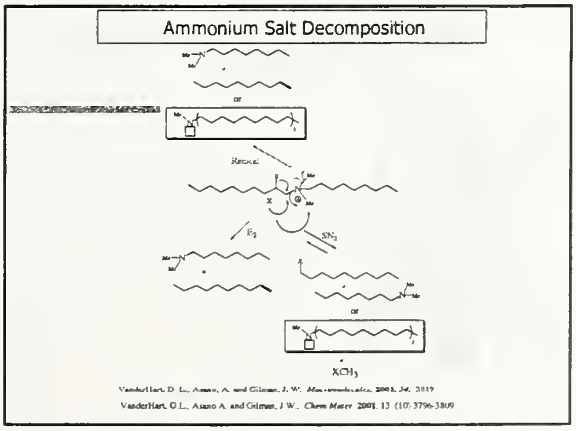
Ammonium Salt Decomposition
or
XCH₃
VanderHart, D.L., Asano, A. and Gilman, J.W., Chem Mater 2001, 13 (10) 3796-3809

pH Sensitive End-group Chemical Shifts

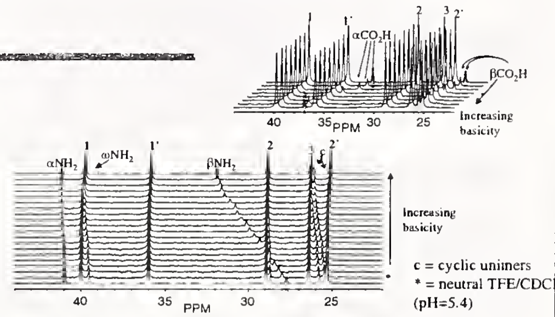

c = cyclic unimers
* = neutral TFE/CDCl
(pH=5.4)

- Davis, R.D.; Steadman, S.J.; Jarrett, W.L.; Mathias, L.J.;, *Macromolecules* 2000, 33, 7088.
- Davis, R.D.; Jarrett, W.L.; Mathias, L.J.;, *Polymer* 2001, 42, 2621.

Nylon 6 and Nylon 6/MMT

Injection molding at 300 °C causes polymer degradation

Polymer	M_n (g/mole)	% ε-Coprolactam*	End-groups*		
			% Amine	% Acid	% Δ
PA-6 as received	13622 ± 1449	0.00	0.83	0.83	0.00
PA-6 injection molded	12311 ± 1489	0.92	0.92	0.92	0.00
Nanocomposite as received	13672 ± 1504	0.19	0.83	0.83	0.00
Nanocomposite injection molded	6321 ± 334	3.80	0.83	1.79	53.4

*uncertainty (2σ) ± 0.1%

What is the affect on properties?

Davis, R., Gilman, J., *Polym. Deg & Stab*, submitted.

Smectite acts as a Bronsted base

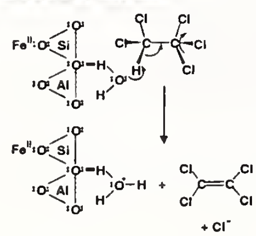

pentachloroethane

tetrachloroethene

Stucki, J., et al. 2000, Clays Clay Miner. 48:132-138

Organic Modification of Clay

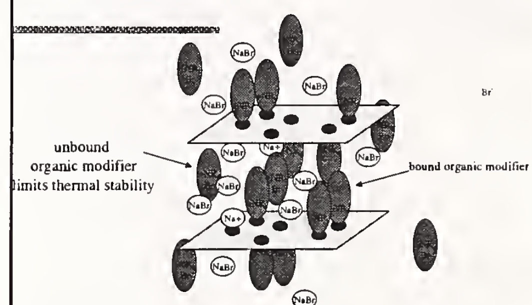

Improved Organoclay Thermal Stability

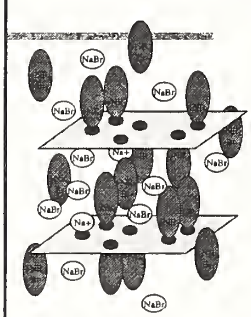

- Thermal gravimetric analysis
- Electrochemical Ion analysis
- Mass spectroscopy
- TGA-FTIR
- X-ray diffraction

Improved Organoclay Thermal Stability

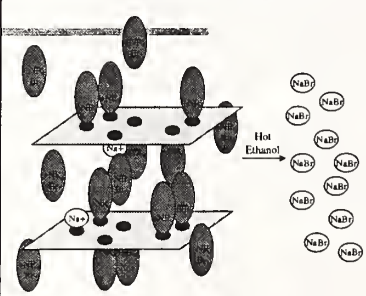

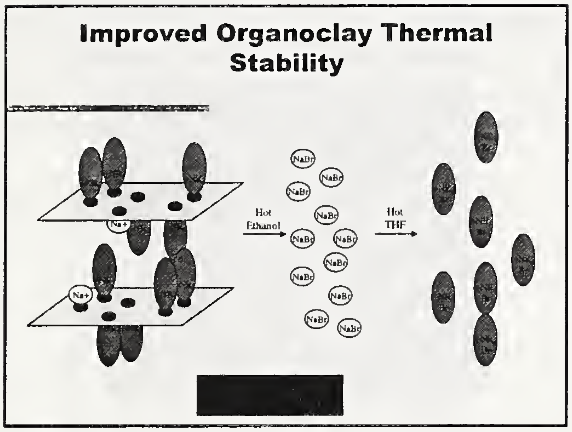
Improved Organoclay Thermal Stability
Na+
Hot Ethanol
NaBr
Hot THF
[redacted]

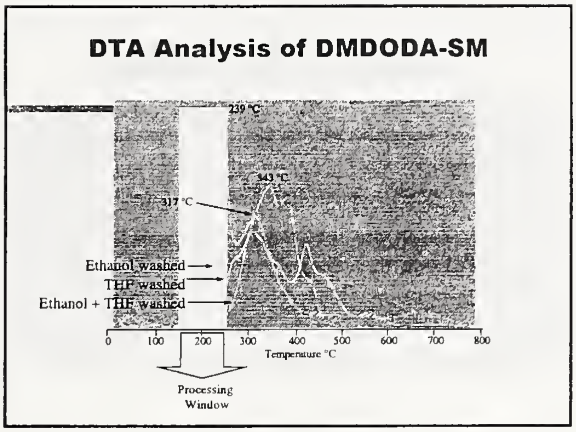
DTA Analysis of DMDODA-SM
239 °C
343 °C
317 °C
Ethanol washed
THF washed
Ethanol + THF washed
0 100 200 300 400 500 600 700 800
Temperature °C
Processing Window

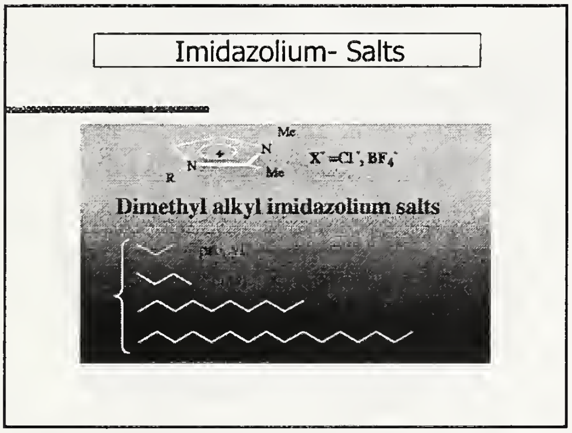
Imidazolium- Salts
Me
N
R
N
Me
X⁻ =Cl⁻, BF₄⁻
Dimethyl alkyl imidazolium salts

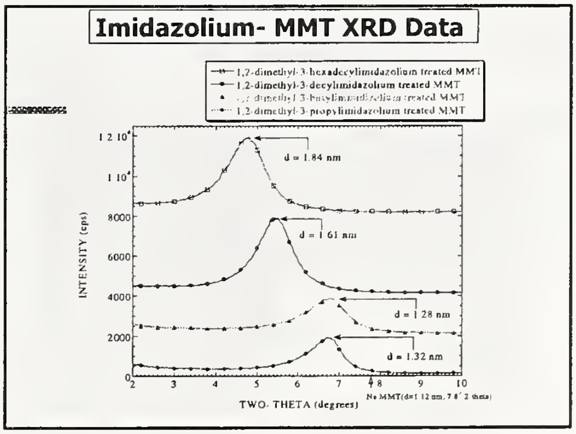
Imidazolium- MMT XRD Data
1,2-dimethyl-3-hexadecylimidazolium treated MMT
1,2-dimethyl-3-decylimidazolium treated MMT
1,2-dimethyl-3-butylimidazolium treated MMT
1,2-dimethyl-3-propylimidazolium treated MMT
d = 1.84 nm
d = 1.61 nm
d = 1.28 nm
d = 1.32 nm
INTENSITY (cps)
TWO- THETA (degrees)

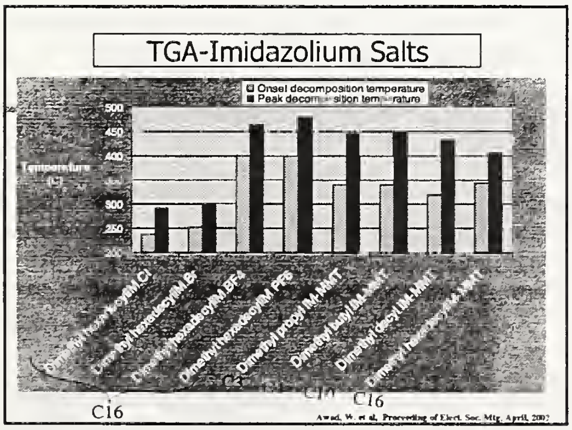
TGA-Imidazolium Salts
Onset decomposition temperature
Peak decomposition temperature
Temperature (C)
C16
C3
C16
Awad, W. et al, Proceeding of Elect. Soc. Mtg. April 2002

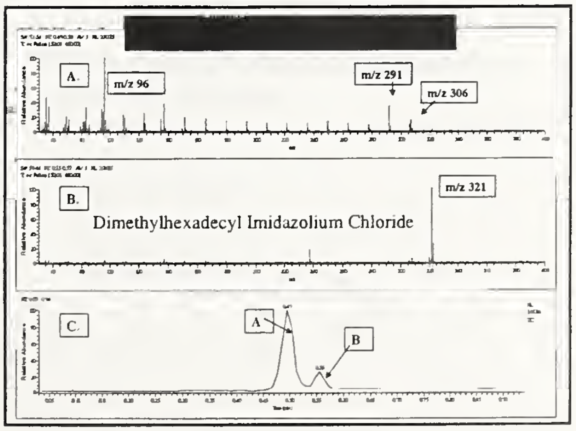
[redacted]
A.
m/z 96
m/z 291
m/z 306
B.
m/z 321
Dimethylhexadecyl Imidazolium Chloride
C.
A
B

[redacted]

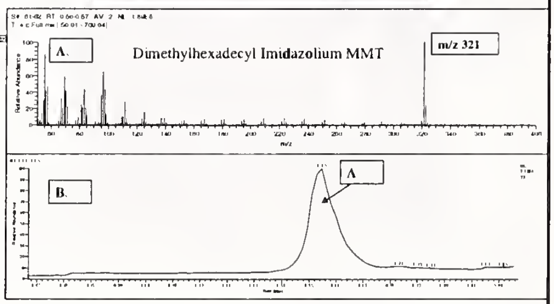

Imidazolium- MMT vs Ammonium-MMT TGA Data

Sample	Onset - T_{dec} °C	Peak - T_{dec} (dTGA) °C
1,2-dimethyl-3-N-hexadecyl imidazolium/MMT	300	375
1-decyl- 2,3-dimethylimidazolium/MMT	300	443
1-butyl- 2,3-dimethylimidazolium/MMT	305	445
dimethyl-di(hydrogenated tallow) ammonium/MMT	200	310

Uncertainty for the onset T_{dec} and peak T_{dec} measurements are ± 0 6 °C

Imidazolium- MMT/ Nanocomposites

DMHDIM-MMT in PA-6

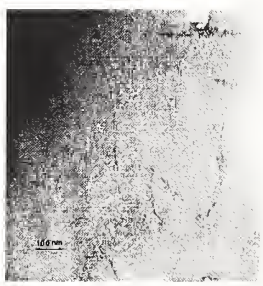

DMHDIM-MMT in PS

Gilman, et al, *Chem. Mater.* In press

PET Homo- and Copolymers

- PET
- PET-5%-co-octanediol (PET-OD)
- Flame Retardant PET (FR-PET)
  - commercial

R= H, C_6H_{13}

*All PET and copolymers provided by KoSa

Davis, C. MS Thesis, U. So. Miss

Effect of Varying Imidazolium Organic Modifier

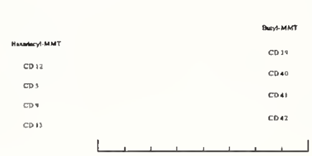

Hexadecyl-MMT/PET nanocomposites

Butyl-MMT/PET nanocomposites

Davis, C. MS Thesis, U. So. Miss

Effect of Varying PET Copolymers

CD 12: hexadecyl-MMT/PET nanocomposite
Screw speed 200 rpm
Residence time. 2 minutes

CD 10: hexadecyl-MMT/PET-OD nanocomposite
Screw speed. 200 rpm
Residence time: 2 minutes

CD 15. hexadecyl-MMT/FR-PET nanocomposite
Screw speed. 200 rpm
Residence time. 2 minutes

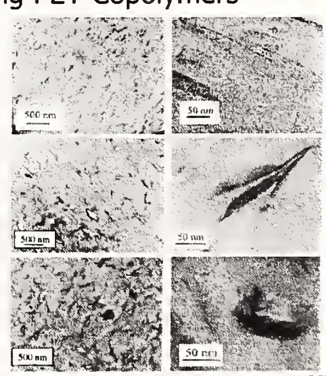

Davis, C MS Thesis, U. So. Miss

GPC Data

Sample*	M_n	M_w	Polydispersity (M_w/M_n)
PET/OD (as received)	21,350	38,650	1.81
PET/OD (processed)	17,750	30,850	1.74
CD 6 (PET-OD nanocomposite)	17,000	30,000	1.76
PET (as received)	32,200	61,850	1.92
PET (processed)	21,100	39,150	1.86
CD 5 (PET nanocomposite)	20,600	38,350	1.86
FR PET (as received)	23,420	45,600	1.94
FR PET (processed)	16,950	31,100	1.83
CD 16 (FR PET nanocomposite)	15,050	27,750	1.84

[illegible]

* Extrusion conditions caused degradation of FR-PET

Parameter Space for Polymer Nanocomposites

Polymer	Nano-additive	Counter-Ion	Organic Treatment	Processing Conditions	Other additives	Flame Retardant
PE PP PS PA6 PU PVC PC PEO PMMA EVA	MMT Mica Hectorite Saponite Laponite Silica POSS	Na Ca Cu Fe...	Alkylammonium Imidazolium Crown Ether Silated Carboxylate	Temperature Shear Residence time	Stabilizers Processing UV Antioxidant Fillers Pigments	Phosphate Halogenated Silicon Based
~ 10	~ 5	~ 5	~ 10	~ 10	~ 10	~ 10

(~ 10^6 Experiments)

High-Throughput Methods: The Approach

- Design → Define Parameter Space
  polymer + FR + additives...
- Fabricate → Prepare Sample Library
  parallel synthesis, extrusion
- Measure → Sample Characterization and Performance On-line probes, microhotplates, IR imaging, HRR
- Analyze → What does it mean?
  Data visualization, mining and models
- Informatics → Focus Library
  correlations

Primary Screening 1000's of samples............Secondary optimization of 100's of samples

Extrusion of Gradient Samples

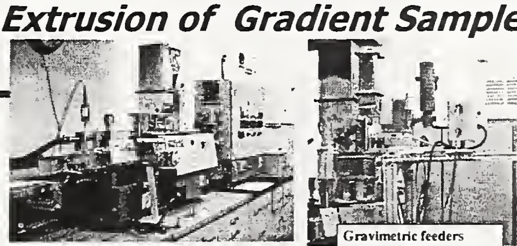

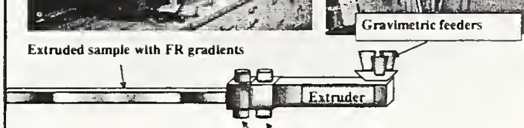

– and Off line High Throughput:
TGA, X-Ray scattering, nanoindentation

– In-line sensors:
UV-Vis, FTIR, optical, dielectric

Sample Characterization

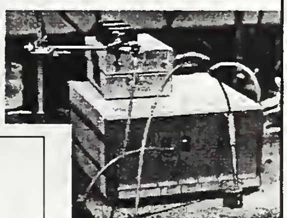

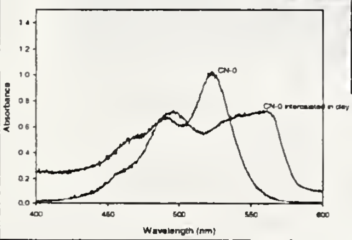

Fluoreneyl-benzimidazolium Layered Silicate.

- The fluoreneyl-benzimidazolium LS (FBIM-LS) will be evaluated as an intercalated sensor for monitoring exfoliation.

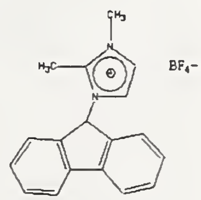

Horizontal Ignition and Flammability Test

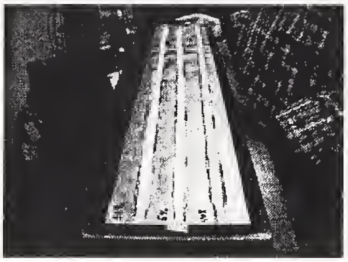

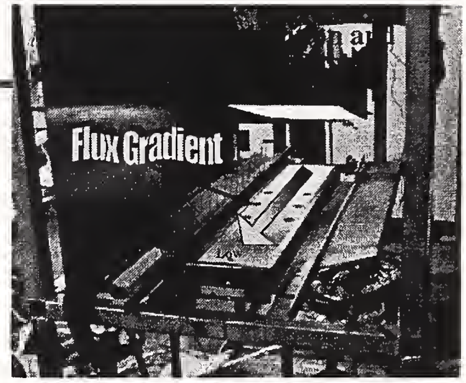

Flux Gradient in HIFT

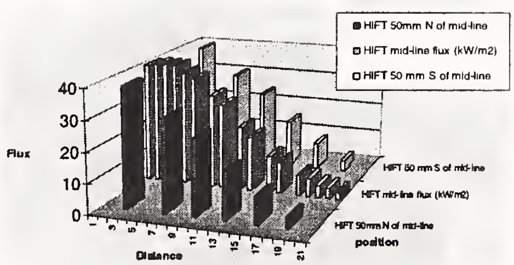

Gradient Flux Test

HIFT

HIFT

Different Critical Fluxes for Flame-Spread

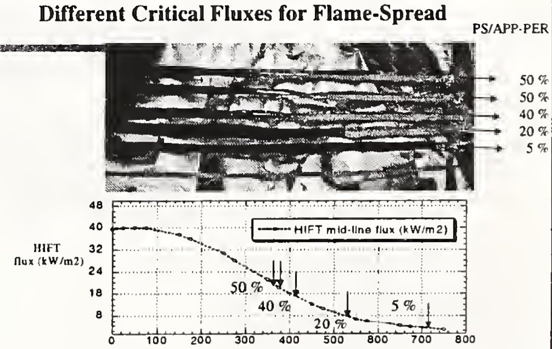

Radiant Panel Test

Flame Spread

~ $HRR^{2/3}/T_{ign}$

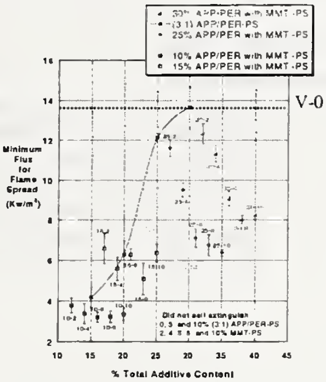

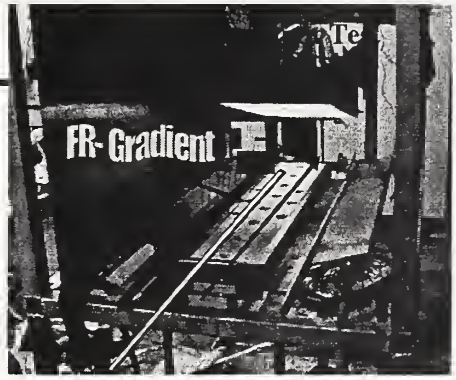

High Throughput Test

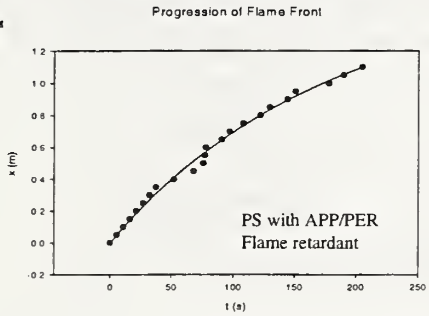

High Throughput Test

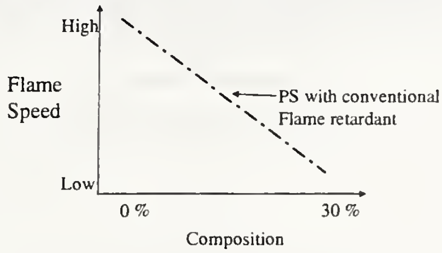

High Throughput Test

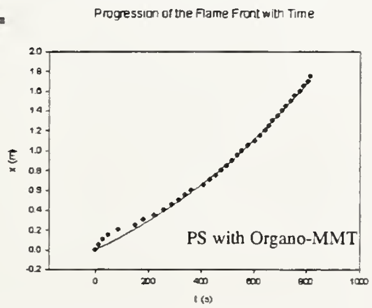

Conventional vs High Throughput Flammability Measurements

Method	Repeatability (+/-)	Data-sets/day	Data Quality
UL-94 V	Poor (10%)	2-5	Qualitative
Cone	Excellent (5%)	2-5	Multi-parameter Highly Quantitative
HFT using gradient sample	Excellent (5%)	50-100	Quantitative

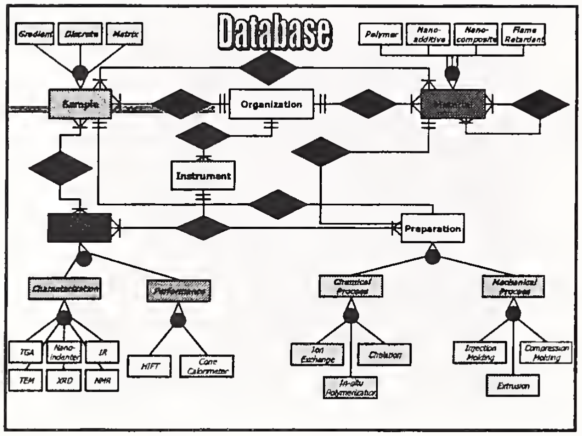

Conclusions

By combining nanotechnology with high-throughput experimentation, we can maximize the effect of additives and thereby provide industry with a powerful tool for the development of a new generation of high performance, low flammability materials.

High Throughput Methods
for
Flammability Research

Focused Project Consortium

For information:
wwww.bfrl.nist.gov/focused_project

RESEARCH TEAM

Marc Nyden, Rick Davis, John Shields, Walid Awad,
Takashi Kashiwagi, Richard Harris, Lori Brassell, Kathy Butler, Michael Smith, Roy McLane
BFRL/NIST

David VanderHart, Tony Bur, Atsuchi Asano
MSEL/NIST

Doug L. Hunter
Southern Clay Products Inc.

Thomas Sutto[1], Paul C. Trulove[2], and Hugh DeLong[3]

[1]Naval Research Laboratory, Washington, DC
[2] Air Force Office of Scientific Research, Arlington, VA
[3] Naval Academy, Annapolis, MD

Advanced Technology Program -Monitored by John Hewes and Felix Wu
FAA, Richard Lyon at William J. Hughes Technical Center (Interagency Agreement DTFA03-99-X-90009)
Air Force Office of Scientific Research (ISSA - AFOSR- ISSA-01-0001)

Materials and Products Group

Michael Smith, Richard Harris, Takashi Kashiwagi, Tom Ohlemiller, Marc Nyden
Rick Davis, Kathy Butler, Greg Linteris, Lori Brassell, John Shields, Ruth Perkins,
Wes Demory, David Wentz, Walid Awad

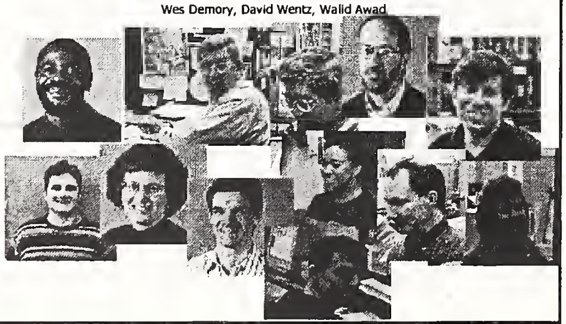

3) Ramanan Krishnamoorti, **“Melt Rheology of Polymer Nanocomposites”** [PowerPoint] [PDF]

(Talk presented by Charles Han due to family illness.)

This talk emphasized the effect of nanoparticles on the rheological properties of polymer melts. Melt measurements were contrasted for exfoliated (e.g., nylon-6) and intercalated clay-filled polymers. First, small amplitude linear dynamic measurements were considered for a clay-filled block copolymer system and gelation was observed with increasing filler concentration. This was attributed to the formation of a filler network structure, although scattering evidence is not yet available to support this hypothesis. Notably time-temperature superposition applied to the viscoelastic properties of these complex materials. Qualitatively similar behavior was found for intercalated and exfoliated clay-filled materials. Carbon nanotube (single wall) filled materials (polystyrene) were also considered and gelation (reinforcement) was similarly observed with increasing filler concentration-provided the nanotubes were functionalized to improve dispersion. At high concentration of clay, beyond the concentration of gelation, yield was observed and large amplitude oscillatory shear was shown to cause alignment followed by a slow recovery after the cessation of oscillation. An analogy to aging and rejuvenation effects in glass-forming liquids was discussed for these filled materials.

Melt Rheology of Polymer Nanocomposite

Ramanan Krishnamoorti
Department of Chemical Engineering
University of Houston

Introduction

- Need to understand the effect of adding nanoparticles on the melt dynamics and processing.
- How does the dispersion of the nanoparticles affect the rheology of the composites?
- How does processing affect the dispersion (or equivalently rheology) and how does the system recover?

Layered Silicate based Nanocomposites

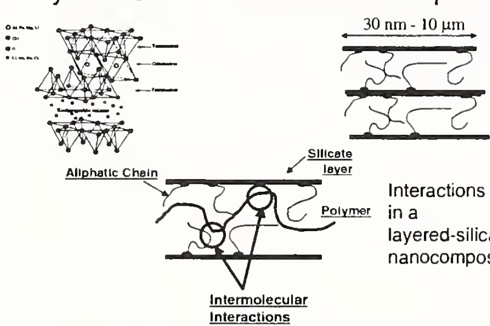

Interactions in a layered-silicate nanocomposite

Nanocomposite Classification

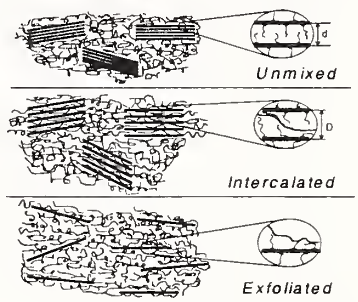

Nanocomposites

- Melt State Viscoelastic Measurements
- Exfoliated – Nylon 6 and Poly(ε-caprolactone)
- Intercalated – Polystyrene, Polyisobutylene based random copolymers, Polystyrene – Polyisoprene Diblock Copolymers, polycarbonate.
- Layered Silicates – Organically Modified
  - Montmorillonite (Natural Occurring)
  - Synthetic including Laponite, Fluorohectorite and Fluoromicas.

Quiescent State Characterization of Nanocomposites

- Linear Dynamic Viscoelastic properties
  - Oscillatory Strain (small amplitude)

Dynamic Oscillatory Behavior

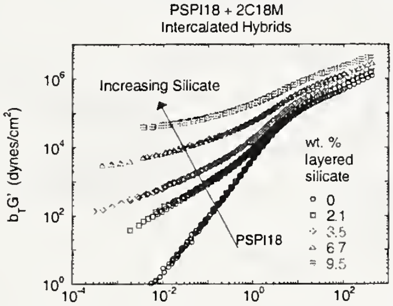

- Disordered block copolymer
- Intercalated Nanocomposites with gallery spacing of 2.5nm.
- Time-Temperature Superposed mastercurves
- Solid like character for nanocomposites with 6.7 and 9.5 wt. % OLS

Shift Factors

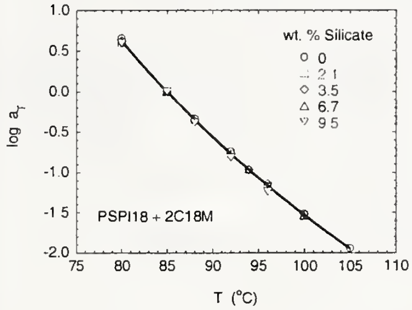

- Horizontal or Frequency shift factors

$a_T = \eta(T)/\eta(T_0)$

- Independent of silicate loading
- Obeys the WLF scaling.

Dynamic Oscillatory Behavior

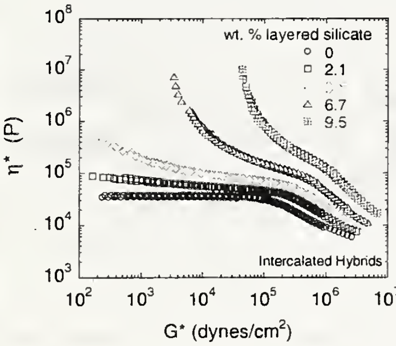

- PSPI18 + 2C18M
- Divergence of viscosity is consistent with the formation of a filler network structure.

Nanocomposite Linear Viscoelasticity

- Time – Temperature Superpositioning works.
- Stress relaxation in quantitative agreement with Dynamic Behavior.
- Transition from liquid-like to solid-like behavior with increasing silicate loading.
- Qualitatively similar behavior for intercalated and exfoliated hybrids.

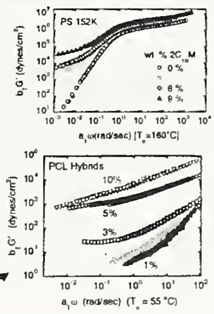

Exfoliated
Hybrid Similar to Nylon -6

Nanotube Composites

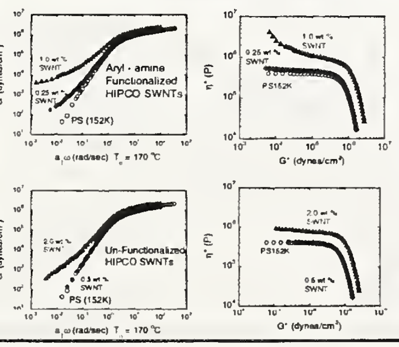

- Aryl Amine Functionalized SWNTs are compatible with PS.
- Unfunctionalized SWNTs demonstrate little reinforcement.
- In collaboration with Tour (Rice) and Arepalli (NASA).

Percolation Hypothesis

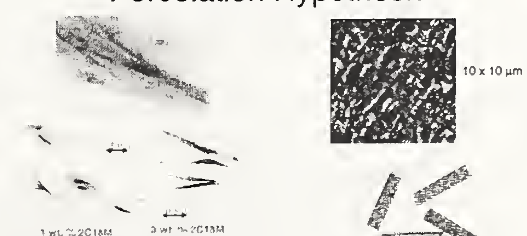

$$n_p = \frac{4}{3\phi_p}\frac{R_h}{h_s}\left[\frac{w_{s,p}\rho_o}{w_{s,p}\rho_o + (1-w_{s,p})\rho_s}\right]$$

2

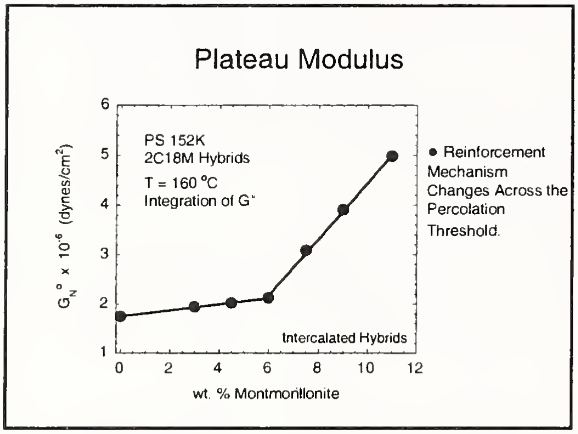
Plateau Modulus
PS 152K
2C18M Hybrids
T = 160 °C
Integration of G"
Intercalated Hybrids
$G_N^o \times 10^{6}$ (dynes/cm^2)
wt. % Montmorillonite
• Reinforcement Mechanism Changes Across the Percolation Threshold.

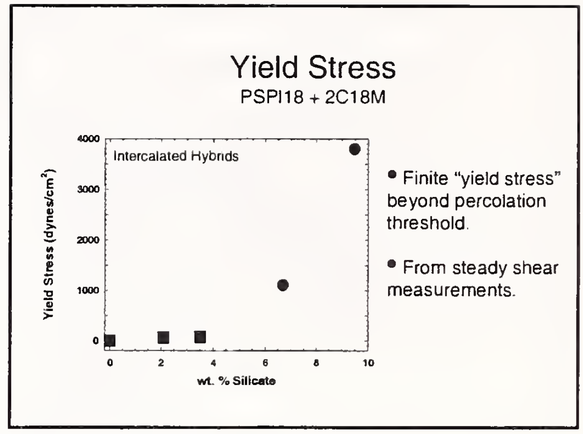
Yield Stress
PSPI18 + 2C18M
Intercalated Hybrids
Yield Stress (dynes/cm^2)
wt. % Silicate
• Finite "yield stress" beyond percolation threshold.
• From steady shear measurements.

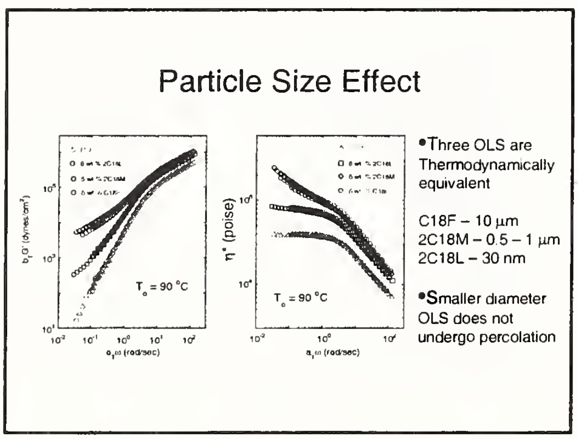
Particle Size Effect
T_o = 90 °C
η^* (poise)
•Three OLS are Thermodynamically equivalent
C18F – 10 μm
2C18M – 0.5 – 1 μm
2C18L – 30 nm
•Smaller diameter OLS does not undergo percolation

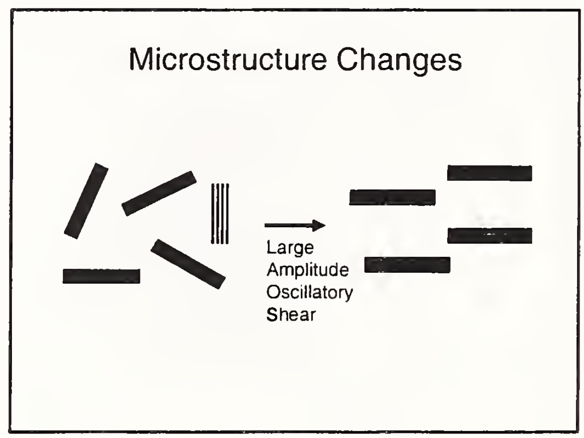
Microstructure Changes
Large
Amplitude
Oscillatory
Shear

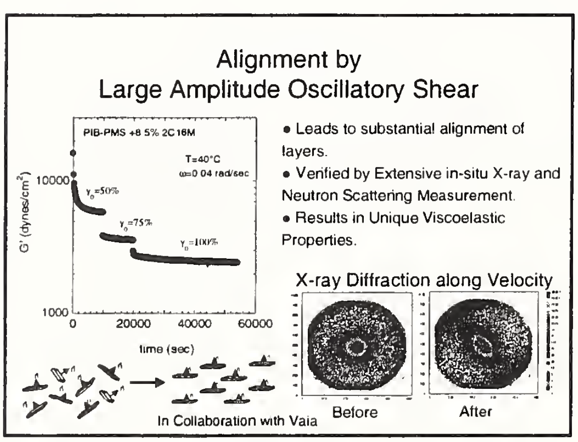
Alignment by
Large Amplitude Oscillatory Shear
PIB-PMS +8.5% 2C18M
T=40°C
ω=0.04 rad/sec
γ_o=50%
γ_o=75%
γ_o=100%
G' (dynes/cm^2)
time (sec)
• Leads to substantial alignment of layers.
• Verified by Extensive in-situ X-ray and Neutron Scattering Measurement.
• Results in Unique Viscoelastic Properties.
X-ray Diffraction along Velocity
Before
After
In Collaboration with Vaia

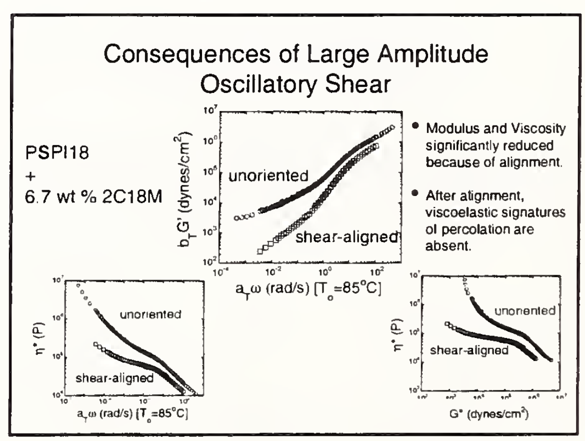
Consequences of Large Amplitude
Oscillatory Shear
PSPI18
+
6.7 wt % 2C18M
unoriented
shear-aligned
$b_T G'$ (dynes/cm^2)
$a_T\omega$ (rad/s) [T_o=85°C]
η^* (P)
G* (dynes/cm^2)
• Modulus and Viscosity significantly reduced because of alignment.
• After alignment, viscoelastic signatures of percolation are absent.

Recovery after Oscillatory Shear Alignment ?

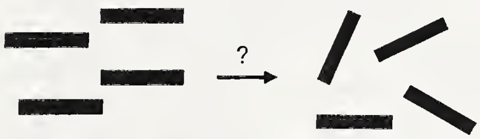

Recovery after Shear Alignment ?

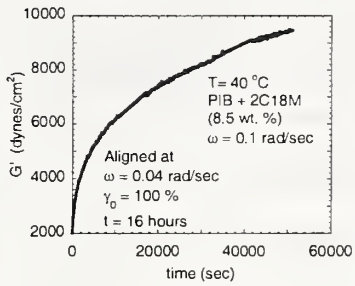

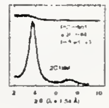

- After prolonged large amplitude oscillatory shear
  - ➢apply small oscillatory strain and monitor G'

Recovery after Shear Alignment

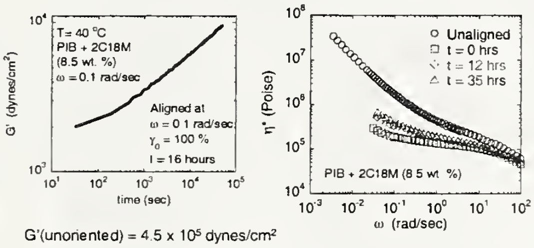

G'(unoriented) = 4.5 x 10^5 dynes/cm^2

Recovery is very slow!

Recovery after Shear Alignment
Temperature Effect

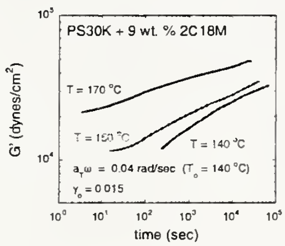

- G'(unoriented, $a_T\omega$ = 0.04) = 4.0 x 10^5 dynes/cm^2
- Very Slow Relaxation with Temperature (or matrix viscosity) having very little Effect.
- Origin of Orientational Relaxation?
  - If Brownian:

$$D_{r0} = \frac{3kT}{16\pi\eta_{matrix}a^3}\left(2\ln\left(2\frac{a}{b}\right)-1\right)$$

- Typically, a ~ 500 nm and a/b ~ 20

	η_{matrix}	D_{r0}
140 °C	~ 2.5 x 10^4 Pa S	2.9 x 10^{-7} s^{-1}
150 °C	~ 4.7 x 10^3 Pa S	1.6 x 10^{-6} s^{-1}
170 °C	~ 3.4 x 10^2 Pa S	2.3 x 10^{-5} s^{-1}

Recovery after Shear Alignment
Particle Size Effect

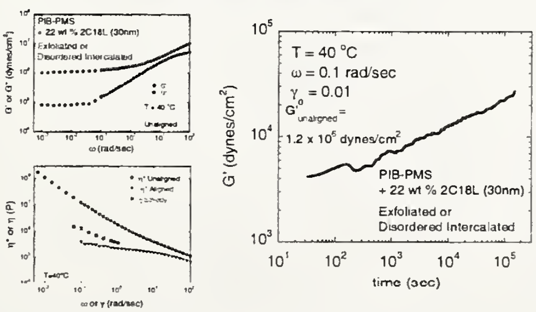

Aging and Rejuvenation

- Leibler, Solich et al. have noted the analogy between the rheology of concentrated soft dispersions to the dynamics of glass formation:
  - —Their Internal Structure is Intrinsically Disordered and Metastable.
  - —History Dependent Viscoelasticity of Pastes is Characteristic of Aging.
  - —In pastes, rejuvenation occurs by the application of large stress and metastability and aging appear when flow ceases.
  - —Do these layered silicate based nanocomposites demonstrate the same physical aging behavior?
    - The recovery after large amplitude oscillatory flow appears to follow that behavior.

4

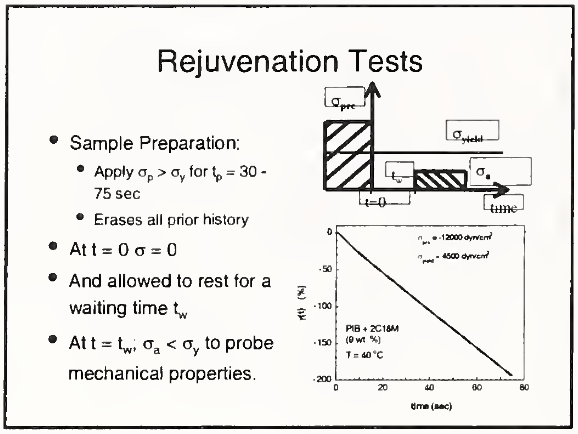
Rejuvenation Tests
Sample Preparation:
Apply $\sigma_p > \sigma_y$ for t_p = 30 - 75 sec
Erases all prior history
At t = 0 σ = 0
And allowed to rest for a waiting time t_w
At t = t_w; $\sigma_a < \sigma_y$ to probe mechanical properties.
σpre
σyield
σa
t=0
time
PIB + 2C18M
(9 wt %)
T = 40 °C
time (sec)

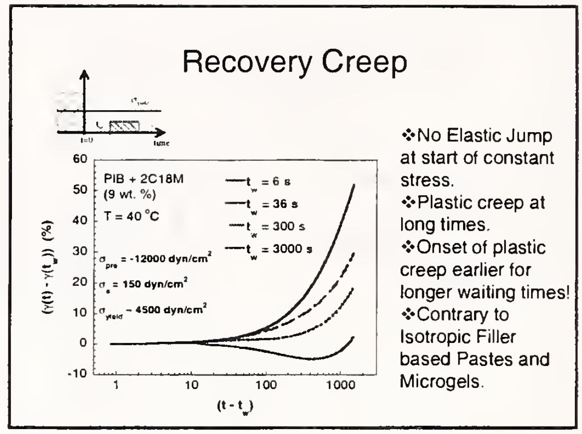
Recovery Creep
PIB + 2C18M
(9 wt. %)
T = 40 °C
σpre = -12000 dyn/cm²
σa = 150 dyn/cm²
σyield ~ 4500 dyn/cm²
tw = 6 s
tw = 36 s
tw = 300 s
tw = 3000 s
(γ(t) - γ(tw)) (%)
(t - tw)
❖No Elastic Jump at start of constant stress.
❖Plastic creep at long times.
❖Onset of plastic creep earlier for longer waiting times!
❖Contrary to Isotropic Filler based Pastes and Microgels.

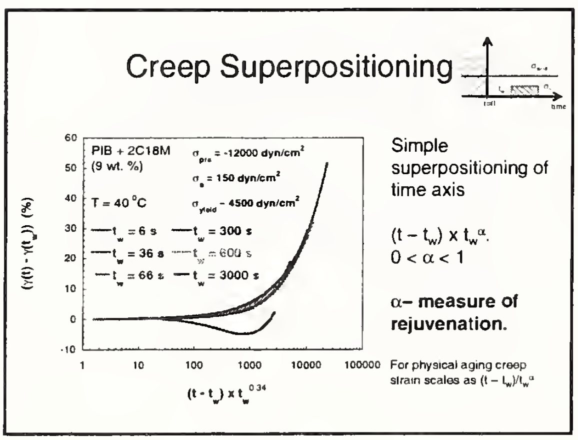
Creep Superpositioning
PIB + 2C18M
(9 wt. %)
T = 40 °C
σpre = -12000 dyn/cm²
σa = 150 dyn/cm²
σyield ~ 4500 dyn/cm²
tw = 6 s
tw = 36 s
tw = 66 s
tw = 300 s
tw = 600 s
tw = 3000 s
(γ(t) - γ(tw)) (%)
(t - tw) x tw^0.34
Simple superpositioning of time axis
(t – tw) x tw^α.
0 < α < 1
α– measure of rejuvenation.
For physical aging creep strain scales as (t – tw)/tw^α

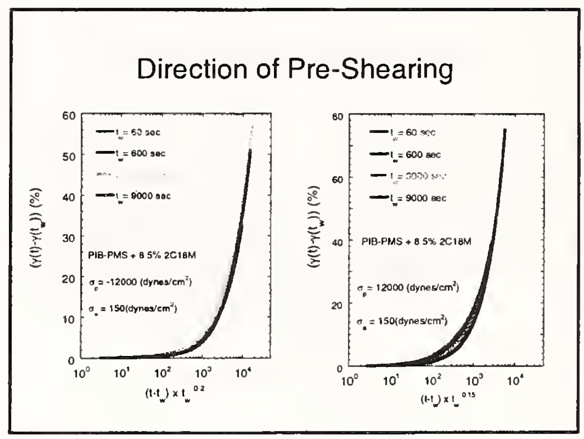
Direction of Pre-Shearing
tw = 60 sec
tw = 600 sec
tw = 9000 sec
PIB-PMS + 8.5% 2C18M
σp = -12000 (dynes/cm²)
σa = 150(dynes/cm²)
σp = 12000 (dynes/cm²)
(γ(t)-γ(tw)) (%)
(t-tw) x tw^0.2
(t-tw) x tw^0.15

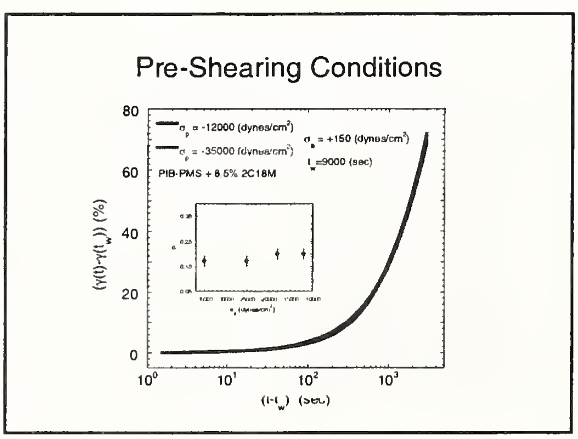
Pre-Shearing Conditions
σp = -12000 (dynes/cm²)
σp = -35000 (dynes/cm²)
σa = +150 (dynes/cm²)
tw = 9000 (sec)
PIB-PMS + 8.5% 2C18M
(γ(t)-γ(tw)) (%)
(t-tw) (sec)

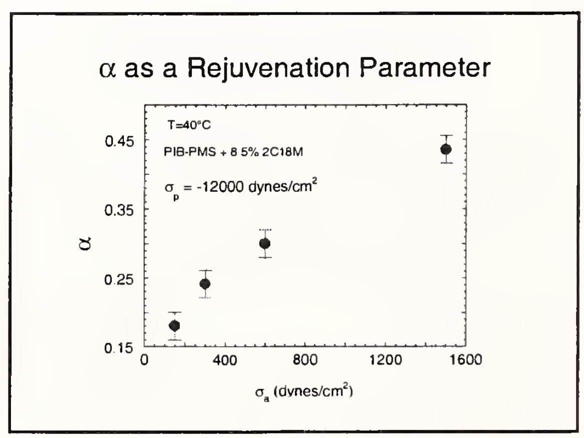
α as a Rejuvenation Parameter
T=40°C
PIB-PMS + 8.5% 2C18M
σp = -12000 dynes/cm²
α
σa (dynes/cm²)

Hypothesis for Unique Creep Recovery

- Large Constant Stress (& Steady Shear) do not lead to exclusively parallel orientation (layer normals in velocity gradient direction).
- Most Likely Scenario – Mixed Parallel + perpendicular orientation.(Preliminary scattering measurements support this hypothesis); Other possible hypothesis – Disaggregation and Reaggregation.
- The perpendicular aligned layers are unstable and disorient rapidly in the absence of flow.

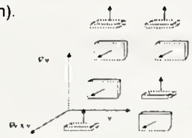

Conclusions

- Linear Viscoelasticity Sensitive to Mesoscale Structure.
- Recovery from Oscillatory Alignment appears to follow Physical Aging Like Kinetics.
- Recovery from Large Constant Stress – Unique and illustrative of the anisotropic layers influence on orientation.
  - No Dependence on Pre – Shear Magnitude and Direction.
  - Simple scaling of t_w allows for superpositioning of creep data.
  - α appears to be a powerful parameter to capture the rejuvenation of the nanocomposites.

Acknowledgements

- Koray Yurekli
- Jiaxiang Ren
- Dr. Adriana Silva
- Cynthia Mitchell
- Barbara Casanueva

- Hsien Wang
- Mun Fu Tse
- Jay Dias

Financial Support

- American Chemical Society (PRF)
- Texas Coordinating Board for Higher Education(ATP)
- Welch Foundation
- NIST
- ARL
- ExxonMobil Chemical Company

4) Satish Kumar, **"Processing, Structure, and Properties of Nano Composite Fibers and Films"** [PowerPoint not available] [PDF]

Dr. Kumar spent some time reviewing the field of nanocomposites as viewed from the perspective of a composite engineer. The geometrical structure of both single and multi-walled materials was reviewed and some measurements on melt-spinning these filler particles in polymer matrices were described. Some impressive improvements in compressive strength and tensile modulus of filled polypropylene and PMMA fibers were noted. Other notable observations include the observation of length changes in the single wall tubes upon blending and fiber spinning and the influence of the tubes on the size and rate of growth of polypropylene spherulites. It was also shown that highly conducting films could be formed from solutions of single wall nanotubes dispersed in Oleum.

Processing, Structure, and Properties of Nano Composite Fibers and Films

Satish Kumar
School of Textile and Fiber Engineering
Georgia Institute of Technology, Atlanta GA 30332
satish.kumar@textiles.gatech.edu

Nano Composites - Reinforcements

- **SWNT**
  - Diameter ~ 1 nm, From Rice University, HiPCO process
- **MWNT** or Carbon Nano Fibers
  - (Diameter 50 – 200 nm, Applied Sciences Inc., OH)

Nano Composites – Matrix Systems

- **Insitu Polymerization**
  - PBO and PBZT
- **Melt Blending**
  - PP
  - PET
  - PMMA

Carbon Nanotubes – Historical Perspective

- Flexible Polymer – such as Polyethylene (1930s). High modulus PE fiber commercialized in 1980s.

$-[CH_2-CH_2]-$

- Rigid Polymers – such as PBZT and PBO (1980s). Zylon fiber commercialized in 1998.

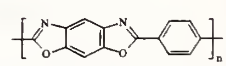

- Carbon Nanotubes – 1990s. By compariosn, synthesis, purification, and processing of these tubes is in its infancy.

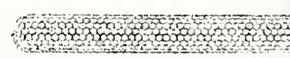

$[\eta] = K M^a$

Flexible polymer	0.5
Semi-flexible polymer	~1
Rigid polymer	1.8
SWNT	?

MWNT

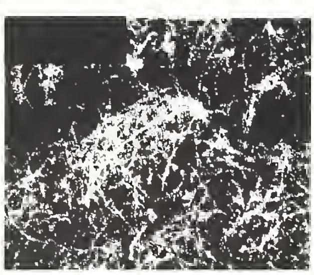

PR-21-PS

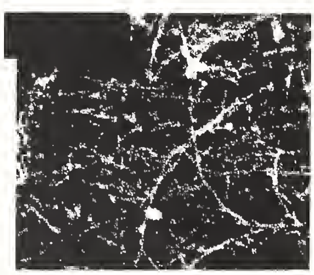

PR-24-PS

MWNT

TEM image of the wall of a carbon nanotube grown by ASI's Pyrograf™-III process.

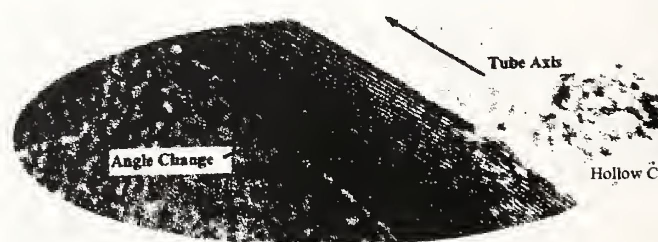

Photograph from Applied Sciences Inc.

MWNT

MWNT	Processing method	Oxygen content (wt%)	Sulfur content (wt%)
PR-21-PS	Pyrolytically stripped	1.2	0.3
PR-24-PS	Pyrolytically stripped	0.6	0.4
PR-24-HT	Graphitized at 3000 °C	0.3	0.0
PR-24-AG	As Grown Fiber	2.2	0.5
PR-24-PPO	Post processing oxidation of PR-24-AG	2.1	0.4
PR-24-ISO	In situ oxidation of PR-24-AG	2.2	1.1

CNFs were provided by Applied Sciences, Inc. (Cedarville, Ohio)

Raman Spectra of MWNT

CNF	Raman intensity ratio of D to G band
PR-24-HT	0.7
PR-24-PS	1.6
PR-21-PS	3.1
PR-24-AG	1.5
PR-24-PPO	1.6
PR-24-ISO	1.8

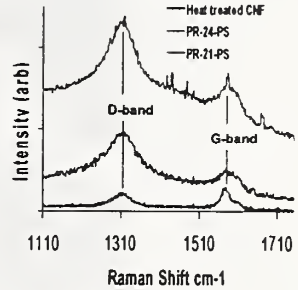

Melt Blending and Fiber Processing

PET melt blended with 5 wt% carbon nano fibers

- Dry Mixing
  - Ball Milling
  - Hand Mixing
- Melt Compounding
  - Haake Twin-screw extruder TW-100
  - Haake mixer
- Spinning
  - 290°C, 250 μm spinneret
- Drawing
  - 120°C, draw ratio 4X or 6X
- Heat treatment
  - 150 °C at constant length

PP and PMMA melt blended at 240 °C

Melt spinning set up

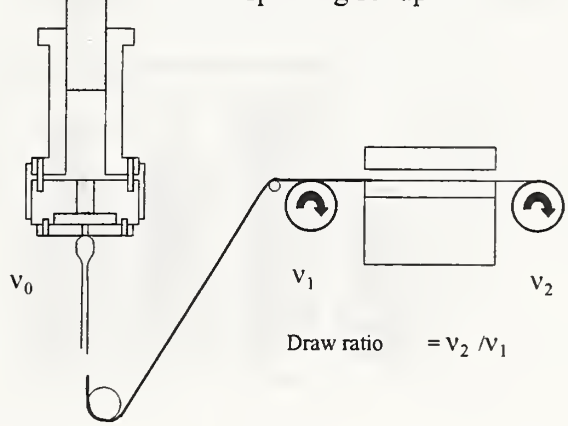

PET/MWNT Composite Fibers

PP/ MWNT Composite Fiber

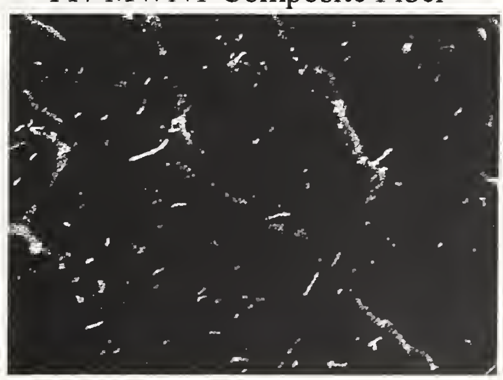

PMMA/MWNT

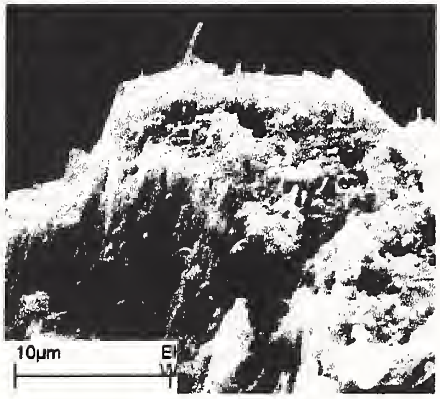

Tensile Modulus of Various PET/CNF fibers

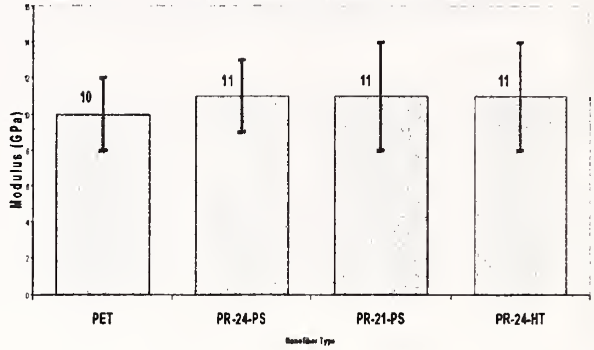

PET/MWNT Composite Fibers

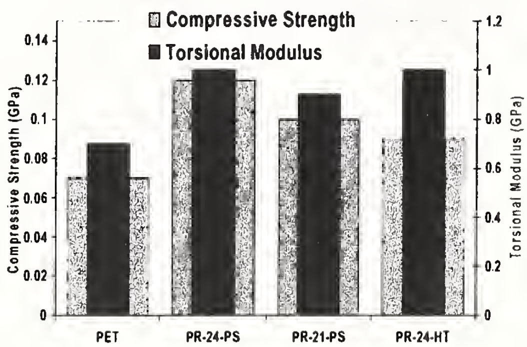

PP/ MWNT Fibers

Sample	Tensile Strength (MPa)	Tensile Modulus (GPa)	Elongation to Break (%)	Compressive Strength (MPa)
PP- control	490 ± 60	4.6 ± 0.7	23 ± 5	25 ± 1
PP + 5 wt % VGNCF	570 ± 70	7.1 ± 0.9	16 ± 2	48 ± 10

PMMA/MWNT Composite Fibers

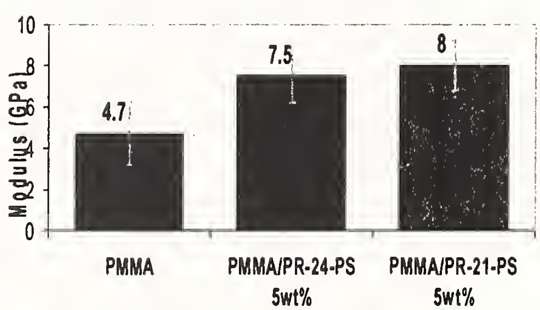

PMMA/MWNT Composite Fiber

Sample	Tensile Modulus GPa	Tensile Strength GPa	Elongation at break (%)	Compressive Strength (MPa)
PMMA Control	4.7±1.5	0.20±0.04	16±3	28±2
PMMA/PR-24-PS 5wt%	7.5±1.3	0.16±0.03	10±3	66±20
PMMA/PR-21-PS 5wt%	8.0±1.2	0.17±0.04	10±6	73±11

Thermal stability of PMMA/MWNT Composites

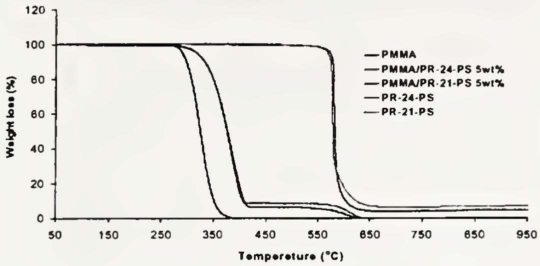

	PMMA	PMMA/PR-24-PS 5wt%	PMMA/PR-21-PS 5wt%
5% weight loss temperature (°C)	**289**	**318**	**315**

Shrinkage Behavior - PMMA/MWNT Fibers

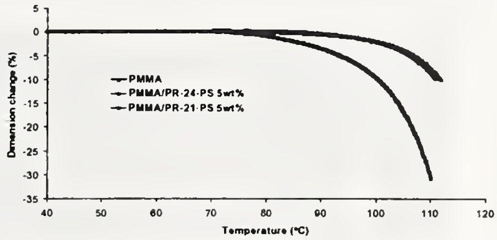

	PMMA	PMMA/PR-24-PS 5wt%	PMMA/PR-21-PS 5wt%
Temp at 0.5% shrinkage (°C)	**78**	**88**	**92**
Shrinkage at 100°C	**9.0**	**2.4**	**2.0**

MWNT Length Reduction During Melt Blending and Fiber Spinning

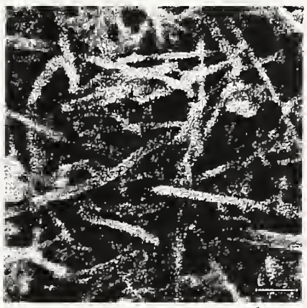

1 μm

Fiber Tensile Modulus - PET/CNF Composite

Modified Cox model:

$$\beta = \frac{l}{d}\sqrt{\frac{E_m}{(1+v)E_f \times \ln(\pi/4V)}}$$

$$E_c = (1-V)E_m + q\left(1-\frac{\tanh\beta}{\beta}\right)VE_f$$

***l*: nano fiber length**
***d*: nano fiber diameter**
***V*: volume fraction**
E_m: matrix modulus
***v*: Poisson's ratio**
E_f: axial tensile modulus
***q*: orientation factor**

Cox HL. Brit. J. Appl. Phys. 3 72-79(1952)

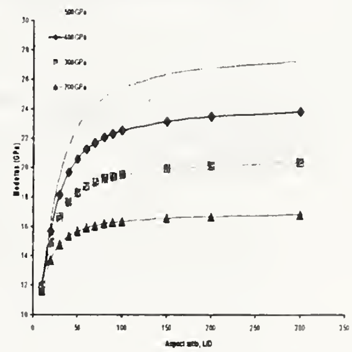

PET/MWNT Composite Fiber WAXD

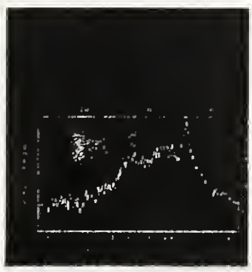

Optical Microscopy-PP/SWNT Melt

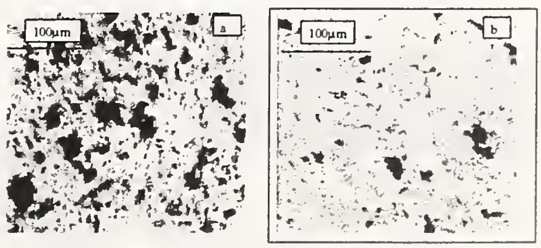

PP/SWNT Composite (a) before filtration and (b) after filtration

Georgia Tech

Optical Microscopy - Sperulitic Growth

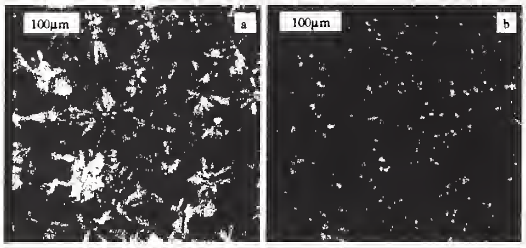

PP PP/SWNT

Georgia Tech

TGA

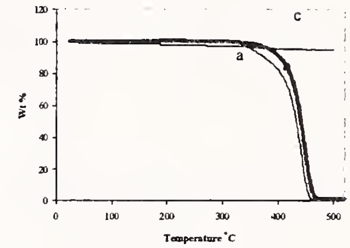

(a) PP (b) PP/SWNT (c) SWNT

Georgia Tech

PP/SWNT - Isothermal Crystallization

The addition of 0.8 wt % SWNT increases the PP crystallization rate.

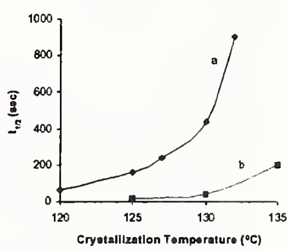

(a) PP (b) PP/SWNT

Georgia Tech

PP/SWNT - Raman Spectroscopy

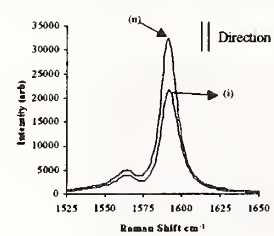

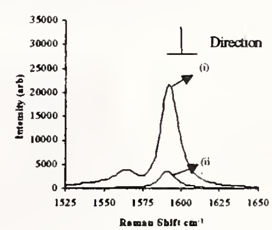

PP/SWNT fiber Draw Ratio	Raman Ratio Intensity ∥/⊥
1	1.0
4.7	8.9

(i) Draw ratio = 1 & (ii) Draw ratio = 4.7

The increase in Raman ratio indicates SWNT alignment.

Georgia Tech

SYNTHESIS OF POLYBENZOBISOXAZOLE

AFRL / MLBP MATERIALS DIRECTORATE

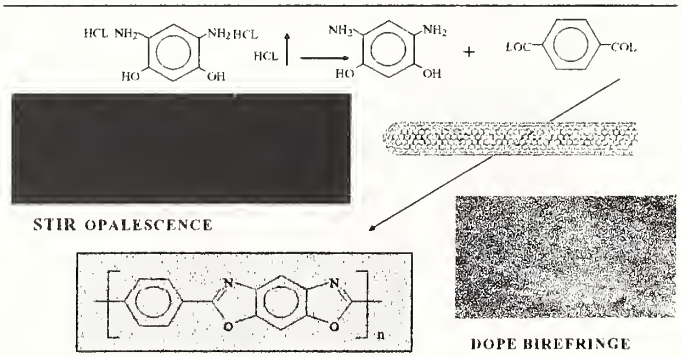

Fred Arnold and Thuy Dang – AFRL/WPAFB

PBO-SWNT Fiber Spinning Conditions

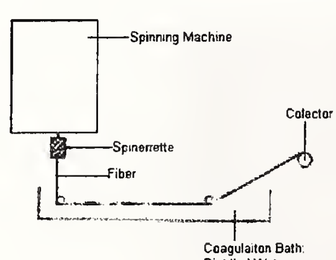

- Spinning temperature 100~130 °
- As-spun fiber washed in water fo one week.
- Fiber heat-treated under tension 400 °C in nitrogen.

PBO/SWNT Fiber Mechanical Properties

	E (GPa)	ε (%)	σ_t (GPa)
PBO HT	138	2.0	2.6
PBO/SWNTHT (95/5)	156	2.3	3.2
PBO/SWNTHT (90/10)	167	2.8	4.2

PBO/SWNT – Thermal Shrinkage

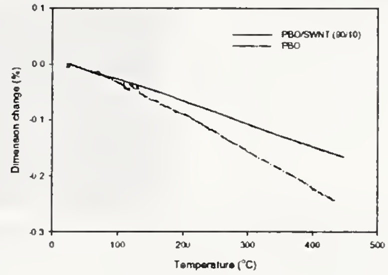

PBO/SWNT Creep Behavior at 400 °C

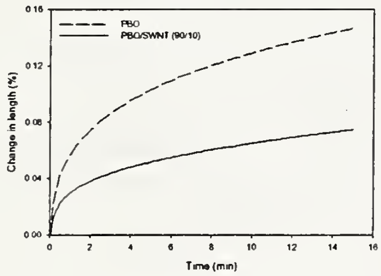

WAXD: Equatorial Scan

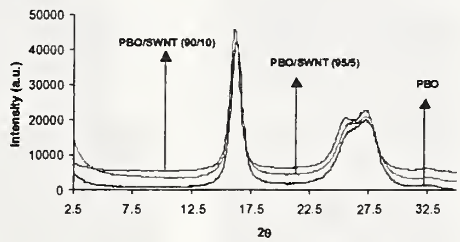

Richard A. Vaia – AFRL/WPAFB

Raman Spectroscopy

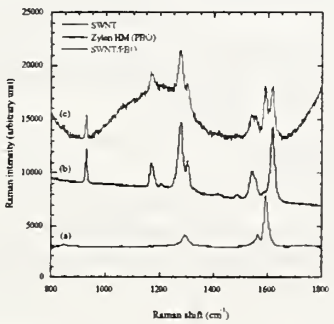

Cheol Park – NASA Langley

PBO and PBO/SWNT Fibers
Fracture Behavior

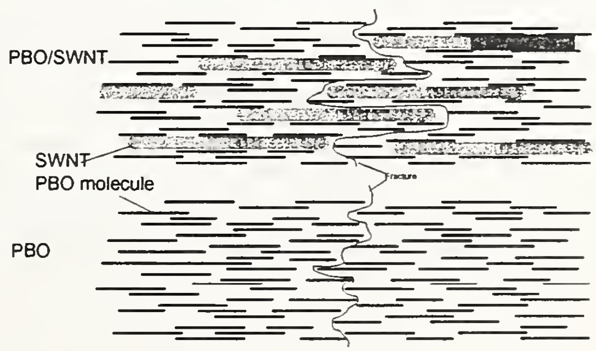

SWNT Film

Optical micrographs of 0.25wt% SWNT in Oleum (H_2SO_4:30% SO_3)

Without cross-polars | **With cross-polars**

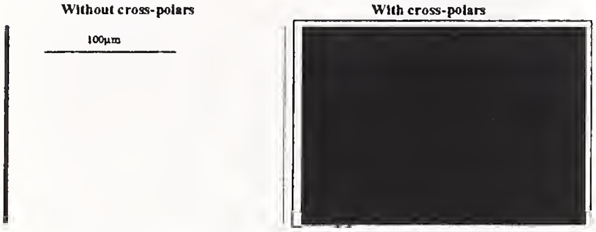

The 0.25 wt% SWNT solution in Oleum is non birefringent, indicating an isotropic solution. This solution is stable for months at room temperature when kept under dry inert environment.

SWNT Film

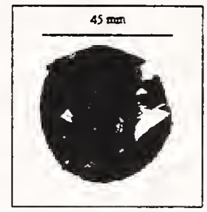

Scanning Electron Micrographs of the SWNT Film

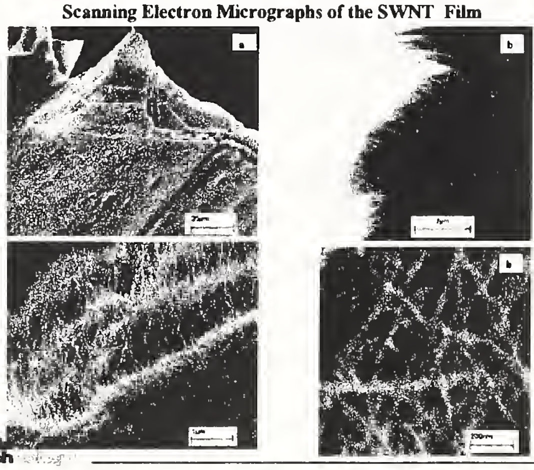

Stress-strain curve of the heat-treated SWNT film

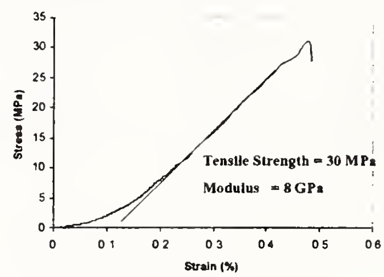

SWNT Film
Electrical Conductivity

- **The electrical conductivity in the plane of the film = 1.3 X 10^5 S/m (Four probe method)**
- **The electrical conductivity through the thickness = 1.1×10^{-2} S/m. (HP4192A LF impedance analyzer)**

Summary

- Polymer/nanotube composite fibers can be spun using the typical polymer spinning equipment /conditions.
- MWNT exhibit good dispersion in PET, PP, and PMMA. PP and PMMA appears to have good interaction with MWNTs.
- High tensile strength fibers can be processed from PBO/SWNT.
- SWNT act as nucleating agent for PP.
- SWNT films with in plane DC electrical conductivity of the order of 10^5 S/m have been processed from isotropic solutions in oleum.

Acknowledgements

- Funding
  - AFOSR, ONR, NSF, KoSa, and CNI
- MWNT – Applied Sciences Inc.
- SWNT work is being done in collaboration with Professor Smalley's group at Rice University and Air force Research Laboratory (Fred Arnold, Thuy Dang, and Richard Vaia).
- Cheol Park - NASA
- Hongming Ma, Jijun Zeng, Harit Doshi, Byung Min, T. V. Sreekumar, Arup R. Bhattacharyya, Xiefei Zhang.

5) Alex Morgan, **"Polypropylene Nanocomposites: Clay Organic Treatment Concentration Effects on Mechanical Properties, Flammability Properties and Clay Dispersion"** [PowerPoint] [PDF]

Dr. Morgan summarized some of the efforts at Dow at exploiting clay-filled thermoset and thermoplastic nanocomposites. These materials show major improvements in mechanical properties, gas barrier properties, thermal stability and flame retardancy and the factors influencing these property changes were summarized- synthesis method, extent of dispersion, clay type and organic treatment, polymer matrix type. The presentation emphasized the complexity of understanding and controlling the properties of these complex materials. Particular emphasis was given to property changes that accompany the variation in the amount of organic modifier in the material. The presentation covered a wide range of experimental methodologies (x-ray diffraction, transmission electron microscopy, thermal gravimetric analysis, mechanical property testing, Flammability property testing, NMR, Atomic force microscopy, neutron scattering calorimetry and optical microscopy) since no single method allows for the characterization of these multi-scale materials. The extensive efforts in characterizing these materials are an important factor in slowing the development of these materials and the need for faster and additional validation methodologies for characterization emphasized, especially methods relating to the characterization of polymer-clay and polymer-organic interactions that important for dispersion stability.

Polypropylene Nanocomposites: Clay Organic Treatment Concentration Effects on Mechanical Properties, Flammability Properties and Clay Dispersion

Alex Morgan
Inorganic Materials
Corporate R&D
The Dow Chemical Company
05/29/02

Current Polymer Nanocomposite Technology

- Polymer Nanocomposites are composed a polymeric material (thermoset or thermoplastic) and a re-enforcing nanoscale material
- The most commonly studied re-enforcing nanoscale materials are layered materials, or clays
- Polymer-clay nanocomposites show major improvements in mechanical properties, gas barrier properties, thermal stability, and flame retardancy
- Many factors affect the polymer-clay nanocomposite properties
  - Synthesis method
    - Melt Compounding, solvent blending, in-situ polymerization, emulsion polymerization
  - Polymer nanocomposite morphology
  - Clay type and clay organic treatment
    - Layered clay aspect ratio, structure
    - Organic treatment thermal stability, structure
  - Polymer matrix
    - Crystallinity, molecular weight, polymer chemistry
- Understanding property improvement due to polymer-clay nanocomposite properties very complex

Importance of Organic Treatment for Layered Silicate Nanocomposites

- Sioce layered silicates are hydrophilic materials, they must be made orgaoophilic (or hydrophobic) to become compatible with the polymer.
  - Withont organic treatment, layered silicates only disperse in very polar polymers.
  - Organic treatment is typically done via ion exchange between inorganic alkali cations on the clay surface and the desired organic cation.
- The organic treatmeot, being at the interface between inorganic silicate and organic polymer, will be a vital part of the nanocomposite, and therefore, must be tailored to syothetic cooditions.
  - Synthetic methods inclnde solvent mixing, *in-situ* polymerization, and melt compounding.
- Ooe of the most "industry-frieodly" methods of making nanocomposites is with the use of melt compounding.
  - Polymer and organically treated clay are heated to the melting point of the polymer, and the two are mixed together via compounding equipment (extruder, mixing head, etc.)

Preparation of Polymer Clay-Nanocomposites

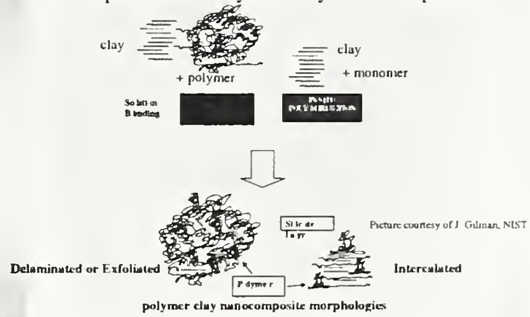

Soxhlet Extraction of Organoclays

- An organoclay (fluorinated synthetic mica (FSM), Somasif ME-100 from Co-op Chemical) treated with an alkyl ammonium chloride (dimethyl, dihydrogenated tallow ammonium, Arquad 2HT from Akzo-Nobel) was extracted with a Soxhlet apparatus from 1 to 4 days with ethanol.
- Each batch of extracted clay (1 day, 2 days, 3 days, 4 days) was analyzed by TGA and XRD.
- By using Soxhlet extraction, excess organic treatment (physisorbed, or non-ion exchanged treatment) can be washed off, possibly improving the thermal stability of the organoclay, as well as removing plasticizing organic treatment.

XRD of Soxhlet Extracted Organoclay

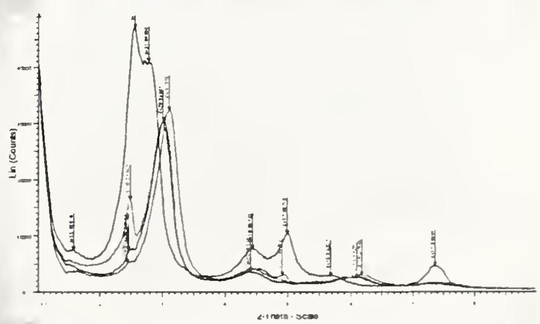

1

TGA of Soxhlet Extracted Organoclay

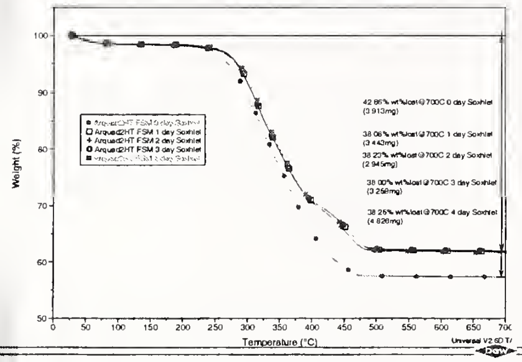

dTGA of Soxhlet Extracted Organoclay

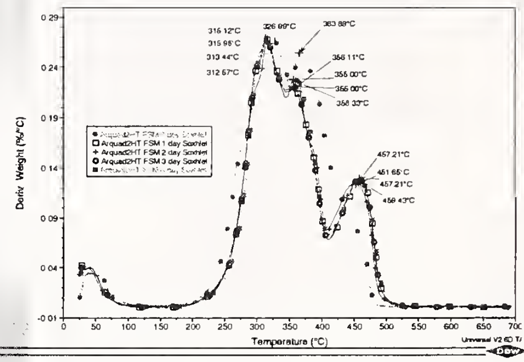

XRD, TGA data for Extracted Clays

- Soxhlet extraction of organoclays removes excess (physisorbed) organic treatment from the clay surface
  - TGA data shows that after 1 day, all excess organic treatment is removed. Additional extraction removes no more treatment (TGA data unchanged)
  - XRD data changes. Main d-spacing (100) peak drops with 1 day extraction time, and then another peak appears with increasing extraction time (organic treatment re-arrangement?)

Soxhlet Extracted Organoclay Nanocomposites

ABM-I-45 Series: PP/PPgMA nanocomposites + soxhlet extracted organoclays
All samples are PP (PD191) + PPgMA (Aldrich PPgMA)
Processing conditions 190 C, 20 min mixing of PP, PPgMA, then 10 min mixing of organoclay into PP+PPgMA

Sample	wt% organoclay	wt% PP	wt% PPgMA	XRD (100) d-spacing change (nm)	TEM Microscale Dispersion	TEM Nanoscale Dispersion	Mechanical Properties Flex Mod (ksi)	Mechanical Properties Izod (R.T.) (ft-lb/in)
ABM-I-45A	0	72	28	N/A	N/A	N/A	188	1.1
ABM-I-45B	8.5	65.9	25.6	0.2	Fair	Good	289	0.7
ABM-I-45C	7.9	66.3	25.8	0.13	Good	Good	312	0.5
ABM-I-45D	7.9	66.3	25.8	0.06	Good	Good	304	0.6
ABM-I-45E	7.9	66.3	25.8	0.01	Good	Good	304	0.6
ABM-I-45F	7.9	66.3	25.8	-0.06	Good	Good	303	0.7

ABM-I-45A Control
ABM-I-45B PP+0-day extracted clay
ABM-I-45C: PP+1-day extracted clay
ABM-I-45D: PP+2-day extracted clay
ABM-I-45E: PP+3-day extracted clay
ABM-I-45F: PP+4-day extracted clay

Soxhlet Extracted Organoclay Nanocomposites

- Extraction improves some mechanical properties.
  - Flex modulus improved with extraction
  - Izod impact properties decreased.
- Improvement in properties occurs with initial (1 day extraction)
  - Prolonged extraction does not seem to improve properties.
- While TEM and XRD of the polymer nanocomposites seem to change with increasing extraction time, mechanical properties do not change much with increasing extraction time

TEM, PP+Clay (No Extraction)

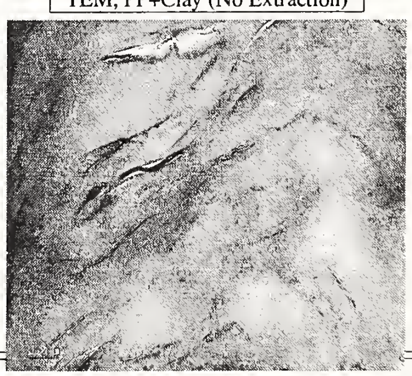

2

TEM, PP+Clay (1-day Extraction)

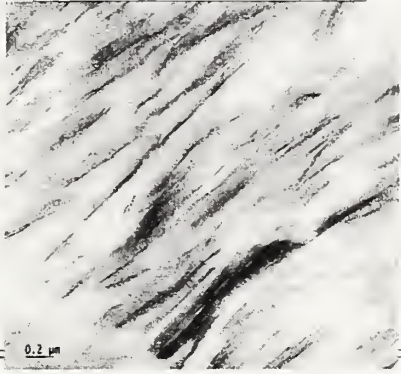

TEM, PP+Clay (2-day Extraction)

TEM, PP+Clay (3-day Extraction)

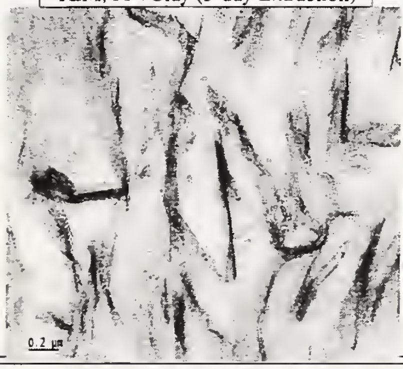

TEM, PP+Clay (4-day Extraction)

Flammability of Polypropylene Nanocomposites

- Flammability does appear to be affected by extraction times
  - T_{ig} slightly delayed with increasing extraction times.
  - Peak HRR (Peak q) goes ap with 1 day extraction time, then slowly begins to lower again to 0-day extraction time Peak HRR value.

PP/PPgMA nanocomposites + soxhlet extracted organoclays
Clay #1: 0 day extraction time. Clay#2: 1 day extraction time
Clay #3: 2 day extraction time. Clay#4: 3 day extraction time. Clay#5: 4 day extraction time.

	Units	PP+PPgMA Control	PP+PPgMA+ Clay#1	PP+PPgMA+ Clay#2	PP+PPgMA+ Clay#3	PP+PPgMA+ Clay#4	PP+PPgMA+ Clay#5
Heat Flux	kW/m²	35	35	35	35	35	35
Tig	s	62	59	65	66	68	70
Peak q	kW/m²	1435.4	498.4	518.6	510.3	494.1	491.0
Mean q	kW/m²	769.9	406.4	429.3	423.8	418.4	405.1
180sec q	kW/m²	684.3	450.1	476.3	465.2	450.5	456.4
300sec q	kW/m²	410.6	386.1	379.3	374.4	376.6	378.1
Total q	MJ/m²	122.9	115.8	113.7	112.3	112.9	113.4
Effective Heat	MJ/kg	43.1	41.2	40.6	40.1	40.8	40.6

Conclusions

- Soxhlet extraction of organoclays removes excess organic treatment after 1 day extraction time.
  - TGA, dTGA data shows materials to be identical in organic content after 1 day extraction time. Additional extraction removes no more material.
  - XRD patterns do change with increasing extraction time. Reason unknown
- Removal of excess organic treatment does improve mechanical, flammability properties.
  - Flex modulus improved with removal of organic treatment, but Izod impact diminished. (Org. treatment acts as plasticizer)
  - Mechanical property changes only occur going from unextracted to 1 day extracted clay. Additional extraction seems to provide no additional benefit, despite changes in XRD (d-spacing decrease with increasing extraction time) and TEM (better dispersion with increasing extraction time)
  - Extraction time seems to have a larger influence on flammability properties.
    - Peak HRR lowest for unextracted clay nanocomposite, goes up for 1 day extracted material, and then slowly goes back to unextracted clay nanocomposite peak HRR level.
    - T_{ig} delayed with clay extraction (excess organic treatment does cause early ignition.

3

Nanocomposite Analysis Techniques

- Many different techniques used for Polymer-Clay Nanocomposite analysis
- Commonly used techniques.
  - X-ray Diffraction (XRD)
  - Transmission Electron Microscopy (TEM)
  - Thermal Gravimetric Analysis (TGA)
  - Mechanical Property Testing (Flex modulus, Izod Impact)
  - Flammability Property Testing (Cone calorimeter)
- Other techniques:
  - Nuclear Magnetic Resonance (NMR)
  - Atomic Force Microscopy (AFM)
  - Neutron scattering
  - Thermal analysis (Rheology, Differential Scanning Calorimetry)
  - Optical Microscopy

Nanocomposite Analysis Techniques: XRD

- XRD measures the spacing between the ordered crystalline layers of the clay
- Spacing change (increase or decrease) can help determine the type of nanocomposite made
  - Immiscible (no d-spacing change)
  - Decomposed/De-intercalated (d-spacing decrease)
  - Intercalated (d-spacing increase)
  - Exfoliated (d-spacing outside of wide-angle XRD, or so far apart and disordered to give a signal
- XRD however, affected by many parameters:
  - Sampling (powder vs. solids, alignment of clay plates, sample orientation)
  - Experimental parameters (slit width, count time, angle step rate)
  - Layered Silicate order (disorded/amorphous materials give no signal by XRD)
- XRD measures d-spacing, not overall (global) clay dispersion in sample

Clay Organic Treatment - XRD Changes

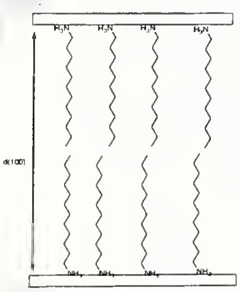

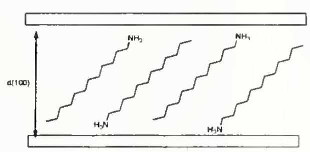

- Stacking/Orientation of organic treatment can have an effect on XRD d(100) spacing
- Clay synthesis conditions, polymer processing, melting point of organic treatment can change orientation.

Nanocomposite Analysis Techniques: TEM

- TEM measures the overall clay dispersion in the sample
- Clay dispersion and structure observed under the microscope can determine the nature of a clay nanocomposite.
  - Immiscible (Usually large clay tactoids, undispersed clay particles)
  - Intercalated (Clay layers in ordered stacks can be observed)
  - Exfoliated (Single clay layers can be observed)
  - Can determine global microscale dispersion as well as nanoscale dispersion/structure
- TEM has limitations and drawbacks
  - Sampling (heterogeneous samples will give false results)
  - Labor intensive analysis, expensive analytical instrument
  - Cannot measure d-spacing of clay, therefore, cannot easily determine difference between intercalated clay nanocomposite and well-dispersed immiscible nanocomposite
- TEM measures overall clay dispersion, but should be combined with XRD data

Nanocomposite Analysis Techniques: Property Testing

- Current property tests follow ASTM or other standards.
- Tests determine property of materials, but do not indicate why properties were obtained
- Example: Flex Modulus Measurement. Shows what flex modulus of property is, but does not indicate why stiffness of nanocomposite has improved.
- Exceptions:
  - Cone Calorimeter: Measures additional parameters, such as heat release rate and mass loss rate, thus suggesting some polymer nanocomposite properties.
  - Drawback: Must rely upon other techniques to confirm nanocomposite dispersion. Technique measures flammability, but cannot explain why improved flammability was obtained on its own.

Nanocomposite Analysis Needs

- No one technique answers all questions about a polymer nanocomposite. Several techniques needed to understand polymer nanocomposite
- Time to get back all data can slow development of polymer nanocomposite formulation
- Other techniques show promise at nanocomposite analysis, but need to be validated.
  - Neutron scattering - similar issues to XRD, limited access.
  - AFM: "Tip" resolution - uncertainty around images of clay plates (single clay plate, or stack of 2-3 very tightly packed together?)
  - NMR: Currently only works for clays with Iron in the clay structure. Technique would need to be adapted for synthetic clays (no Iron).
  - Rheology/DSC: Suggestions made in literature that clay dispersions can be observed by DSC and rheological changes, but this may be specific to certain nanocomposites only
  - XRD: Possible greater use (peak height/broadness analysis relating to clay dispersion, d-spacing changes - what is significant?) - needs to be validated.

4

Conclusions

- Polymer-clay naoocomposites present a complex analytical problem
  - Properties of polymer clay nanocomposite dependent on many factors
  - No one analytical technique analyzes these many factors
- TGA, XRD, TEM currently major tools for polymer-clay nanocomposites.
  - Techniques in combination give a better description/analysis of polymer-clay nanocomposite
  - Each technique has positive and negative aspects
- Time to complete analysis on polymer-clay nanocomposite slow step
  - New analytical techniques needed to speed up analysis.
  - Techniques that address polymer-clay/polymer-organic treatment interactions are needed.

Acknowledgements

- Inorganic Materials, Chemical Sciences:
  - Steve Lakso, Juan Garces, Mike Paquette, Wanda Stringfield
- Analytical Sciences:
  - Joe Harris
- Fabricated Products:
  - Sylvie Boukami

6) Atsushi Takahara, **"Structure and Mechanical Properties of Natural Inorganic Nanofiller / Polymer Hybrids"** [PowerPoint] [PDF]

Dr. Takahara discussed a novel inorganic counterpart to carbon nanotubes that should be useful in dispersing nanotubes in polymer polar matrices without the need of surfactant additives. This type of nanotube ('imogolite') has an aluminum silicate composition and has molecular dimensions comparable to single wall carbon nanotubes, and naturally occurs in certain volcanic ashes found near Kyushu University. The environmentally friendly nature of this nanofiller and advantages for chemical functionalization were emphasized. After the extraction of the imogolite from volcanic ash was discussed, the properties were characterized by a variety of techniques (TEM, AFM, wide angle x-ray diffraction) and a tendency towards gel formation was observed. The functionalization of the imogolite was characterized though the adhesive force with an AFM cantilever tip and it was shown that the functionalized imogolite could be dispersed in an organic solvent (hexane). Films of PVA and PMMA and imogolite were prepared and the viscoelastic properties were characterized. Modified imogolite was also dispersed in PMMA and formed fibrous network of gelling nanotubes within the polymer matrix. Notably the transparency of the PMMA was not sacrificed for these nanotube additives. This could be important for applications where carbon nanotubes have a negative impact on appearance because of the characteristic black color of the filled polymers. Finally, clay-filled polymer (nylon) composites and the fatigue and mechanical properties of these materials were considered. The resulting materials are excellent in comparison to glass-fiber reinforced nylon.

A. Takahara

Structure and Mechanical Properties of Natural Inorganic Nanofiller/Polymer Hybrids

Atsushi Takahara
Institute for Fundamental Research of Organic Chemistry,
Kyushu University, FUKUOKA, JAPAN

Coworkers
K. YAMAMOTO, R. MATSUNO, H. OTSUKA, S.-I. WADA*,
A. YAMASHITA, T. KAJIYAMA

A. Takahara

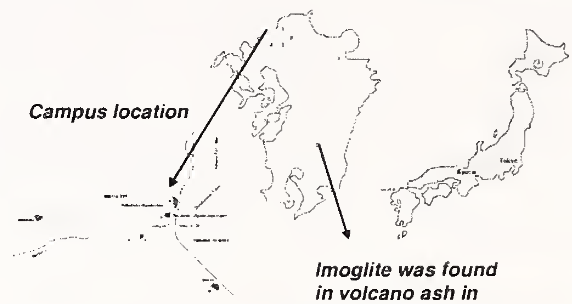

A. Takahara

Content

- Characterization of natural nanofiber "Imogolite"
- Surface modification of natural nanofiber "Imogolite"
  Chem. Lett., 1162(2001)
- Preparation of novel polymer nanohybrid from natural nanofiber "Imogolite"
  J. Adhesion, (2002).
- Fatigue behavior of nylon clay hybrid based on dynamic viscoelastic measurement during the fatigue process
  Composite Interfaces, 6, 247(1999).

A. Takahara

What is Imogolite?

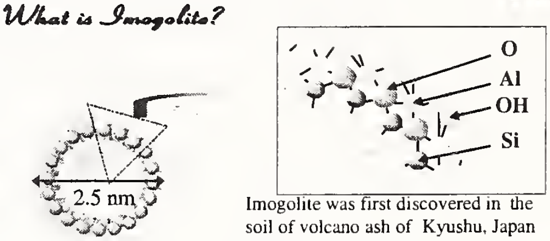

Imogolite was first discovered in the soil of volcano ash of Kyushu, Japan in 1962.

Characteristics of imogolite

- Nanotube with an external diameter of 2.5 nm and length in the range of several 100nm to several μm.
- Fibril formation in acidic condition.

A. Takahara

Nanofillers

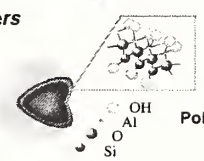

Polar surface

Diameter□3-5 nm
Allophane □1-2SIO$_2$□Al$_2$O$_3$□nH$_2$O□

Diameter 2.5 nm
Imogolite□SiO$_2$□Al$_2$O$_3$□nH$_2$O□

Non-polar surface

Diameter 0.71 nm
Fullerene.C60

Diameter ca.1 nm
Carbon.nanotube

A. Takahara

Nanofiller + **Polymer matrix** → **Nanocomposite**

Imogolite as a nanofiller

Extremely high aspect ratio of imogolite
- Imogolite forms space filling gel at the concentration of 0.2wt%
- Improve mechanical, thermal,flame - retardant, barrier properties

Chemical modification of Al-OH group of the external surface of imogolite
- Control interaction between imogolite and matrix polymer

Imogolite retain water in soil
- Environmentally benign nanocomposite "Green Nanohybrid" can be realized.

Purpose
Prepare novel (natural nanofiller /inorganic) nanohybrids

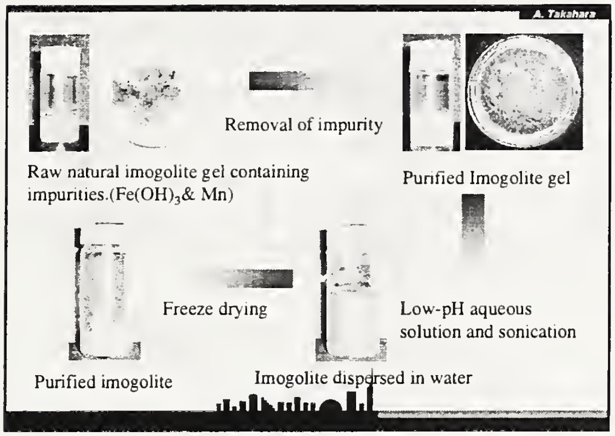
A. Takahara
Removal of impurity
Raw natural imogolite gel containing impurities.(Fe(OH)3& Mn)
Purified Imogolite gel
Freeze drying
Low-pH aqueous solution and sonication
Purified imogolite
Imogolite dispersed in water

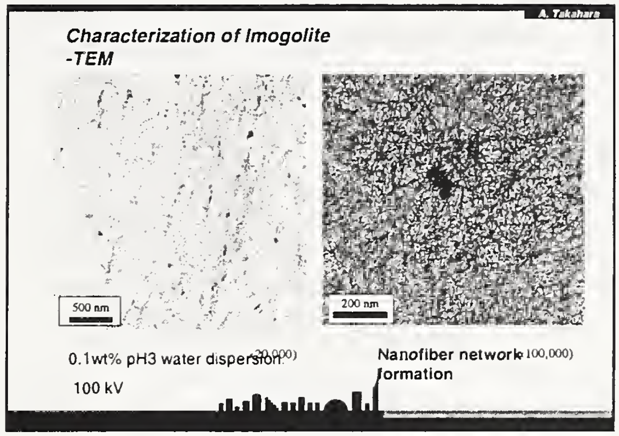
A. Takahara
Characterization of Imogolite -TEM
500 nm
200 nm
0.1wt% pH3 water dispersion
100 kV
Nanofiber network formation

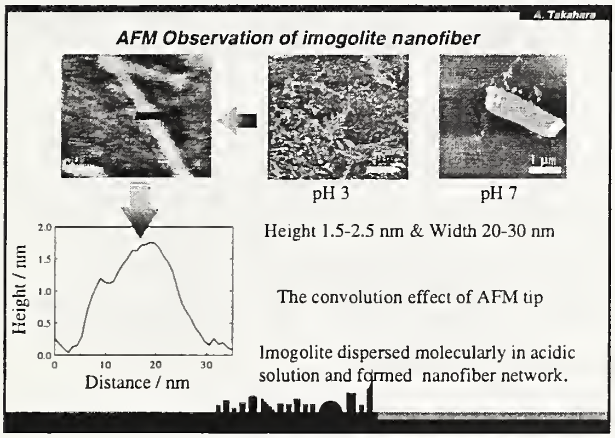
A. Takahara
AFM Observation of imogolite nanofiber
1 μm
pH 3
pH 7
Height / nm
Distance / nm
Height 1.5-2.5 nm & Width 20-30 nm
The convolution effect of AFM tip
Imogolite dispersed molecularly in acidic solution and formed nanofiber network.

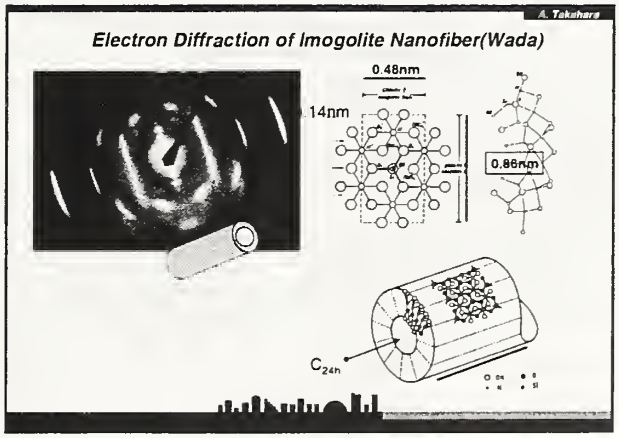
A. Takahara
Electron Diffraction of Imogolite Nanofiber(Wada)
0.48nm
14nm
0.86nm
C24h

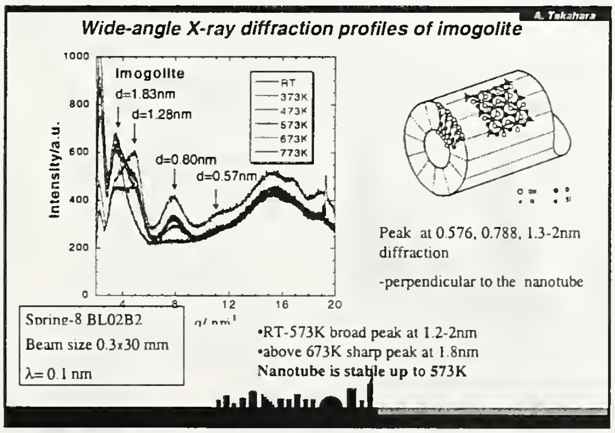
A. Takahara
Wide-angle X-ray diffraction profiles of imogolite
Imogolite
d=1.83nm
d=1.28nm
d=0.80nm
d=0.57nm
RT
373K
473K
573K
673K
773K
Intensity/a.u.
Peak at 0.576, 0.788, 1.3-2nm diffraction
-perpendicular to the nanotube
Spring-8 BL02B2
Beam size 0.3x30 mm
λ= 0.1 nm
•RT-573K broad peak at 1.2-2nm
•above 673K sharp peak at 1.8nm
Nanotube is stable up to 573K

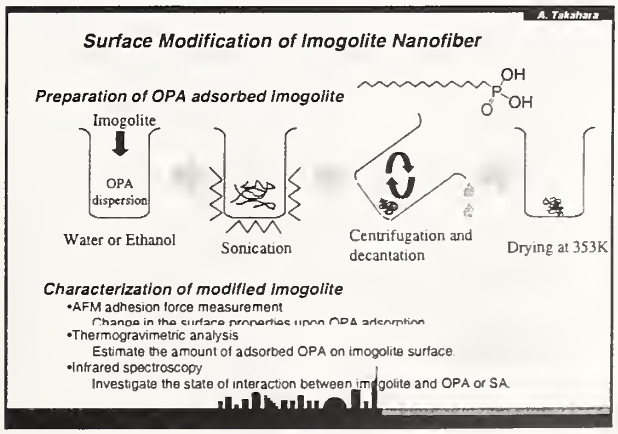
A. Takahara
Surface Modification of Imogolite Nanofiber
Preparation of OPA adsorbed imogolite
OH
OH
Imogolite
OPA dispersion
Water or Ethanol
Sonication
Centrifugation and decantation
Drying at 353K
Characterization of modified imogolite
•AFM adhesion force measurement
Change in the surface properties upon OPA adsorption
•Thermogravimetric analysis
Estimate the amount of adsorbed OPA on imogolite surface
•Infrared spectroscopy
Investigate the state of interaction between imogolite and OPA or SA

A. Takahara

Adsorption of OPA and SA on surface of imogolite

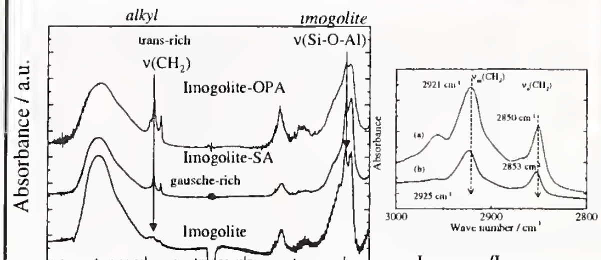

$I_{\nu(Si\text{-}O\text{-}Al)}/I_{\nu(CH_2)}$

R-PO(OH)$_2$ > R-COOH
[OPA] [SA]

Sample.imogolite OPA and SA adsorbed from ethanol solution

A. Takahara

TGA
-Evaluation of amount of adsobed OPA

Effect of water on adsorption of OPA on surface of imogolite

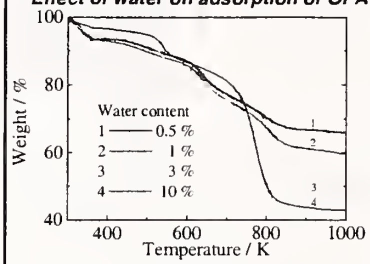

Water content ↑

Amount of adsorption ↑

Water influences the adsorption behavior of OPA onto imogolite.

Samples : Imogolite:OPA=1:2(w/w) from water and ethanol mixture solution.

A. Takahara

Concentration dependence of amount of adsorption of OPA on surface of imogolite

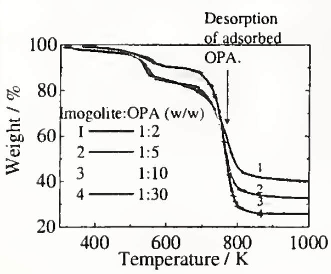

Imo:OPA	Ads.OPA/ Imo	Ads.OPA/ Water
1:2	0.89	3.15
1:5	1.29	3.77
1:10	1.68	6.33
1:30	2.07	12.8

Amount of adsorbed OPA on imogolite increased with an increase in relative amount of OPA.

Samples : Imogolite:OPA=1:2(w/w) from water and ethanol (2:3v/v) mixture solution.

A. Takahara

IR spectra of imogolite after desorption of OPA

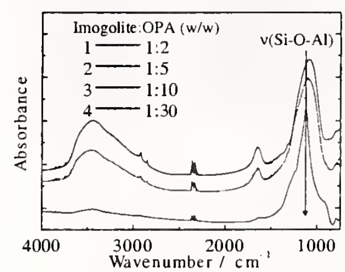

OPA adsorbed imogolite

Heating above decomposition temperature of OPA

ν(CH$_2$) peak decreased
ν(Si-O-Al) peak shifted

OPA desorbed

Presence of Imogolite

Samples : Imogolite:OPA from water and ethanol (2:3v/v) mixture solution. Heat upto 1273K

A. Takahara

Evidence of OPA adsorption onto imogolite
-Evaluation of adhesion force between cantilever tip and surface of imogolite

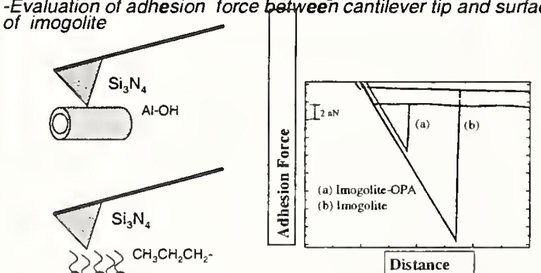

Force-distance curve

A. Takahara

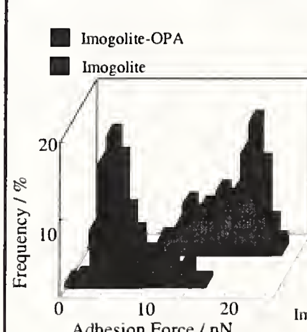

Samples imogolite:OPA=1:5 (w/w) from ethanol and water solution

Lower adhesion force of OPA adsorbed imogolite than that of imogolite.

Formation of alkyl layer on the surface of imogolite after exposure to OPA solution.

Imogolite can be dispersed in organic solvent.

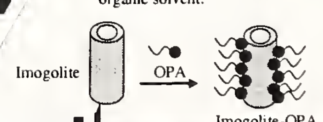

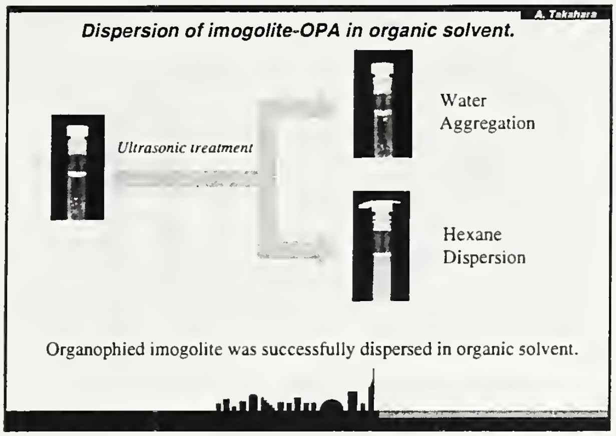
A. Takahara
Dispersion of imogolite-OPA in organic solvent.
Ultrasonic treatment
Water
Aggregation
Hexane
Dispersion
Organophied imogolite was successfully dispersed in organic solvent.

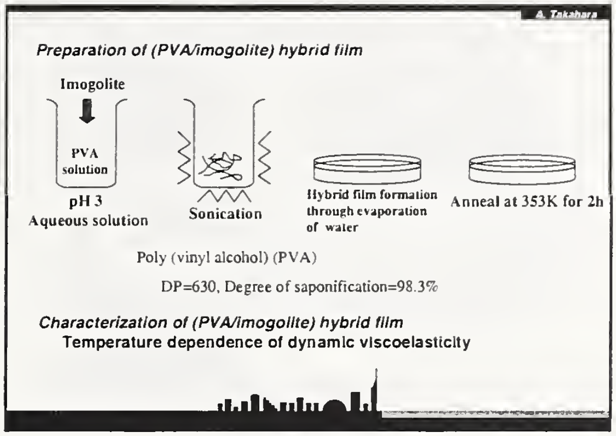
A. Takahara
Preparation of (PVA/imogolite) hybrid film
Imogolite
PVA solution
pH 3
Aqueous solution
Sonication
Hybrid film formation through evaporation of water
Anneal at 353K for 2h
Poly (vinyl alcohol) (PVA)
DP=630, Degree of saponification=98.3%
Characterization of (PVA/imogolite) hybrid film
Temperature dependence of dynamic viscoelasticity

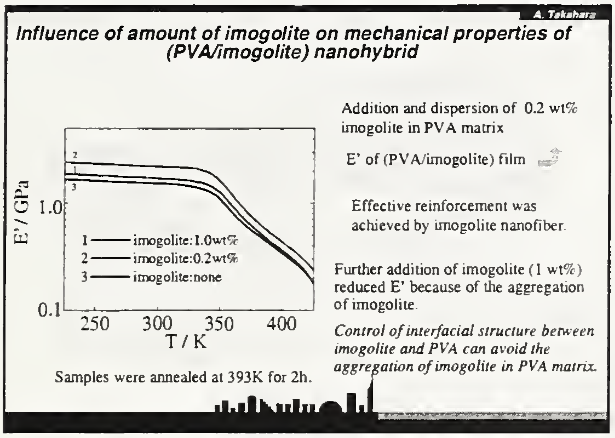
A. Takahara
Influence of amount of imogolite on mechanical properties of (PVA/imogolite) nanohybrid
E' / GPa
1.0
0.1
250
300
350
400
T / K
1 imogolite:1.0wt%
2 imogolite:0.2wt%
3 imogolite:none
Samples were annealed at 393K for 2h.
Addition and dispersion of 0.2 wt% imogolite in PVA matrix
E' of (PVA/imogolite) film
Effective reinforcement was achieved by imogolite nanofiber.
Further addition of imogolite (1 wt%) reduced E' because of the aggregation of imogolite.
Control of interfacial structure between imogolite and PVA can avoid the aggregation of imogolite in PVA matrix.

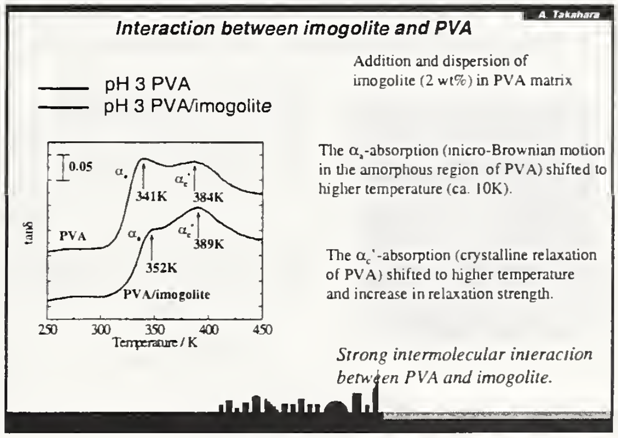
A. Takahara
Interaction between imogolite and PVA
pH 3 PVA
pH 3 PVA/imogolite
tanδ
0.05
341K
384K
PVA
352K
389K
PVA/imogolite
250
300
350
400
450
Temperature / K
Addition and dispersion of imogolite (2 wt%) in PVA matrix
The α_a-absorption (micro-Brownian motion in the amorphous region of PVA) shifted to higher temperature (ca. 10K).
The α_c'-absorption (crystalline relaxation of PVA) shifted to higher temperature and increase in relaxation strength.
Strong intermolecular interaction between PVA and imogolite.

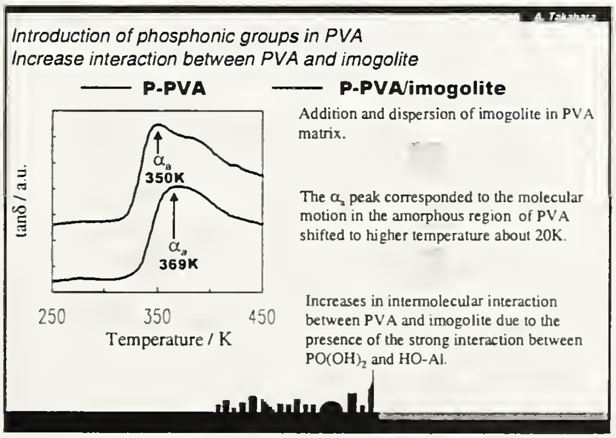
A. Takahara
Introduction of phosphonic groups in PVA
Increase interaction between PVA and imogolite
P-PVA
P-PVA/imogolite
tanδ / a.u.
α_a
350K
α_a
369K
250
350
450
Temperature / K
Addition and dispersion of imogolite in PVA matrix.
The α_a peak corresponded to the molecular motion in the amorphous region of PVA shifted to higher temperature about 20K.
Increases in intermolecular interaction between PVA and imogolite due to the presence of the strong interaction between $PO(OH)_2$ and HO-Al.

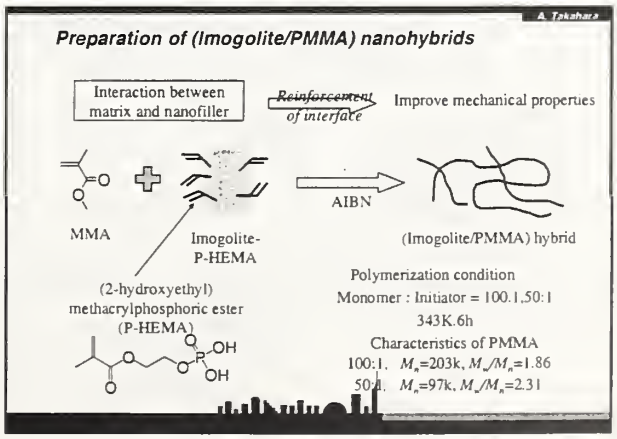
A. Takahara
Preparation of (Imogolite/PMMA) nanohybrids
Interaction between matrix and nanofiller
Reinforcement of interface
Improve mechanical properties
MMA
Imogolite-P-HEMA
AIBN
(Imogolite/PMMA) hybrid
(2-hydroxyethyl) methacrylphosphoric ester (P-HEMA)
Polymerization condition
Monomer : Initiator = 100:1, 50:1
343K, 6h
Characteristics of PMMA
100:1, M_n=203k, M_w/M_n=1.86
50:1, M_n=97k, M_w/M_n=2.31

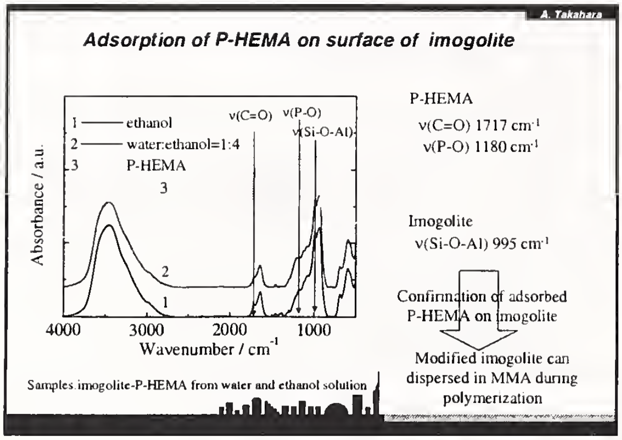
A. Takahara
Adsorption of P-HEMA on surface of imogolite
1 ethanol
2 water:ethanol=1:4
3 P-HEMA
v(C=O)
v(P-O)
v(Si-O-Al)
Absorbance / a.u.
4000 3000 2000 1000
Wavenumber / cm-1
Samples imogolite-P-HEMA from water and ethanol solution
P-HEMA
v(C=O) 1717 cm-1
v(P-O) 1180 cm-1
Imogolite
v(Si-O-Al) 995 cm-1
Confirmation of adsorbed P-HEMA on imogolite
Modified imogolite can dispersed in MMA during polymerization

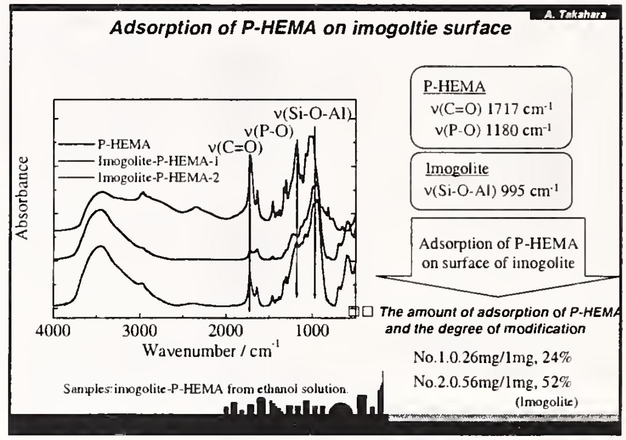
A. Takahara
Adsorption of P-HEMA on imogoltie surface
P-HEMA
Imogolite-P-HEMA-1
Imogolite-P-HEMA-2
v(Si-O-Al)
v(P-O)
v(C=O)
Absorbance
4000 3000 2000 1000
Wavenumber / cm-1
Samples: imogolite-P-HEMA from ethanol solution
P-HEMA
v(C=O) 1717 cm-1
v(P-O) 1180 cm-1
Imogolite
v(Si-O-Al) 995 cm-1
Adsorption of P-HEMA on surface of imogolite
The amount of adsorption of P-HEMA and the degree of modification
No.1.0.26mg/1mg, 24%
No.2.0.56mg/1mg, 52%
(Imogolite)

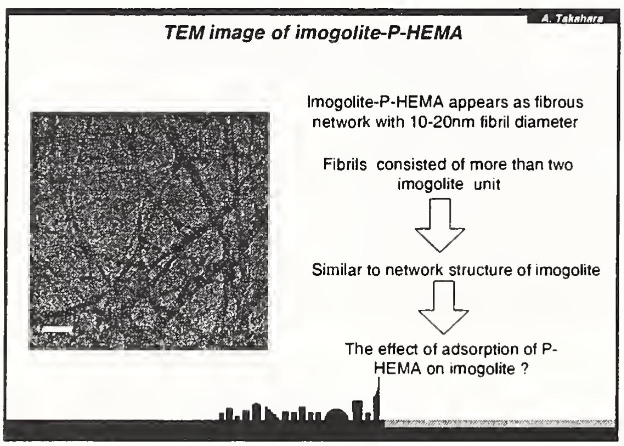
A. Takahara
TEM image of imogolite-P-HEMA
Imogolite-P-HEMA appears as fibrous network with 10-20nm fibril diameter
Fibrils consisted of more than two imogolite unit
Similar to network structure of imogolite
The effect of adsorption of P-HEMA on imogolite ?

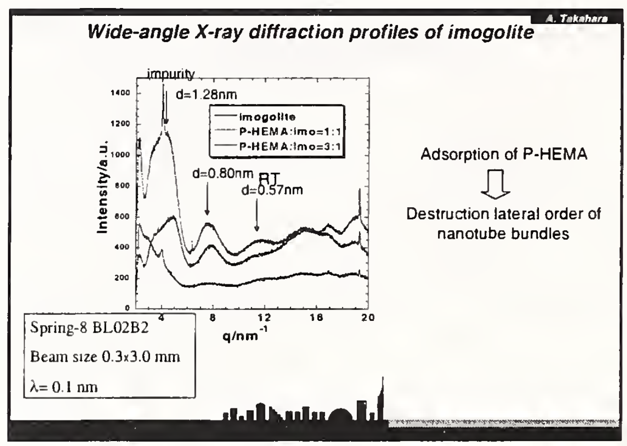
A. Takahara
Wide-angle X-ray diffraction profiles of imogolite
impurity
d=1.28nm
imogolite
P-HEMA:Imo=1:1
P-HEMA:Imo=3:1
d=0.80nm
RT
d=0.57nm
Intensity/a.u.
q/nm-1
Spring-8 BL02B2
Beam size 0.3x3.0 mm
λ= 0.1 nm
Adsorption of P-HEMA
Destruction lateral order of nanotube bundles

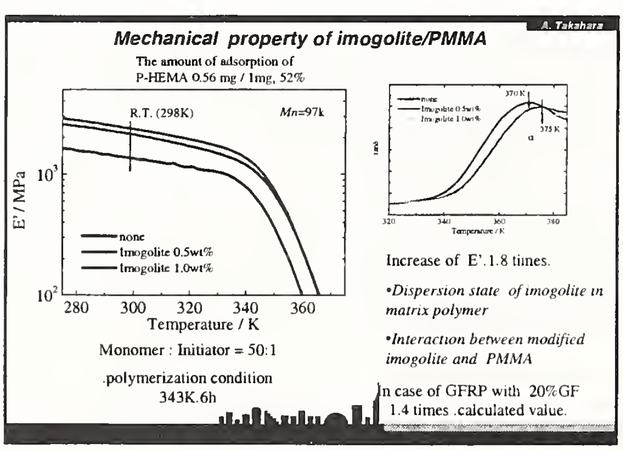
A. Takahara
Mechanical property of imogolite/PMMA
The amount of adsorption of P-HEMA 0.56 mg / 1mg, 52%
R.T. (298K)
Mn=97k
none
Imogolite 0.5wt%
Imogolite 1.0wt%
E' / MPa
280 300 320 340 360
Temperature / K
Monomer : Initiator = 50:1
.polymerization condition 343K.6h
370 K
373 K
Increase of E'.1.8 times.
•Dispersion state of imogolite in matrix polymer
•Interaction between modified imogolite and PMMA
In case of GFRP with 20%GF 1.4 times .calculated value.

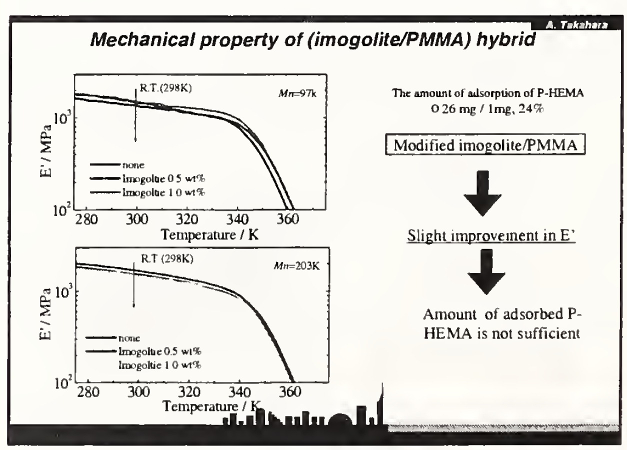
A. Takahara
Mechanical property of (imogolite/PMMA) hybrid
R.T.(298K)
Mn=97k
none
Imogolite 0.5 wt%
Imogolite 1.0 wt%
E' / MPa
280 300 320 340 360
Temperature / K
R.T (298K)
Mn=203K
The amount of adsorption of P-HEMA 0.26 mg / 1mg, 24%
Modified imogolite/PMMA
Slight improvement in E'
Amount of adsorbed P-HEMA is not sufficient

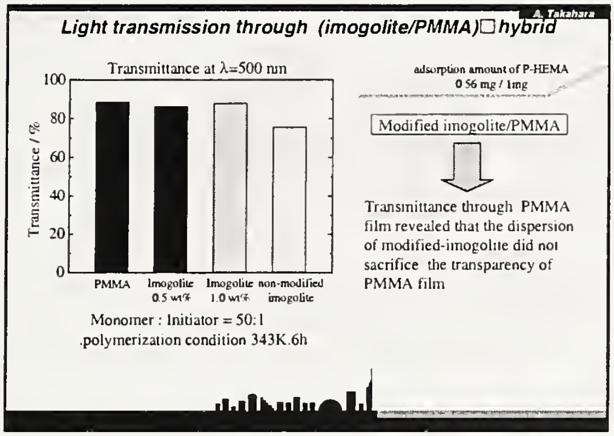

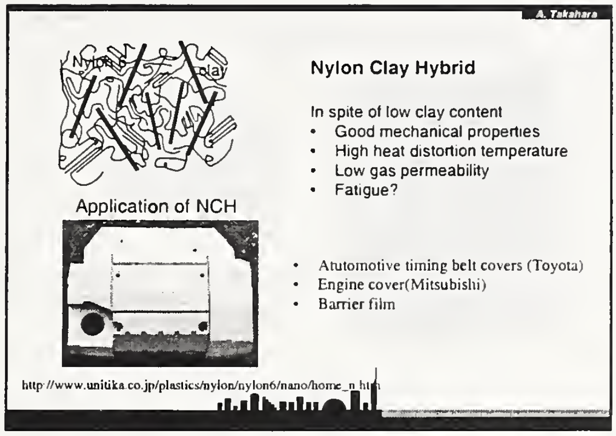

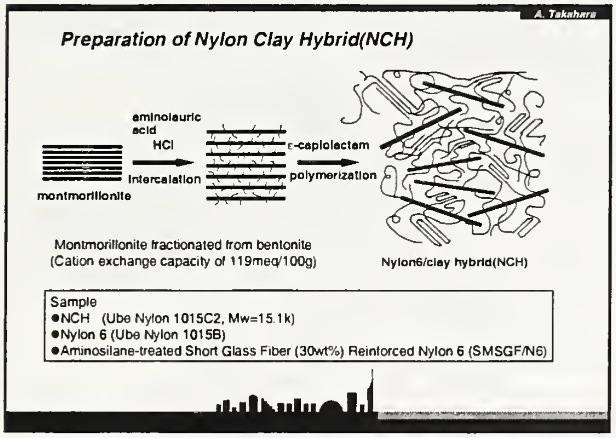

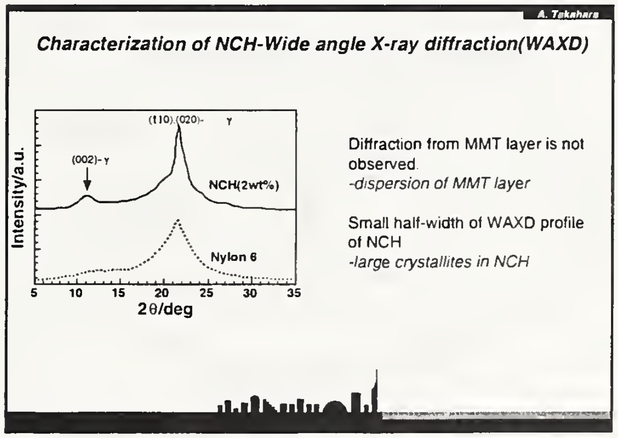

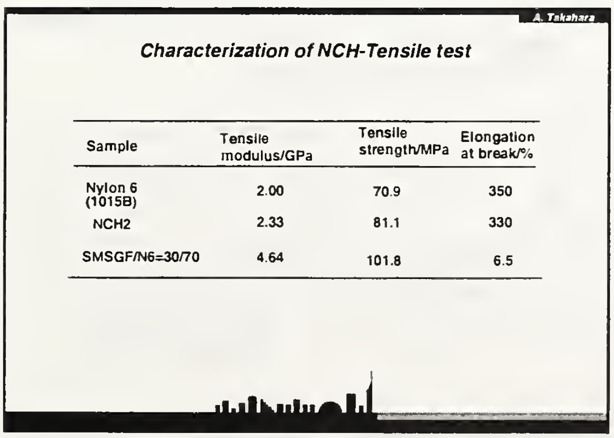

Sample	Tensile modulus/GPa	Tensile strength/MPa	Elongation at break/%
Nylon 6 (1015B)	2.00	70.9	350
NCH2	2.33	81.1	330
SMSGF/N6=30/70	4.64	101.8	6.5

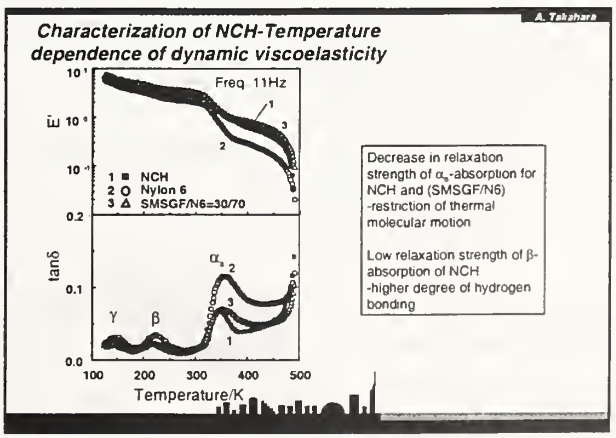

A. Takahara

Characterization of NCH-TEM

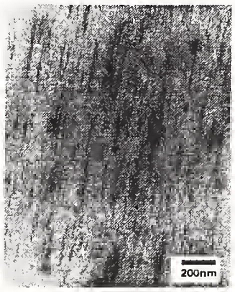

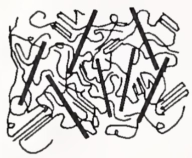

- Finely dispersed silicate layer
- Orientation of silicate layer along direction of flow

A. Takahara

Fatigue Test

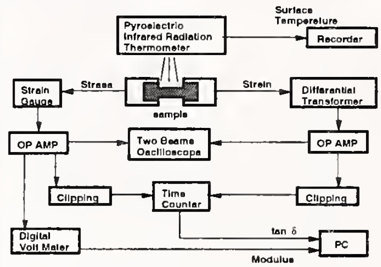

- T=303K
- f=6.91Hz
- Tension-compression
- Strain control

Measure dynamic viscoelasticity and surface temperature during the cyclic fatigue

A. Takahara, K. Yamada, T. Kajiyama, M. Takayanagi, J. Appl. Polym. Sci., 25, 597(1980).

A. Takahara

Relationship between strain amplitude and fatigue lifetime for NCH, Nylon 6 and SMSGF/N6

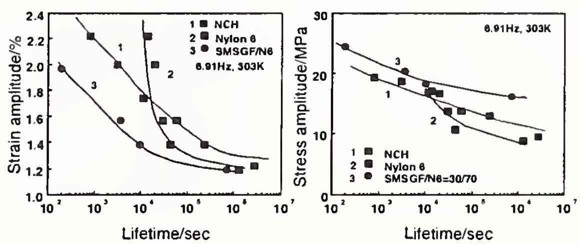

Excellent fatigue strength for NCH

A. Takahara

Variation of E' and surface temperature increase, θ for NCH with time during the fatigue process

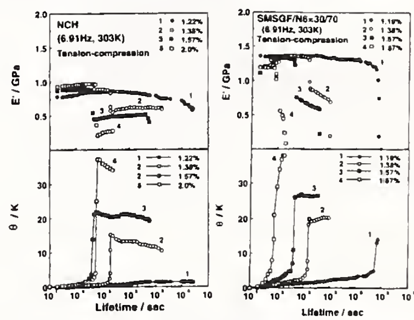

- Heat generation under cyclic fatigue SMSGF/N6 > NCH
- Strain concentration in matrix nylon6

A. Takahara

Fatigue Criterion based on Viscoelastic Energy Loss

Surface temperature increase is smaller than that expected from the viscoelastic energy loss. Some part of the viscoelastic energy did not appear as heat but consumed for irreversible structural change.

$$H = \chi H + (1-\chi)H$$

$$\frac{dT_s}{dt} = \frac{1}{\rho c}\left[\chi\pi f \varepsilon_d^2 E'' - \kappa(T_s - T_0)\right]$$

H

□

$$H_{s,av} = \frac{1}{t_f}\int_0^{t_f}(1-\chi)H\,dt$$

Fatigue failure criterion

$$(H_{s,av} - H_0)t_f = C$$

Evaluation of heat transfer coefficient, κ

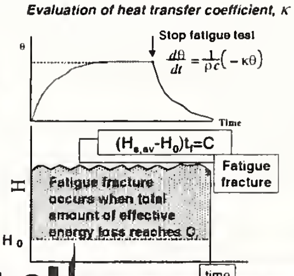

A. Takahara

Relationship between $H_{s,av}$ and lifetime for NCH, Nylon 6 and SMSGF/N6 composite.

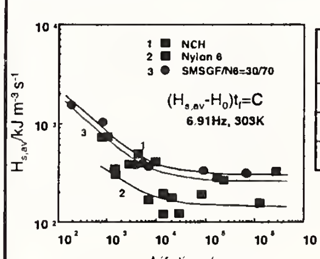

Material	Density /10^3kg m^{-3}	Tensile strength/ MPa	C /10^2MJ m^{-3}
NCH	1.15	81	6.5
Nylon 6	1.14	71	4.1
SMSFG/N6	1.36	102	3.6

NCH showed fatigue strength being superior to nylon6 and glass-fiber reinforced nylon 6 -no macroscopic interface

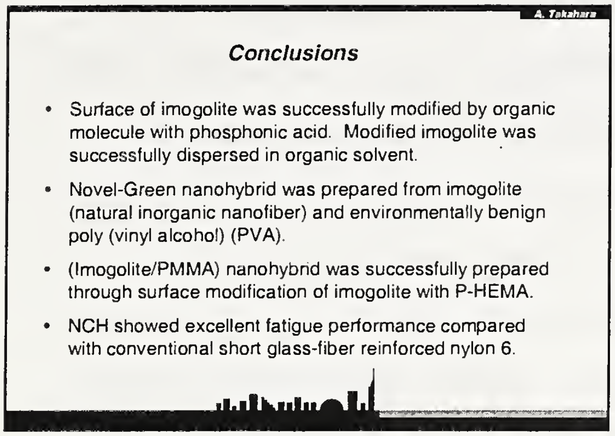
A. Takahara
Conclusions
• Surface of imogolite was successfully modified by organic molecule with phosphonic acid. Modified imogolite was successfully dispersed in organic solvent.
• Novel-Green nanohybrid was prepared from imogolite (natural inorganic nanofiber) and environmentally benign poly (vinyl alcohol) (PVA).
• (Imogolite/PMMA) nanohybrid was successfully prepared through surface modification of imogolite with P-HEMA.
• NCH showed excellent fatigue performance compared with conventional short glass-fiber reinforced nylon 6.

7) R. A. Vaia, **"Impact and control of Ultrastructure (Meso) in Polymer Nanocomposites"** [PowerPoint] [PDF]

Dr. Vaia emphasized the balance between cost and added value in filled materials that drive the development of these materials at the Air Force Research Laboratory and elsewhere. After giving a valuable summary of opportunity areas for development of nanocomposites in aerospace and the challenges for understanding structure-property relationships in these systems, he summarized some experience of filled systems in relation to self-passivation and erosion in aggressive environments. Tools found helpful in characterizing these systems are summarized (SAXS, WAXS). Challenges in understanding filled rubbers and parallels of the filled systems to complex liquids were also considered. It was suggested that many useful properties of these nanocoposites could be obtained by exploiting the high particle anisotropy and field structuring and preliminary work on this topic (e.g., orientation of clay particles with an E-field).

Air Force Research Laboratory — Nanostructured Materials

Impact and Control of Ultrastructure (Meso) in Polymer Nanocomposites

R. A. Vaia, H. Koerner, R. Reuter, G. Price
Air Force Research Laboratory, Polymer Branch
WPAFB, OH, 45433-7750

Air Force Office of Scientific Research
AFRL Materials and Manufacturing Directorate

Outline

Air Force Research Laboratory — Nanostructured Materials

- Introduction & Drivers
- MesoScale Morphology
  - Morphology and Properties
  - Framework
  - Morphology Control
- Summary

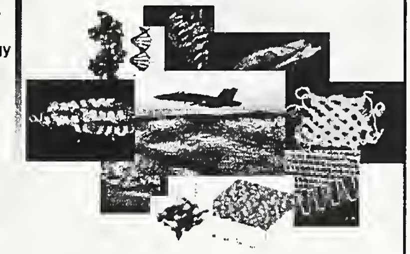

Organic-Inorganic Nanostructured Materials

Air Force Research Laboratory — Nanostructured Materials

Objective:

maintain processibility and cost
modest mechanical enhancements / weight savings
value-added functionality

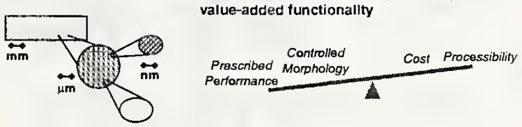

Approaches:

A. Exfoliation
B. In-situ formation (templating)
C. Molecular incorporation

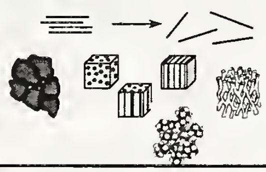

Polymer NanoComposites for Aerospace

Air Force Research Laboratory — Nanostructured Materials

Conductive Plastics electrical - permittivity – stiffness / ductility - processing

Carbon NT
Metal NP
Dielectric Oxide NP

Signal Wires
Static Discharge
Platforms
Flex. Packaging

Photonics NLO – refractive index modulation – PL – lasing - processing

QDs
Hybrid NP
Oxide NP

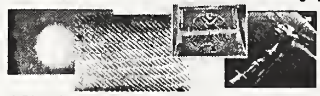

Sensors (bio)
Sources
Flex. Packaging
Optical Elements

MultiFunctional Plastics mechanicals – self-passivation – shape memory – barrier - processing

Layered Silicates
Carbon NT

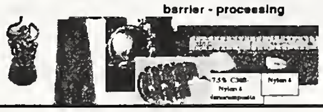

Propulsion
Space Deployables
Tanks
Composites
Tires

Fundamental Challenge: Structure-Property-Processing Relationships

Air Force Research Laboratory — Nanostructured Materials

Multi-Phase Systems: $R_{Soft\ (Polymer)} \sim R_{Hard\ (Nano\text{-}element)}$

$\alpha >> 1$

DESIGN

- **Properties of nanoelements:** inorganic and interfacial polymer; relative contribution to composite properties
- **Properties of polymer:** semicrystalline; network topology — amorphous
- **Interface:** tailoring and responsive — strength v processibility trade-off
- **Properties of composite:** general v system specific

STRUCTURE

- **Thermodynamics:** mean field v site specific — experimental verification
- **De-aggregation:** mechanisms and relation to synthesis and processing
- **Process-morphology relationships:** block copolymer/LC parallel — multi-length scale control; 'defect' control
- **Engineered mophology:** beyond 'dispersion'

PERFORMANCE

- **Mechanics:** continuum v. molecular; experimental database — residual stress; synergism and cooperativity

Outline

Air Force Research Laboratory — Nanostructured Materials

- Introduction & Drivers
- MesoScale Morphology
  - Morphology and Properties
    - Self-Passivation
    - Mechanicals
  - Framework
  - Morphology Control
- Summary

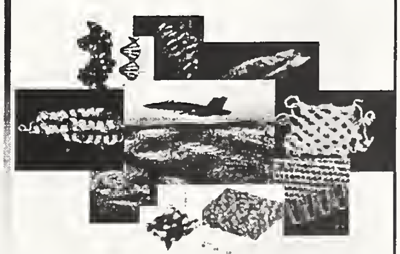

1

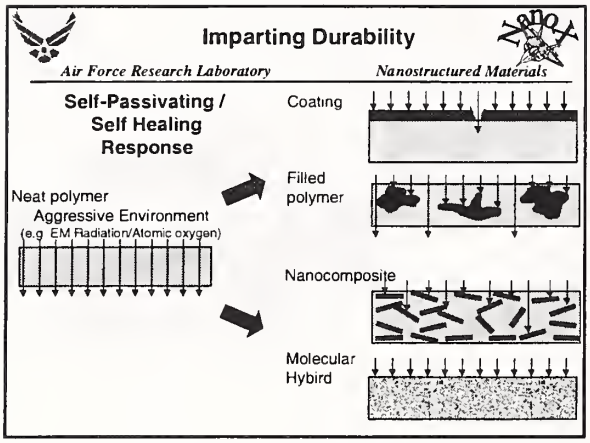
Imparting Durability
Air Force Research Laboratory
Nanostructured Materials
Self-Passivating / Self Healing Response
Neat polymer
Aggressive Environment
(e.g. EM Radiation/Atomic oxygen)
Coating
Filled polymer
Nanocomposite
Molecular Hybird

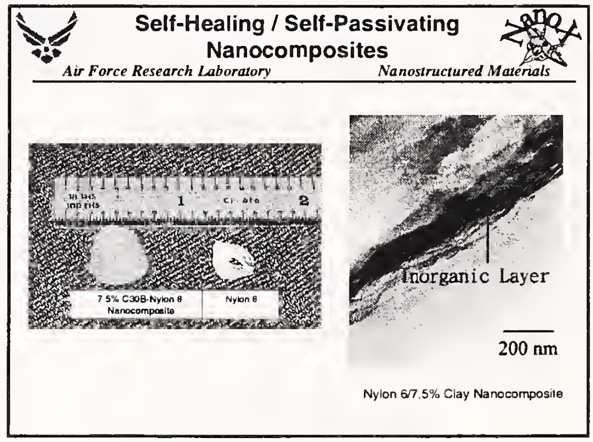
Self-Healing / Self-Passivating Nanocomposites
Air Force Research Laboratory
Nanostructured Materials
7.5% C30B-Nylon 6 Nanocomposite
Nylon 6
Inorganic Layer
200 nm
Nylon 6/7.5% Clay Nanocomposite

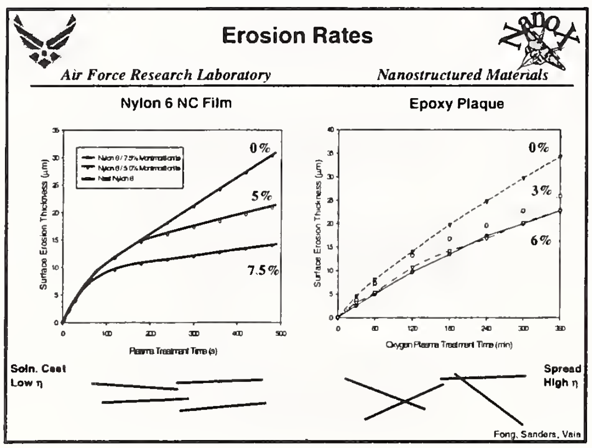
Erosion Rates
Air Force Research Laboratory
Nanostructured Materials
Nylon 6 NC Film
Epoxy Plaque
Surface Erosion Thickness (μm)
0%
5%
7.5%
Plasma Treatment Time (s)
3%
6%
Oxygen Plasma Treatment Time (min)
Soln. Cast
Low η
Spread
High η
Fong, Sanders, Vaia

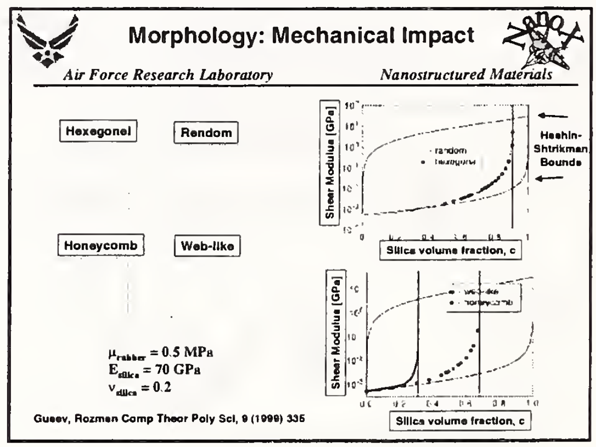
Morphology: Mechanical Impact
Air Force Research Laboratory
Nanostructured Materials
Hexagonal
Random
Honeycomb
Web-like
Shear Modulus [GPa]
Hashin-Shtrikman Bounds
Silica volume fraction, c
μrubber = 0.5 MPa
Esilica = 70 GPa
νsilica = 0.2
Gusev, Rozman Comp Theor Poly Sci, 9 (1999) 335

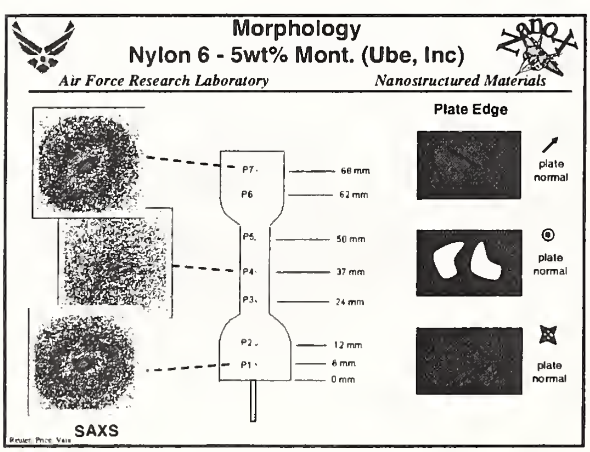
Morphology
Nylon 6 - 5wt% Mont. (Ube, Inc)
Air Force Research Laboratory
Nanostructured Materials
Plate Edge
P7
P6
P5
P4
P3
P2
P1
68 mm
62 mm
50 mm
37 mm
24 mm
12 mm
6 mm
0 mm
plate normal
plate normal
plate normal
SAXS

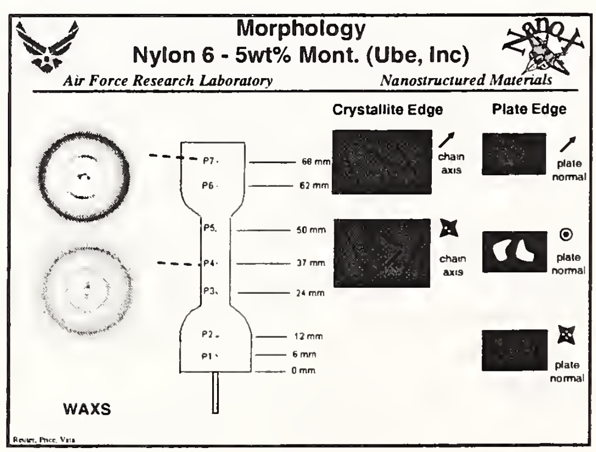
Morphology
Nylon 6 - 5wt% Mont. (Ube, Inc)
Air Force Research Laboratory
Nanostructured Materials
Crystallite Edge
Plate Edge
P7
P6
P5
P4
P3
P2
P1
68 mm
62 mm
50 mm
37 mm
24 mm
12 mm
6 mm
0 mm
chain axis
chain axis
plate normal
plate normal
plate normal
WAXS

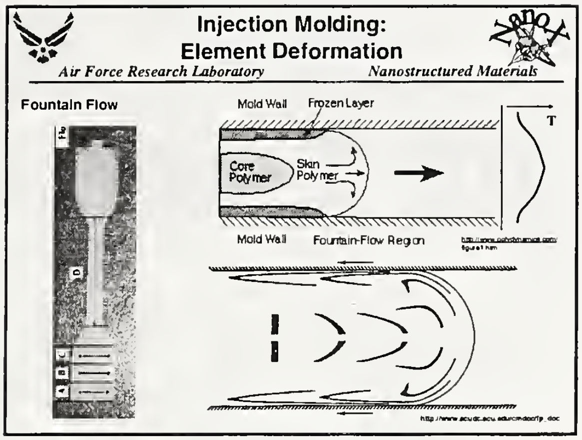
Injection Molding:
Element Deformation
Air Force Research Laboratory
Nanostructured Materials
Fountain Flow
Mold Wall
Frozen Layer
Core Polymer
Skin Polymer
T
Mold Wall
Fountain-Flow Region
D
A B C

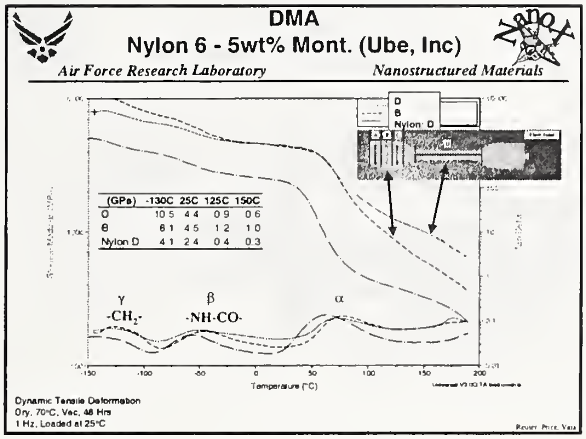
DMA
Nylon 6 - 5wt% Mont. (Ube, Inc)
Air Force Research Laboratory
Nanostructured Materials
D
B
Nylon: D
(GPa) -130C 25C 125C 150C
D 10.5 4.4 0.9 0.6
B 8.1 4.5 1.2 1.0
Nylon D 4.1 2.4 0.4 0.3
γ
-CH₂-
β
-NH-CO-
α
Temperature (°C)
Dynamic Tensile Deformation
Dry, 70°C, Vac, 48 Hrs
1 Hz, Loaded at 25°C
Reuer, Price, Vaia

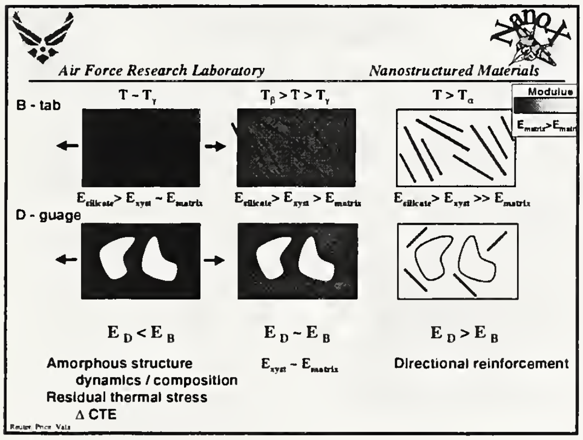
Air Force Research Laboratory
Nanostructured Materials
B - tab
$T \sim T_\gamma$
$T_\beta > T > T_\gamma$
$T > T_\alpha$
Modulus
$E_{matrix} > E_{matrix}$
$E_{silicate} > E_{xyst} \sim E_{matrix}$
$E_{silicate} > E_{xyst} > E_{matrix}$
$E_{silicate} > E_{xyst} >> E_{matrix}$
D - guage
$E_D < E_B$
$E_D \sim E_B$
$E_D > E_B$
Amorphous structure
dynamics / composition
Residual thermal stress
Δ CTE
$E_{xyst} \sim E_{matrix}$
Directional reinforcement
Reuer, Price, Vaia

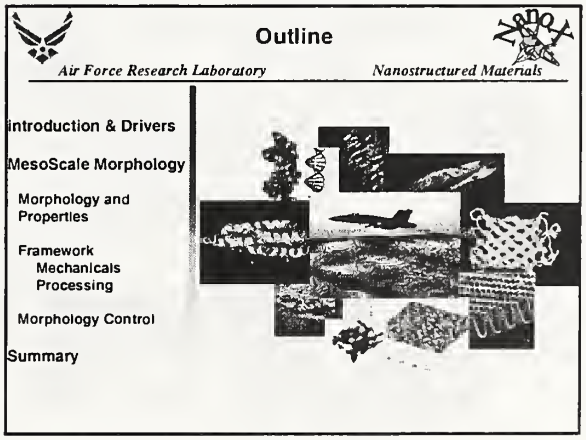
Outline
Air Force Research Laboratory
Nanostructured Materials
Introduction & Drivers
MesoScale Morphology
Morphology and Properties
Framework
Mechanicals
Processing
Morphology Control
Summary

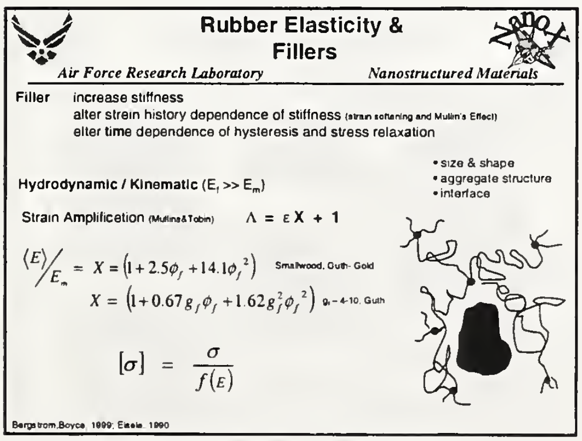
Rubber Elasticity & Fillers
Air Force Research Laboratory
Nanostructured Materials
Filler increase stiffness
alter strein history dependence of stiffness (strain softening and Mullin's Effect)
elter time dependence of hysteresis and stress relaxation
• size & shape
• aggregate structure
• interface
Hydrodynamic / Kinematic ($E_f >> E_m$)
Strain Amplification (Mullins&Tobin) $\Lambda = \varepsilon X + 1$
$\langle E \rangle / E_m = X = (1 + 2.5\phi_f + 14.1\phi_f^2)$ Smallwood, Guth- Gold
$X = (1 + 0.67 g_f \phi_f + 1.62 g_f^2 \phi_f^2)$ $g_f \sim 4$-10, Guth
$[\sigma] = \dfrac{\sigma}{f(E)}$
Bergstrom,Boyce, 1999; Eisele, 1990

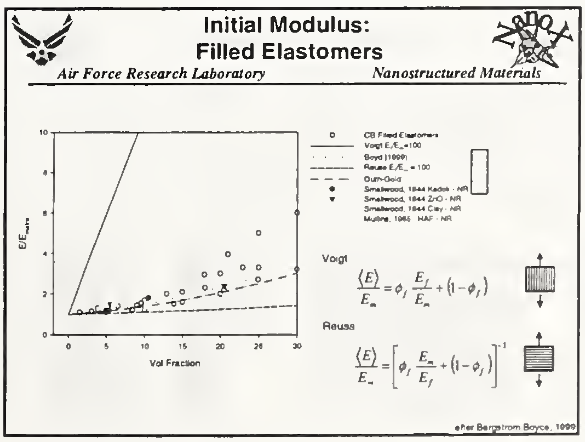
Initial Modulus:
Filled Elastomers
Air Force Research Laboratory
Nanostructured Materials
E/E_{matrix}
Vol Fraction
CB Filled Elastomers
Voigt E_f/E_m=100
Boyd (1999)
Reuss E_f/E_m = 100
Guth-Gold
Smallwood, 1944 Kaolin - NR
Smallwood, 1944 ZnO - NR
Smallwood, 1944 Clay - NR
Mullins, 1965 HAF - NR
Voigt
$\dfrac{\langle E \rangle}{E_m} = \phi_f \dfrac{E_f}{E_m} + (1 - \phi_f)$
Reuss
$\dfrac{\langle E \rangle}{E_m} = \left[\phi_f \dfrac{E_m}{E_f} + (1 - \phi_f) \right]^{-1}$
after Bergstrom Boyce, 1999

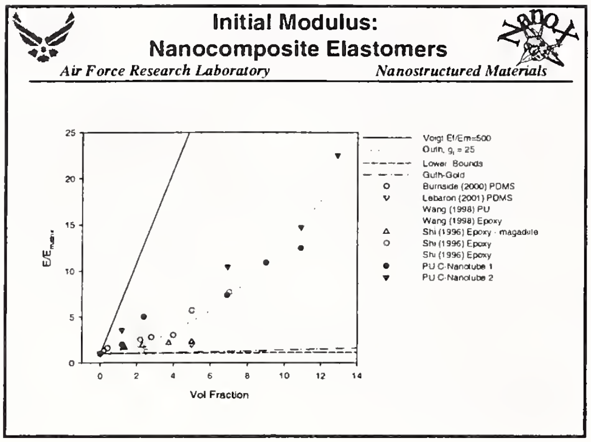
Initial Modulus:
Nanocomposite Elastomers
Air Force Research Laboratory
Nanostructured Materials
E/E_matrix
Vol Fraction
Voigt Ef/Em=500
Guth, g_f = 25
Lower Bounds
Guth-Gold
Burnside (2000) PDMS
Lebaron (2001) PDMS
Wang (1998) PU
Wang (1998) Epoxy
Shi (1996) Epoxy - magadiite
Shi (1996) Epoxy
Shi (1996) Epoxy
PU C-Nanotube 1
PU C-Nanotube 2

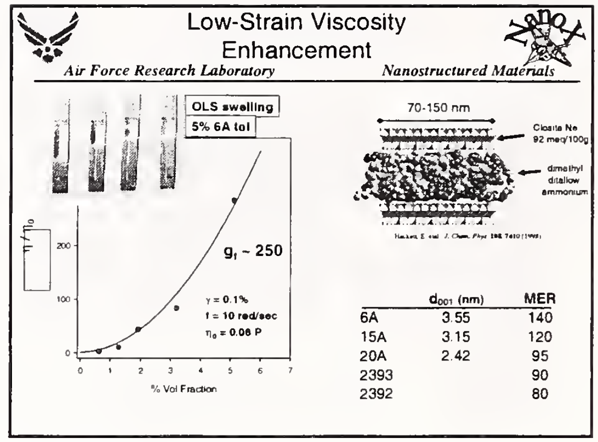
Low-Strain Viscosity
Enhancement
Air Force Research Laboratory
Nanostructured Materials
OLS swelling
5% 6A tol
70-150 nm
Cloisite Na
92 meq/100g
dimethyl ditallow ammonium
g_f ~ 250
γ = 0.1%
f = 10 rad/sec
η_0 = 0.06 P
% Vol Fraction
d_001 (nm) MER
6A 3.55 140
15A 3.15 120
20A 2.42 95
2393 90
2392 80

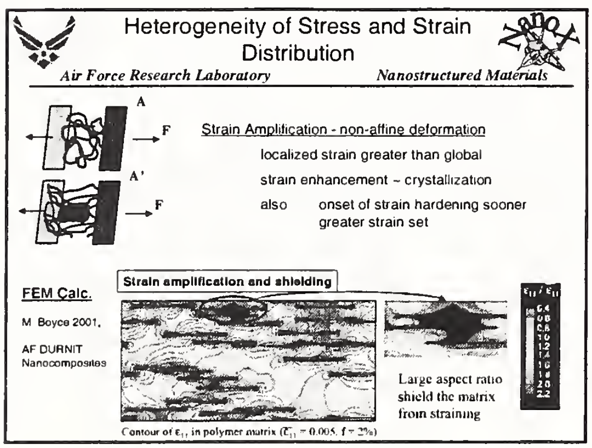
Heterogeneity of Stress and Strain
Distribution
Air Force Research Laboratory
Nanostructured Materials
A
F
A'
F
Strain Amplification - non-affine deformation
localized strain greater than global
strain enhancement ~ crystallization
also onset of strain hardening sooner
greater strain set
FEM Calc.
M Boyce 2001,
AF DURNIT
Nanocomposites
Strain amplification and shielding
Large aspect ratio
shield the matrix
from straining
Contour of ε11 in polymer matrix (ε̄11 = 0.005, f = 2%)

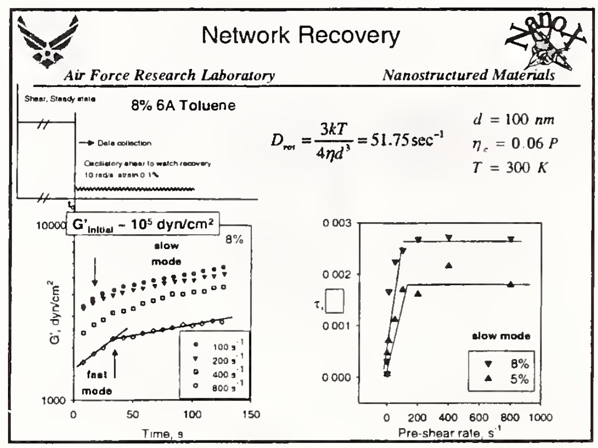
Network Recovery
Air Force Research Laboratory
Nanostructured Materials
Shear, Steady state
8% 6A Toluene
Data collection
Oscillatory shear to watch recovery
$D_{rot} = \frac{3kT}{4\eta d^3} = 51.75\,\mathrm{sec}^{-1}$
d = 100 nm
η_c = 0.06 P
T = 300 K
G'_initial ~ 10^5 dyn/cm^2
8%
slow mode
fast mode
G', dyn/cm^2
Time, s
slow mode
8%
5%
Pre-shear rate, s^-1

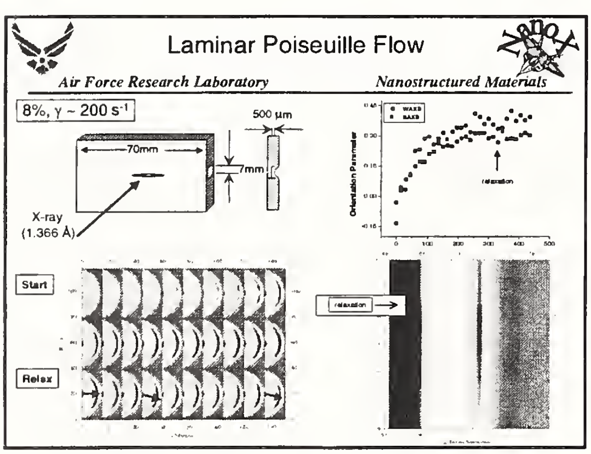
Laminar Poiseuille Flow
Air Force Research Laboratory
Nanostructured Materials
8%, γ ~ 200 s^-1
70mm
500 µm
7mm
X-ray
(1.366 Å)
WAXS
SAXS
Orientation Parameter
relaxation
Start
Relax
relaxation

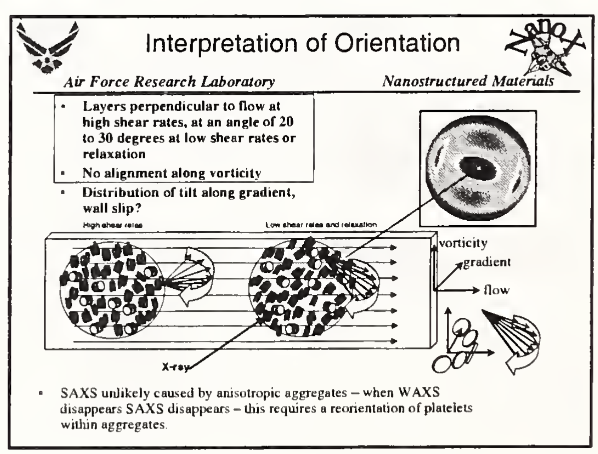
Interpretation of Orientation
Air Force Research Laboratory
Nanostructured Materials
• Layers perpendicular to flow at high shear rates, at an angle of 20 to 30 degrees at low shear rates or relaxation
• No alignment along vorticity
• Distribution of tilt along gradient, wall slip?
High shear rates
Low shear rates and relaxation
vorticity
gradient
flow
X-ray
• SAXS unlikely caused by anisotropic aggregates – when WAXS disappears SAXS disappears – this requires a reorientation of platelets within aggregates.

4

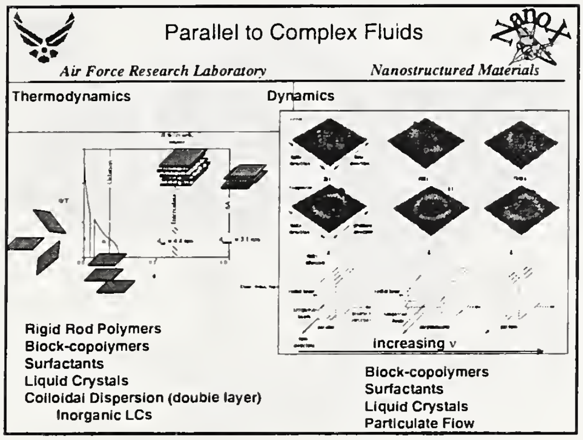

Parallel to Complex Fluids
Air Force Research Laboratory
Nanostructured Materials
Thermodynamics
Dynamics
increasing ν
Rigid Rod Polymers
Block-copolymers
Surfactants
Liquid Crystals
Colloidal Dispersion (double layer)
Inorganic LCs
Block-copolymers
Surfactants
Liquid Crystals
Particulate Flow

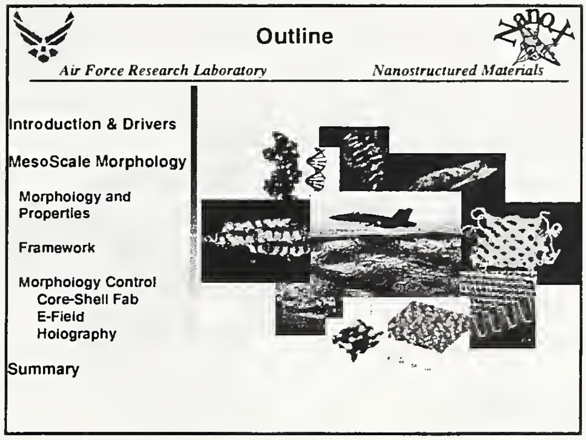

Outline
Air Force Research Laboratory
Nanostructured Materials
Introduction & Drivers
MesoScale Morphology
Morphology and Properties
Framework
Morphology Control
Core-Shell Fab
E-Field
Holography
Summary

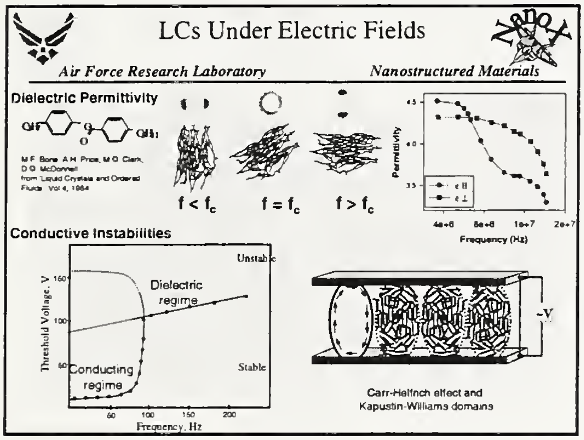

LCs Under Electric Fields
Air Force Research Laboratory
Nanostructured Materials
Dielectric Permittivity
f < fc
f = fc
f > fc
Permittivity
Frequency (Hz)
Conductive Instabilities
Threshold Voltage, V
Frequency, Hz
Dielectric regime
Conducting regime
Unstable
Stable
Carr-Helfrich effect and Kapustin-Williams domains

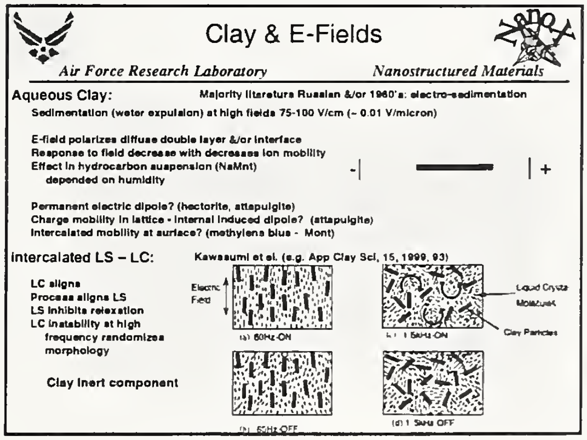

Clay & E-Fields
Air Force Research Laboratory
Nanostructured Materials
Aqueous Clay:
Majority literature Russian &/or 1960's: electro-sedimentation
Sedimentation (water expulsion) at high fields 75-100 V/cm (~ 0.01 V/micron)
E-field polarizes diffuse double layer &/or interface
Response to field decrease with decreases ion mobility
Effect in hydrocarbon suspension (NaMnt) depended on humidity
Permanent electric dipole? (hectorite, attapulgite)
Charge mobility in lattice - internal induced dipole? (attapulgite)
Intercalated mobility at surface? (methylene blue - Mont)
Intercalated LS – LC:
Kawasumi et al. (e.g. App Clay Sci, 15, 1999, 93)
LC aligns
Process aligns LS
LS inhibits relaxation
LC instability at high frequency randomizes morphology
Clay inert component
Electric Field
Liquid Crystal Molecules
Clay Particles

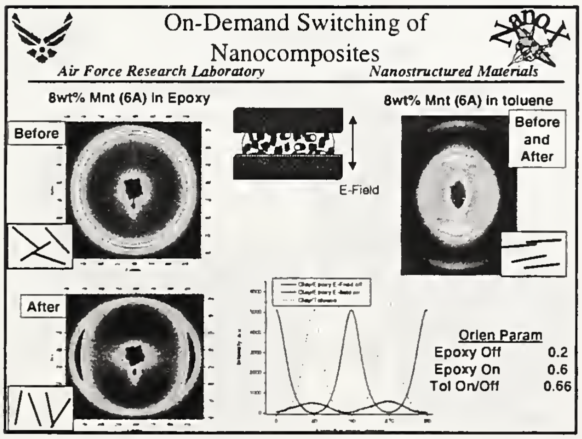

On-Demand Switching of Nanocomposites
Air Force Research Laboratory
Nanostructured Materials
8wt% Mnt (6A) in Epoxy
8wt% Mnt (6A) in toluene
Before
After
Before and After
E-Field
Orien Param
Epoxy Off 0.2
Epoxy On 0.6
Tol On/Off 0.66

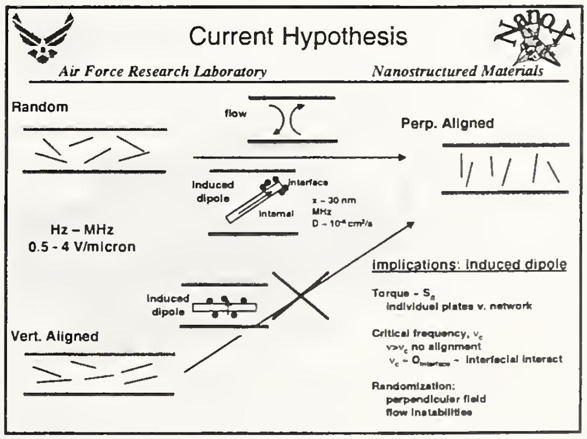

Current Hypothesis
Air Force Research Laboratory
Nanostructured Materials
Random
flow
Perp. Aligned
Induced dipole
interface
internal
Hz – MHz
0.5 - 4 V/micron
Implications: induced dipole
Torque - S
individual plates v. network
Critical frequency, νc
ν>νc no alignment
Randomization:
perpendicular field
flow instabilities
Induced dipole
Vert. Aligned

5

Outline

Air Force Research Laboratory — Nanostructured Materials

- Introduction & Drivers
- MesoScale Morphology
  - Morphology and Properties
  - Framework
  - Morphology Control
- Summary

Conclusions

Air Force Research Laboratory — Nanostructured Materials

General Conclusions

- Nanocomposites – must consider anisotropic aspects
  - Not sufficient to treat as isotropic systems
    - Preferential reinforcement, self-passivation, CTE, etc..
- Initial Frameworks exist to develop SPP Relationships
  - Stiffness enhancements in elastomers ($E_f >> E_m$) primarily aspect ratio
  - Heterogeneity of local stress/strain distribution
- Network history (not just individual particle key)
  - Anisotropic percolation and recovery
  - Aspect ratio ~ persistence length
- Techniques for Hierarchical Morphology Control Necessity
  - Experimental data for SPP theory
  - Unique nanocomposite applications:
    - Electronic packaging, optics, polyelectrolytes

Potential

Air Force Research Laboratory — Nanostructured Materials

Precision Morphology — **Predictive Relationships** — **Cost Effective Manufacturing**

Nanoscale inorganics
- Nanotubes
  - carbon
  - silica
  - V_2O_5
  - etc..
- Nanoparticles (dots, rods, sheets)
  - magnetic
  - photonic
  - metallic
  - ceramic
  - semiconductors
- Biological (proteins, viruses)
- Air

Polymers
- Liquid crystal polymers
- Block copolymers
- Colloidal assemblies
- Electro-optical polymers
- Inorganic polymers
- Thermoplastics
- Thermosets
- Hyperbranched

Objectives
- Multifunctional materials
  - EMI shielding
  - Smart fabrics
  - Embedded antennas
  - Chem/Bio membranes
- Active photonic crystals
- Actuators
- Sensor protection
- Obscurants
- Dielectrics
- Nonlinear-optical materials
- Fuel cell membrane

Nanostructured Polymer Systems Team

Air Force Research Laboratory — Nanostructured Materials

Morphology & Rheology
D. Lincoln
H. Koerner
G. Price
R. Reuter
W. Liu
R. Krishnamoorti (U. Houston)
B. Hsiao (SUNY Stony Brook)
E. Giannelis (Cornell)
MIT DURNIT

Synthesis
T Dang
F Vastuner
E Vasilu
C Co (U. Cinn)
D. Dean (Tuskegee)
W J Brittian (U Akron)

3D Fabrication &NanoPhotonics
R Jakubiak
D Tomlin
B J. Gazdecki
C. Denni
L. Natarajan
V Tondigilia
T Bunning

Simulations
R. Bharadwaj
A Sansuiate
B Farmer

C-Nanotube and Fiber
M. Alexander
F Arnold
S Kumar (G Tech)
C -S Wang
T. Dang

Thermal Stability
W Xie (U W Kentucky)
W P Pan (U W Kentucky)
D. Hunter (Southern Clay Prod)

Space Durability
H. Fong
J. Sanders
C Cerbus
S. Phillips

Thermosets & Mechanics
T. Benson Tolle
J Brown
N Pigano
C Chen
MIT DURNIT

Extra

Air Force Research Laboratory — Nanostructured Materials

Holographic photopolymerization

Air Force Research Laboratory — Nanostructured Materials

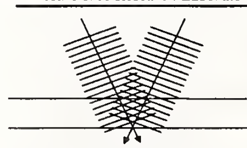

holographic illumination

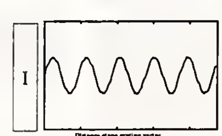

Modulated intensity profile

$$R_i = 2\vartheta I_a f$$

diffusion of monomer

$$R_p = k_p[M](R_i/2k_t)^{1/2}$$

Well-documented; Dupont et al.

Bunning et al

6

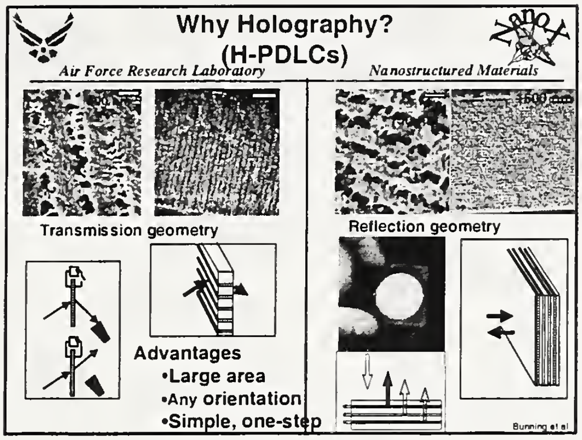

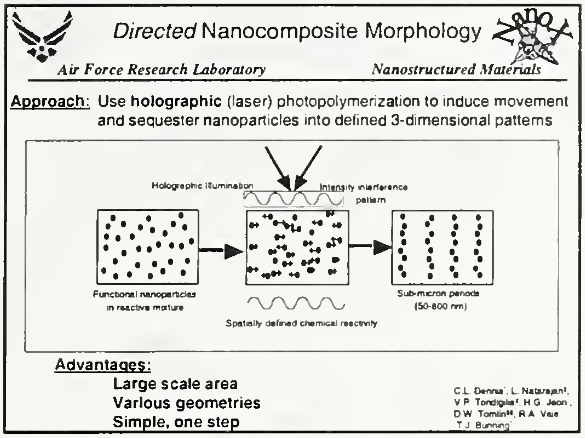

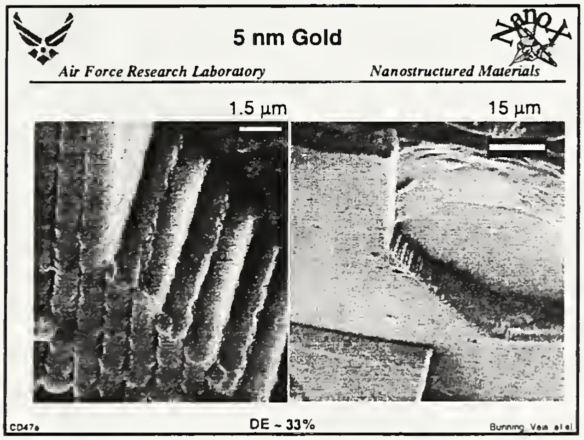

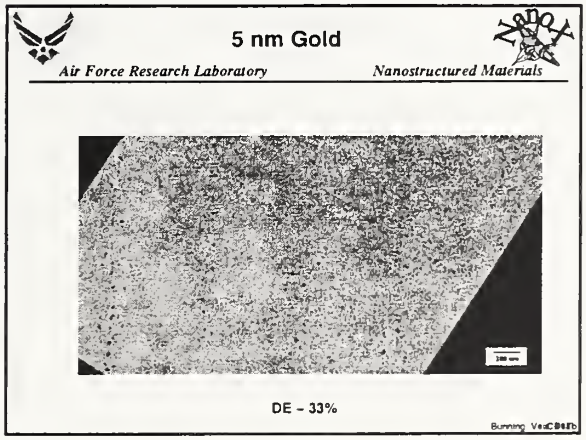

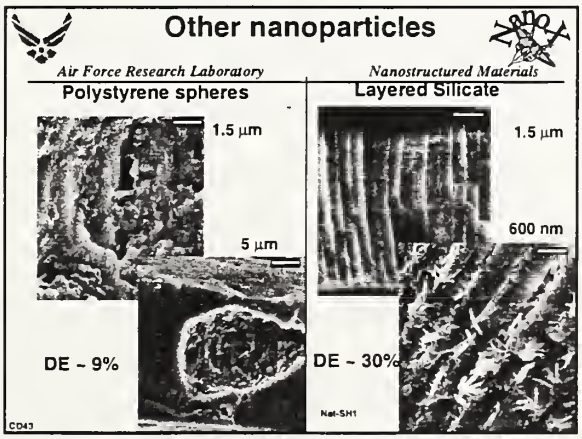

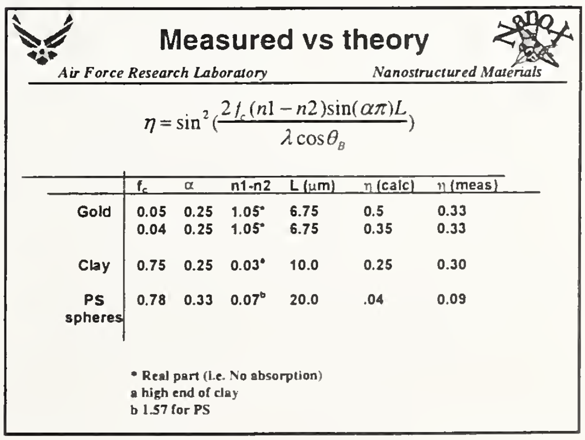

$$\eta = \sin^2\left(\frac{2f_c(n1-n2)\sin(\alpha\pi)L}{\lambda\cos\theta_B}\right)$$

	f_c	α	n1-n2	L (µm)	η (calc)	η (meas)
Gold	0.05	0.25	1.05*	6.75	0.5	0.33
	0.04	0.25	1.05*	6.75	0.35	0.33
Clay	0.75	0.25	0.03ᵃ	10.0	0.25	0.30
PS spheres	0.78	0.33	0.07ᵇ	20.0	.04	0.09

* Real part (i.e. No absorption)
a high end of clay
b 1.57 for PS

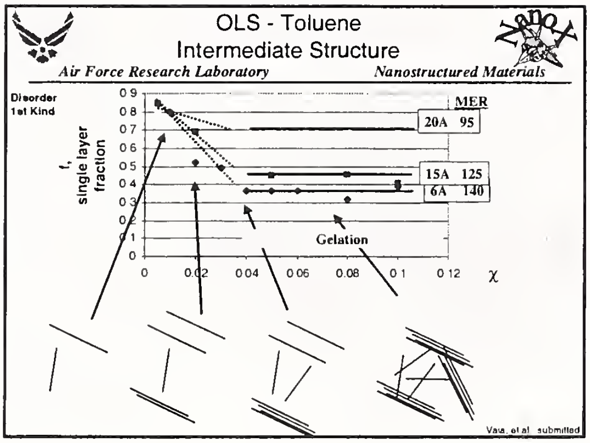
OLS - Toluene
Intermediate Structure
Air Force Research Laboratory
Nanostructured Materials
Disorder 1st Kind
f, single layer fraction
MER
20A 95
15A 125
6A 140
Gelation
χ
Vaia, et al. submitted

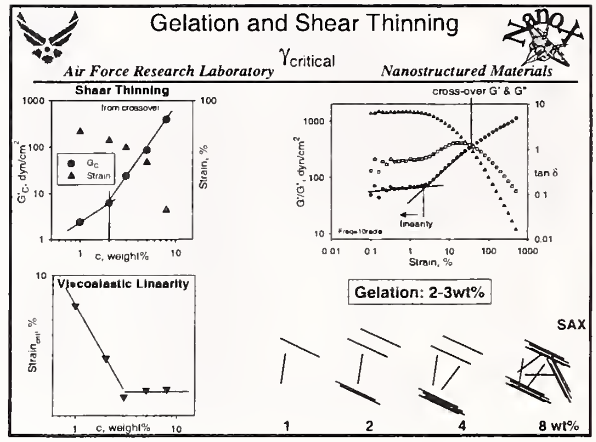
Gelation and Shear Thinning
γcritical
Air Force Research Laboratory
Nanostructured Materials
Shear Thinning
from crossover
c, weight%
Strain, %
cross-over G' & G"
G'/G", dyn/cm²
tan δ
linearity
Strain, %
Viscoelastic Linearity
c, weight%
Gelation: 2-3wt%
SAX
1
2
4
8 wt%

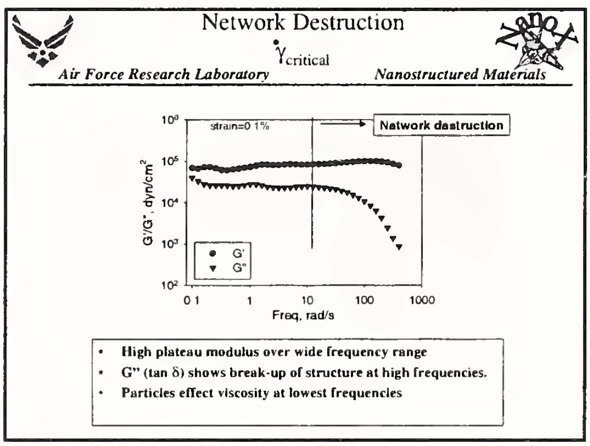
Network Destruction
γcritical
Air Force Research Laboratory
Nanostructured Materials
strain=0.1%
Network destruction
G'/G", dyn/cm²
G'
G"
Freq, rad/s
High plateau modulus over wide frequency range
G" (tan δ) shows break-up of structure at high frequencies.
Particles effect viscosity at lowest frequencies

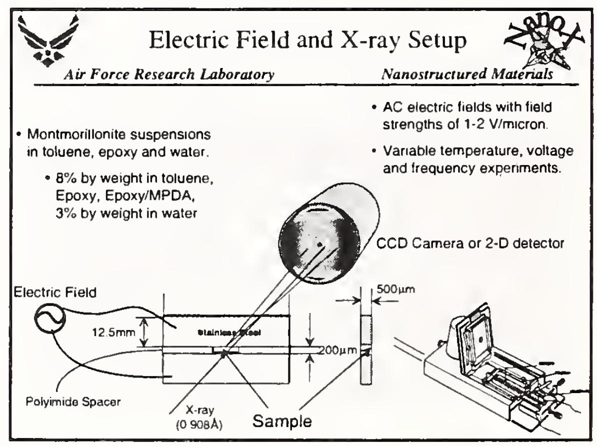
Electric Field and X-ray Setup
Air Force Research Laboratory
Nanostructured Materials
Montmorillonite suspensions in toluene, epoxy and water.
8% by weight in toluene, Epoxy, Epoxy/MPDA, 3% by weight in water
AC electric fields with field strengths of 1-2 V/micron.
Variable temperature, voltage and frequency experiments.
CCD Camera or 2-D detector
Electric Field
500μm
12.5mm
Stainless Steel
200μm
Polyimide Spacer
X-ray (0.908Å)
Sample

8) Francis W. Starr, **"Probing Nanocomposite Structure and properties using Computer Simulations"** [PowerPoint] [PDF]

Dr. Starr emphasized the need to study nanofilled systems using idealized models with the intention of identifying general properties. First, he summarized recent molecular dynamics work by himself and coworkers showing that the glass transition T_g of filled systems can be shifted to higher or lower temperature depending on the polymer particle interaction. This effect was compared to similar results, supported both by experiment and theory, for shifts of T_g in thin polymer films with variable polymer surface interactions at the boundaries. Preliminary results were then shown for simple simulation models of clay sheets and compact nanoparticles. Not surprisingly, the compact nanoparticles aggregated when the polymer-particle interaction was weak. This effect was quantified through the 'phase diagrams' governing the clustering state of the particles in the plane of temperature and polymer-particle interaction and the plane of the concentration of particles versus polymer-particle interaction. The clustering transition was identified through a maximum in the specific that accompanies the particle clustering transition. These observations are consistent with an equilibrium clustering transition that requires further investigation. Useful criteria for identifying this clustering from scattering measurements were then summarized. Finally, the influence of shear on the clustering of model clay particles in a polymer matrix was investigated by molecular dynamics and the thermodynamic clustering line was found to shift under shear. Finally, the importance of developing hierarchical multi-scale modeling approaches was emphasized in order to model nanoparticle systems under more realistic processing conditions.

Probing Nanocomposite Structure and Properties using Computer Simulations

Francis W. Starr
Polymers Division, Center for Theoretical and Computational Materials Science

Jack Douglas, NIST
Sharon Glotzer, NIST & Michigan
Thomas Schrøder, NIST & Roskilde
Barry Farmer, AFRL
Anuchai Sinsuiate, AFRL
Richard Vaia, AFRL

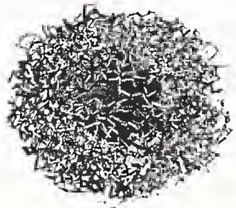

NIST
National Institute of Standards and Technology
Technology Administration, U.S. Department of Commerce

Filled Polymers and Nanocomposites

- Improve mechanical, rheological, dielectric, optical and other properties
- Low tech: tires, bumpers, paints and coatings
- High tech: micro- and nano-electronic devices
- Nanofillers
  - Tailor size and interactions to make specific property modifications
  - Custom designed materials!

Molecular level mechanisms poorly understood!

- Philosophy of this work: Start with simple systems, and work towards complexity

Example Nanofiller Geometries

Spherical/Polyhedral

e.g. colloidal silica, gold

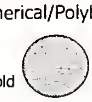

Plates

e.g. clays

Rods, Tubes, and Fibers

e.g. carbon nanotubes

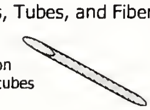

Random/Fractal

e.g. fumed silica, carbon black

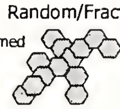

Multiple Length Scales

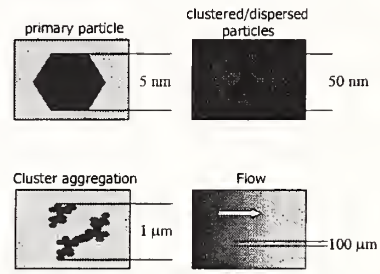

Outline

- Single, Symmetric Nanoparticle in a Dense Melt; consider effect of interactions on:
  - Chain Structure and Dynamics near interface
  - Relation to thin films (geometry implications)
- Nanocomposite: Symmetric nanoparticles in a melt
  - Aggregation and dispersion
  - Response to shear/relation to structure
- Clay-like Nanocomposite:
  - Response to shear (preliminary!)

Single Nanoparticle results: Starr, Schrøder, Glotzer, Phys Rev E 65, 051503 (2001)
Macromolecules 35, 4481 (2002)

MD Simulation Model

"Bead-Spring" Polymer **Icosahedral Nanoparticle**

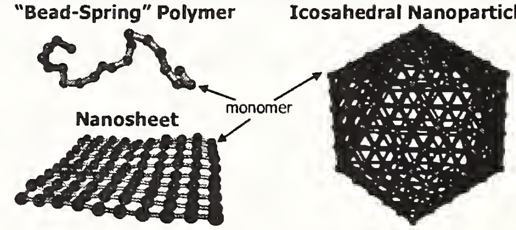

- Interactions:
  - Monomer: Lennard Jones; adjustable monomer-filler attraction
  - Bonds: FENE springs along chains and within nanoparticles
  - Vary polymer-nanoparticle interaction strength!
- Systems:
  - 100-1500 chains; 1-125 nano-fillers (loading 4%-30%)
  - Periodic Boundary Conditions
  - $0.3 < T < 2.0$
  - $10^{-4} < \gamma < 0.2$

Single Nanoparticle "Snapshot"

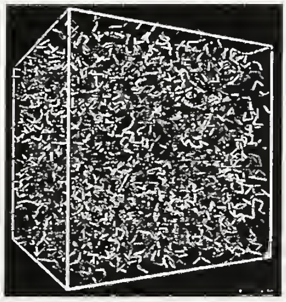

- Bulk System:
  - 100 20-mer chains
  - Fixed density $\rho = 1.0$
- Nanoparticle System:
  - 100/200/400 20-mer chains
  - System size chosen to give ρ_{-} within 0.2% of pure system density
  - $\varepsilon_{mp} = 2\varepsilon_{mm}$ (Attractive and non-attractive)
  - Facet size = R_{ee}
  - Simulation times up to 20×10^{6} MD steps (approx 40ns)

NIST, May 2002

Chain Structure and Glass Transition

- Chain Structure
  - Chains orient with surface
  - Independent of interactions!

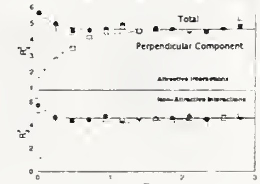

- Glass transition shift
  - T_g increases for attractive interaction
  - T_g decreases for excluded volume interactions
  - Reducing fraction of chains amplifies effects
  - Surface controlled!

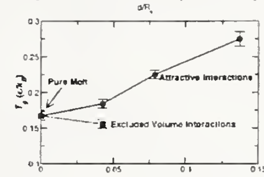

NIST, May 2002

Origin of T_g shift: Surface Dynamics

Effect of Interactions

- Slower surface dynamics with attraction
- Implies increased T_g
- Far from surface recover bulk relaxation time
- Explains ϕ dependence
- Reversal for excluded volume interactions

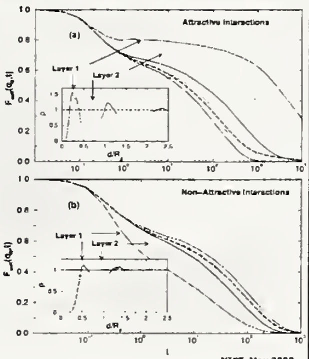

NIST, May 2002

Nano-particle vs. Ultra-thin films

- Nano-particle system
  - Polymers are elongated and flattened near particle surface
  - Strongly (weakly) attractive filler increases (decreases) T_g
  - Strongly (weakly) attractive particle slows (speeds up) monomer dynamics.
  - T_g shifts are more pronounced the higher the filler concentration

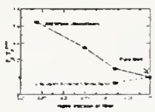

- Ultra-thin films

  - Polymers are elongated and flattened near substrate
  - Strongly (weakly) attractive substrate increases (decreases) T_g
  - Strongly (weakly) attractive substrate slows (speeds up) segmental dynamics.
  - T_g shifts are more pronounced the thinner the film

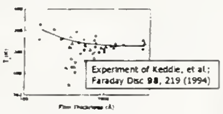

Local Structure/Dynamics weakly affected by geometry

Simulated Nanocomposite

Monitoring particle dispersion

- How do you know material is dispersed?
- Influence on Material Properties
- Role in processing

To control dispersion, you must understand

- Effect of particle-polymer interactions
- Effect of loading, temperature, etc
- Measuring dispersion via scattering?
- Morphology under shear and viscosity

NIST, May 2002

Nanocomposite "Snapshot"

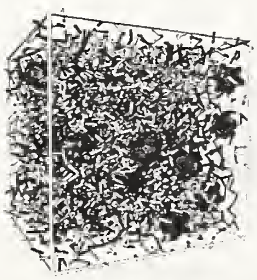

- Nanocomposite:
  - Scale down nanoparticle size
  - 400 10-mer chains
  - Fixed pressure $P = 1.0$
  - Vary number of nanoparticles
  - Vary particle-polymer interaction strength
  - Simulation times up to 10^{8} MD steps (approx 200ns)

NIST, May 2002

2

Nanocomposite: Particle Dispersion

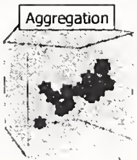

Aggregation for weak polymer-particle interaction

Dispersion for stronger interaction

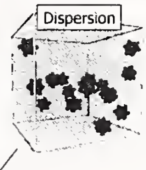

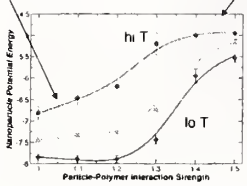

$\phi = 4.6\%$

NIST, May 2002

Clustering "Phase Diagram"

Identify "transition" point by specific heat peak

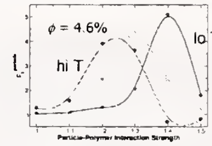

Fixed ϕ; variable T

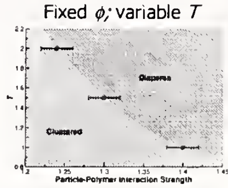

Fixed T; variable ϕ

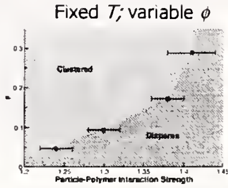

NIST, May 2002

Measuring Particle Dispersion

How do we know the state of dispersion?

- Particle Potential Energy ideal for this system, BUT
  - Experimentally inaccessible
  - Complicated geometries: no information about orientations
- Structure should be apparent in scattering profile
  - Growth of $S(q \rightarrow 0)$ indicates long range ordering

Nano-particle structure factor

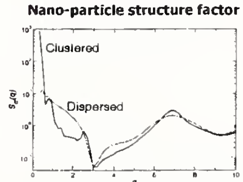

Monomer structure factor

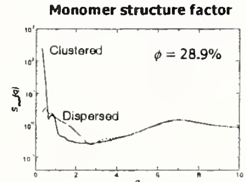

NIST, May 2002

Effect of Shear

- Start from initially clustered state
- Shear rate $\gamma = 0.1$

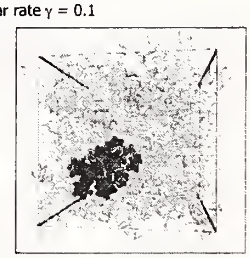

- Nanoparticles disperse in direction of shear quickly
- Disperse fully on longer time scale

NIST, May 2002

Effect of Shear

- Initially clustered state near transition line
- Shear rate $\gamma = 0.1$

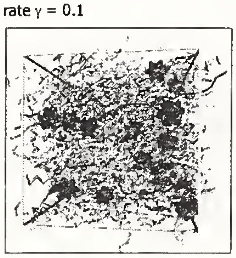

- Nanoparticles disperse in direction of shear quickly
- Disperse fully on longer time scale

NIST, May 2002

Morphology and Shear Viscosity

- Effect of shear on clustering
  - Shear has little effect on dispersed systems
  - Very high shear to disperse systems far from "transition"
  - Shear dependent shift to clustering diagram

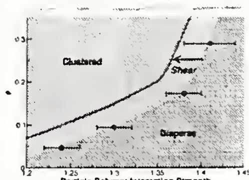

- Strength: Shear Viscosity
  - Shear far from transition (stable morphology)
  - Greater viscosity for dispersed system for $\phi > 0.1$
  - Why no effect for smaller ϕ?

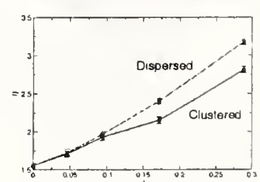

NIST, May 2002

Shear: Clay-like sheets

Intercalated
(stacked sheets)

Exfoliated
(disperse sheets)

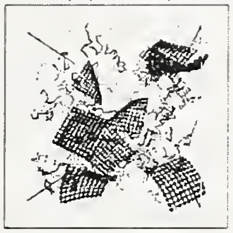

- Loading: $\phi = 0.057$
- Viscosity disparity equivalent to $\phi = 0.2$ for nanoparticles

NIST, May 2002

Conclusions

- Surface Effects
  - Chains align with filler surface
  - Chain conformation insensitive to interaction
  - Interactions dominate surface dynamics and T_g
- Clustering and Dispersion
  - Dispersion dominated by particle-polymer interaction
  - Dispersion measurable via scattering (impractical)
- Response to shear
  - Shear favors disorder here
  - Greater viscosity when dispersed
  - Geometry important for improving properties

NIST, May 2002

What next?

- Filler Geometry and Interactions
  - Expand sheet studies
  - More complex interactions (electrostatic?)
  - Keep models simple
- New Approaches?
  - Larger length scales impractical for MD/MC approach
  - Mesoscopic methods
    - Lattice Boltzmann/Lattice Gas
    - Dissipative particle dynamics

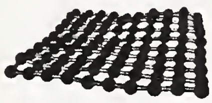

NIST, May 2002

Acknowledgments

Eric Amis
Charles Han
Eric Hobbie
Alamgir Karim
Alan Nakatani
Andrew Roosen
Wen-li Wu

NIST, May 2002

9) Juan J. de Pablo, **"Molecular Simulation and Characterization of Ultrathin Films and Nanoscopic Polymeric Structures: Departures from Bulk Behavior"** (talk presented by Kevin Van Workum) [PowerPoint] [PDF]

Dr. De Pablo's approach to modeling polymer thin films and nanoparticle filled polymer materials stresses the need for molecular modeling (molecular dynamics and Monte Carlo), continuum theory and measurement. As in the talk of Dr. Francis Starr, this contribution emphasizes simple model systems capable of inferring behavior of qualitative importance for process applications. First, recent experimental and simulation studies of the glass transition in thin films are summarized as an illustration of the value of computational methods in interpreting measurement. This is followed by the challenge of understanding finite size effects in polymer lithography applications where the scale of the patterns becomes below the scale of convenient measurement and where continuum theory can no longer be trusted. Simulations provide insight into what might be expected in this nanoscale regime. The Young's modulus of the etched lines depends on the line width and elastic constants become anisotropic. Nanoparticle fillers are shown to offer some promise in improving the properties and stability of these nanoscopic patterns. Further simulation applications explore the alignment of liquid crystal molecules about nanoparticles in connection with the development of sensors based on the binding of biological molecules to liquid crystalline substrates. Segregation of nanoparticles in block copolymer systems was also investigated in connection with the self-assembly of metal nanostructures on diblock copolymer scaffolds.

"Molecular Simulation and Characterization of Ultrathin Films and Nanoscopic Polymeric Structures: Departures from Bulk Behavior"

Kevin Van Workum,

Profs. Juan J. de Pablo and Paul F. Nealey

Department of Chemical Engineering
and the Center for NanoTechnology
University of Wisconsin - Madison

1

Introduction

Understanding Structure-Property relationships at nanometer length scales is becoming increasingly important.

Three Distinct Applications:

- Mechanical Properties of Nanostructures and Nanocomposites
- Nanoparticles dispersed in Liquid Crystals
- Nanoparticles dispersed in Block Copolymers

Vital Research Tools:

Molecular Modeling, Continuum Theory, Experiments

2

Multiscale Modeling of the Mechanical Properties of Polymeric Nanoscopic Structures

3

Glass Transition Temperature of Thin Polymer Films

Experimental Results

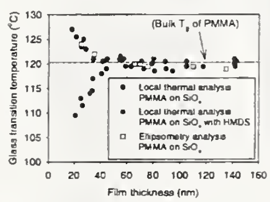

Molecular Dynamics Results

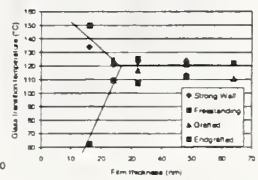

•*Fryer, Nealey, and de Pablo , Macromol., 2000.*
•*Torres, Nealey and de Pablo, Phys.Rev.Lett., 2000.*

4

Industry Goals

2001
Linewidth (Dense Features) = 150 nm
Aspect Ratio = 3.0 - 4.0

2002
Linewidth (Dense Features) = 130 nm
Aspect Ratio = 3.0 - 4.0

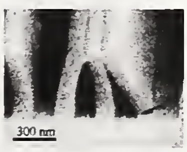

2008
Linewidth (Dense Features) = 70 nm
Aspect ratio = 3.0 - 4.0

At the 150nm or 130 nm node collapse of dense and semi-dense photoresist structures may limit our ability to stay on the SIA roadmap.

5

Continuum Model Results

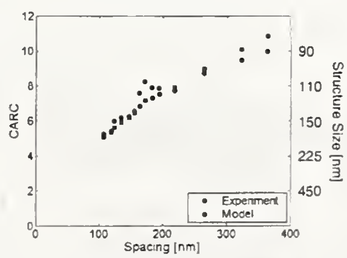

When does continuum mechanics fail?

Experiments become very difficult below 90 nm

Continuum mechanics cannot completely explain resist collapse ⟹ Molecular Simulations

6

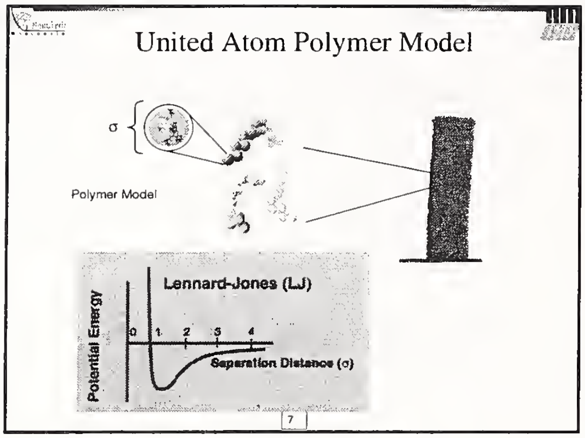
United Atom Polymer Model
σ
Polymer Model
Lennard-Jones (LJ)
Potential Energy
Separation Distance (σ)
0 1 2 3 4
7

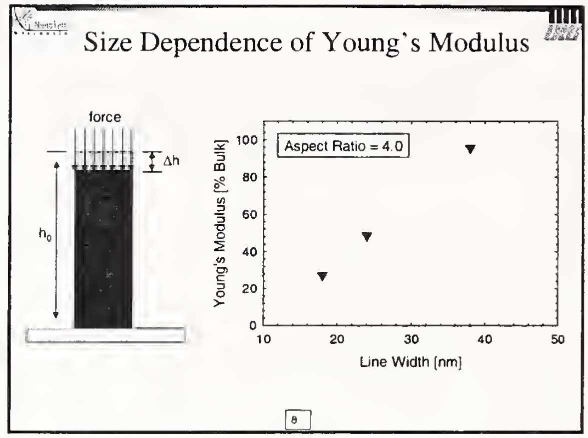
Size Dependence of Young's Modulus
force
Δh
h_0
Aspect Ratio = 4.0
Young's Modulus [% Bulk]
Line Width [nm]
8

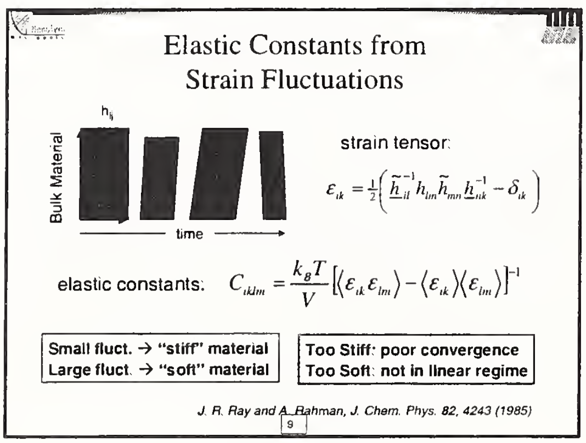
Elastic Constants from Strain Fluctuations
h_{ij}
Bulk Material
time
strain tensor:
$\varepsilon_{ik} = \frac{1}{2}\left(\tilde{h}_{il}^{-1} h_{lm} \tilde{h}_{mn} h_{nk}^{-1} - \delta_{ik}\right)$
elastic constants: $C_{iklm} = \frac{k_B T}{V}\left[\langle \varepsilon_{ik}\varepsilon_{lm}\rangle - \langle \varepsilon_{ik}\rangle\langle \varepsilon_{lm}\rangle\right]^{-1}$
Small fluct. → "stiff" material
Large fluct. → "soft" material
Too Stiff: poor convergence
Too Soft: not in linear regime
J. R. Ray and A. Rahman, J. Chem. Phys. 82, 4243 (1985)
9

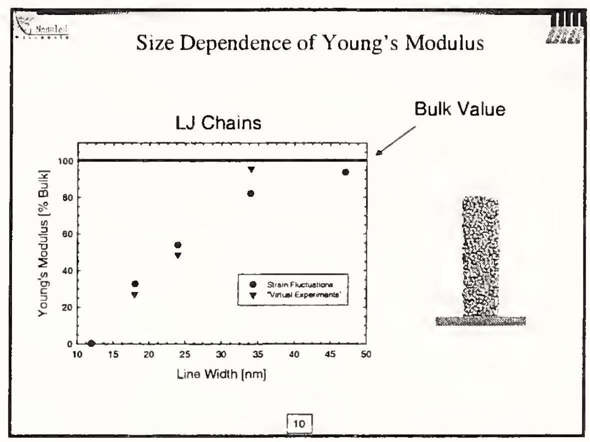
Size Dependence of Young's Modulus
LJ Chains
Bulk Value
Young's Modulus [% Bulk]
Strain Fluctuations
"Virtual Experiments"
Line Width [nm]
10

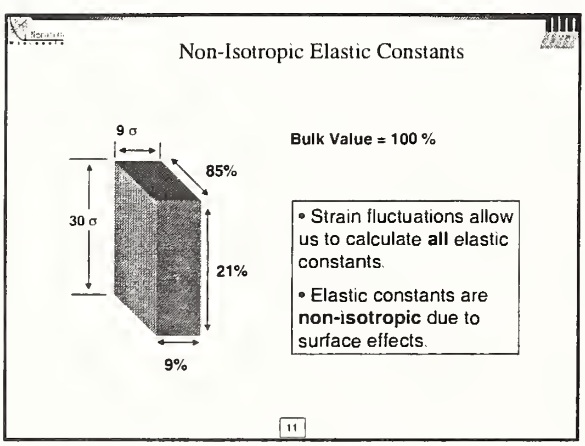
Non-Isotropic Elastic Constants
9 σ
30 σ
85%
21%
9%
Bulk Value = 100 %
• Strain fluctuations allow us to calculate all elastic constants.
• Elastic constants are non-isotropic due to surface effects.
11

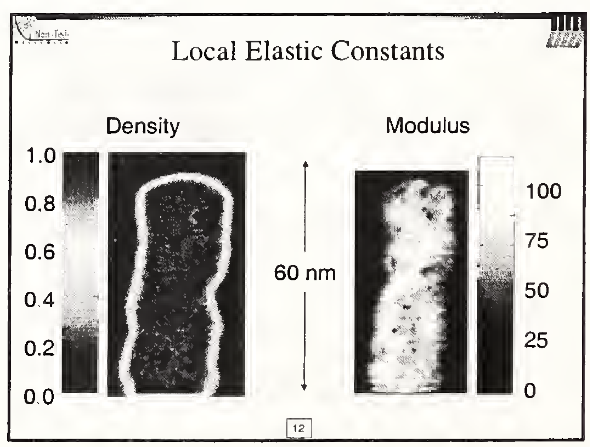
Local Elastic Constants
Density
Modulus
1.0
0.8
0.6
0.4
0.2
0.0
60 nm
100
75
50
25
0
12

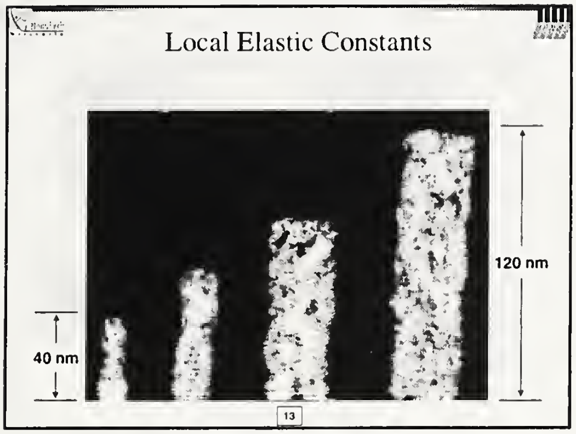
Local Elastic Constants
120 nm
40 nm
13

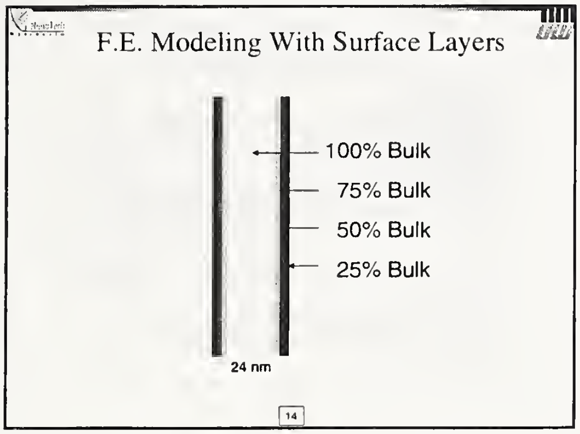
F.E. Modeling With Surface Layers
100% Bulk
75% Bulk
50% Bulk
25% Bulk
24 nm
14

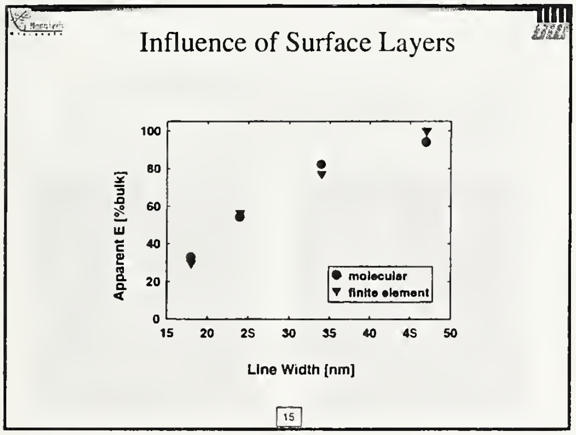
Influence of Surface Layers
Apparent E [%bulk]
100
80
60
40
20
0
15 20 25 30 35 40 45 50
Line Width [nm]
molecular
finite element
15

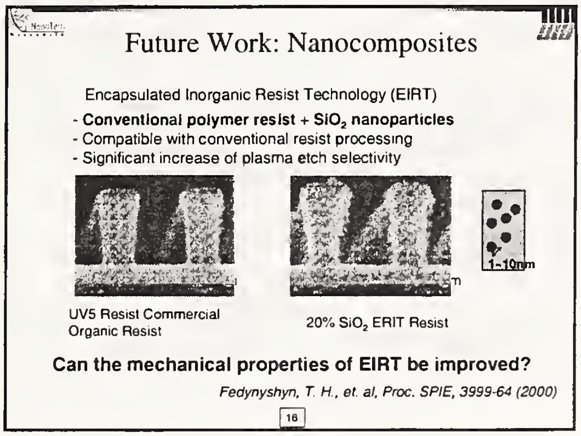
Future Work: Nanocomposites
Encapsulated Inorganic Resist Technology (EIRT)
- Conventional polymer resist + SiO_2 nanoparticles
- Compatible with conventional resist processing
- Significant increase of plasma etch selectivity
1~10nm
UV5 Resist Commercial Organic Resist
20% SiO_2 ERIT Resist
Can the mechanical properties of EIRT be improved?
Fedynyshyn, T. H., et. al, Proc. SPIE, 3999-64 (2000)
16

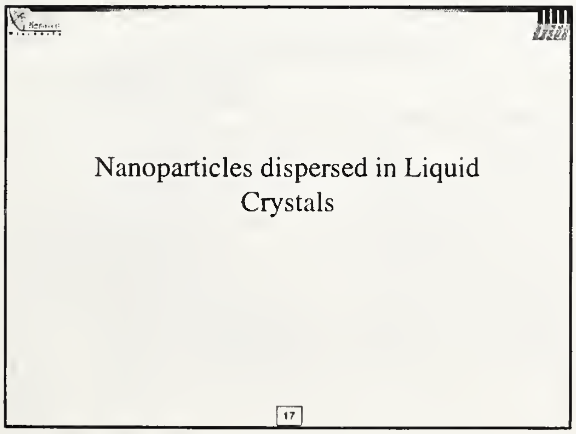
Nanoparticles dispersed in Liquid Crystals
17

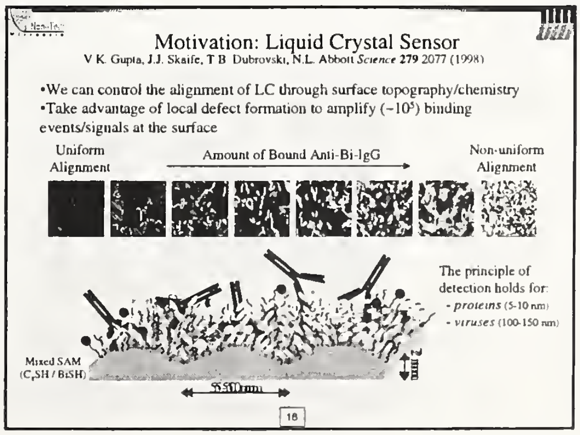
Motivation: Liquid Crystal Sensor
V K Gupta, J.J. Skaife, T B Dubrovski, N.L. Abbott Science 279 2077 (1998)
•We can control the alignment of LC through surface topography/chemistry
•Take advantage of local defect formation to amplify (~10^5) binding events/signals at the surface
Uniform Alignment
Amount of Bound Anti-Bi-IgG
Non-uniform Alignment
The principle of detection holds for:
- proteins (5-10 nm)
- viruses (100-150 nm)
Mixed SAM (C_7SH / BiSH)
~500nm
18

3

Multi-Scale Modeling

- Can we use models to anticipate which defect structure arises for specific systems?
- Can we use theory to establish quantitative relations between bound-particle concentration and shape and defect structure?
- Can we use these results to design optimal substrates?
- Can we make use of transient or time-dependent observations to infer additional information ?

19

Multi-scale Modeling

- use *detailed models* to study defect structure on *nm* length scales
- use *continuum models* to study defect structure and amplification over *μm* length scales

protein ~ 5nm long

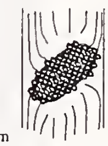

virus ~ 145x100nm

20

Different approaches to computational studies of LC

Molecular Simulations:	Approximate theories:
- Monte Carlo/Molecular Dynamics -Gay-Berne, interatomic forces	- Onsager approach (rigid rods) - *Continuum theory* (Frank free energy)
Advantages: •direct defect structure	*Advantages:* •mesoscale ~10nm – 1μm •longer time scale
Disadvantages: •cover length scales ~0.2 – 5 nm •short time scale	*Disadvantages:* •need input from experiment or molecular simulations •approximate
Challenges: •Difficulties associated with sampling of phase space	*Challenges:* •Approximations and coarse-graining might introduce artifacts

21

Simulation Details

•Monte Carlo NVT simulations with a sphere fixed at (0,0,Zsph)
•purely repulsive Gay-Berne potential (cut-off and shifted at the minimum) between LC, LC/surface, and LC/sphere
•repulsive potential results in homeotropic anchoring
•N~11,500, kT=1

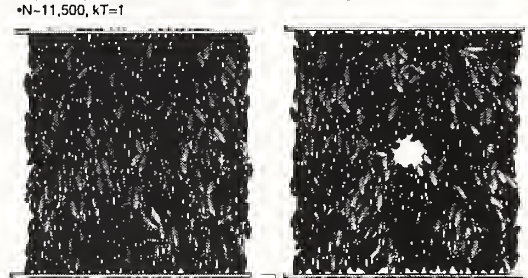

22

Confined System

•tune density and Zwall for a "bulk-like" region in the middle
•undamped oscillations in density profile seemed to be minimal for Zwall = 34

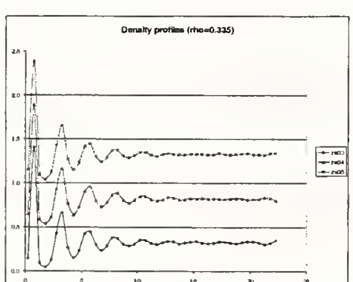

23

Molecular Simulations of LC

•Detailed representation of the system on the nm length scale

•Defect structure from intermolecular interactions

•Can investigate fundamental characteristics such as the influence of surfaces and molecular interactions on the type of defect that arises

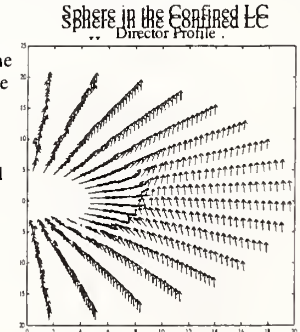

24

Continuum Theory

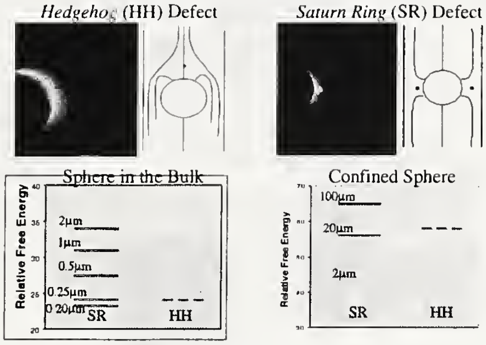

25

Solid sphere in a nematic LC (5CB)

(Y. Gu and N.L. Abbott *PRL* 85(22) 4719 (2000))

•Experiment confirms theoretical predictions!

•For R ~ 10 – 50 μm *Saturn Ring* defect is stabilized in the confined system compared to *Hedgehog* defect

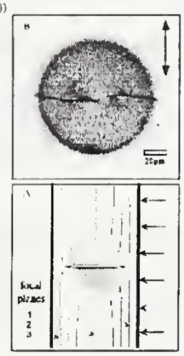

26

Sphere/Confined LC System

•sphere at a fixed position
•a sphere is repelled from the surface for z<4,
F(z=4) = 0;
force oscillates between repulsive to attractive till it is roughly 0 for z>9
•big gaps between datapoints

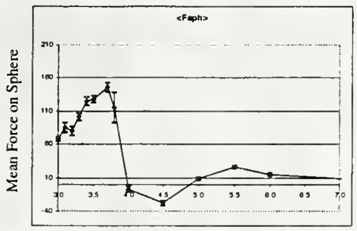

27

Expanded Ensemble using Density of States Formalism

•expand in z_{sph}
*m*th state ≡ $z_{sph}(m) = \Delta z(m - ½)$
•want uniform probability of visiting any state *m*
•use *Density of States formalism* to update weights
•will not follow Markov chain, but can rerun without updating the weights once a reasonable estimate is obtained

$$\Omega = \sum_{m=1}^{M} Q_m(N,V,T,m) g_m$$

$$g_m \propto \frac{1}{Q_m}$$

$$P_{acc}(old \to new) = \min\{1, \exp(-\beta\Delta U + \ln[g_{old}] - \ln[g_{new}])\}$$

DOS: any time a state *m* is visited, update $g_m \to \ln(g_m) + f$

$w(z) = -kT \ln Q_m = -kT \ln g_m$	←PMF from weights g_m
$w(z) = -\int_{z0}^{z1} F_{sph}(z)dz$	←PMF from integrating F_{sph}

Engkvist O, Karlstrom, J. Chem. Phys. 213 (1996) 63-76

28

Expanded Ensemble

•z range of interest [3,13]
•tried 1 window;
3 overlapping windows;
9 overlapping windows [z,z+2]
•much more efficient in collecting detailed data

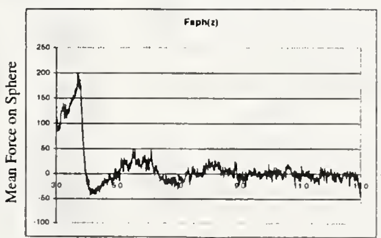

29

What happens physically?

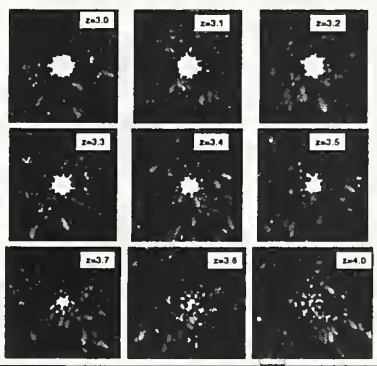

At z=3.8, surfece layer is completely filled

Equilibrium Sphere Location

5

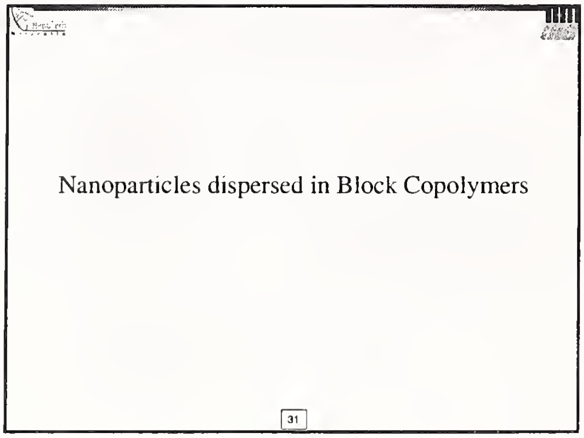
Nanoparticles dispersed in Block Copolymers
31

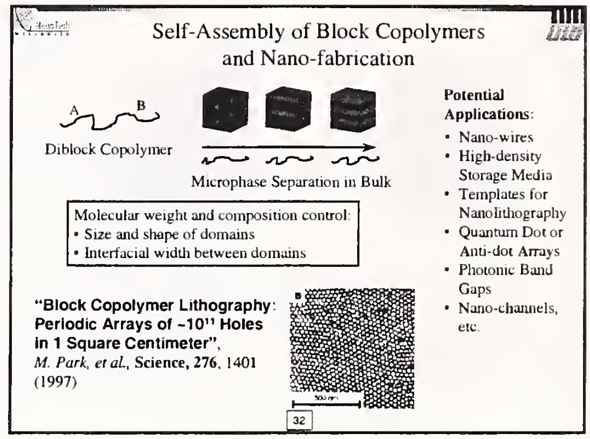
Self-Assembly of Block Copolymers and Nano-fabrication
A
B
Diblock Copolymer
Microphase Separation in Bulk
Molecular weight and composition control:
• Size and shape of domains
• Interfacial width between domains
"Block Copolymer Lithography: Periodic Arrays of ~10^11 Holes in 1 Square Centimeter", M. Park, et al., Science, 276, 1401 (1997)
Potential Applications:
• Nano-wires
• High-density Storage Media
• Templates for Nanolithography
• Quantum Dot or Anti-dot Arrays
• Photonic Band Gaps
• Nano-channels, etc.
32

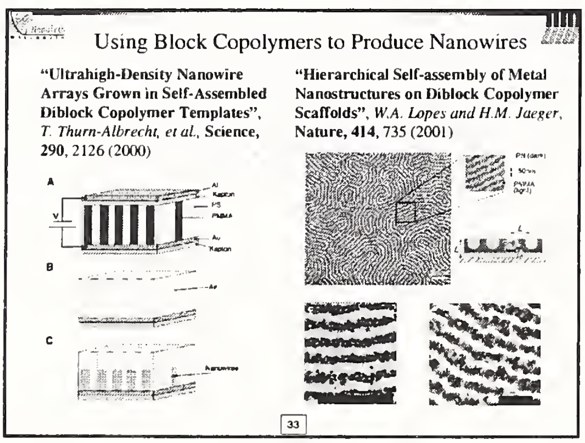
Using Block Copolymers to Produce Nanowires
"Ultrahigh-Density Nanowire Arrays Grown in Self-Assembled Diblock Copolymer Templates", T. Thurn-Albrecht, et al., Science, 290, 2126 (2000)
"Hierarchical Self-assembly of Metal Nanostructures on Diblock Copolymer Scaffolds", W.A. Lopes and H.M. Jaeger, Nature, 414, 735 (2001)
A
B
C
33

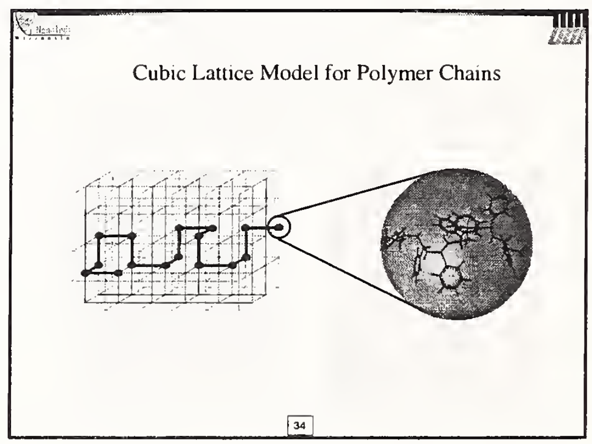
Cubic Lattice Model for Polymer Chains
34

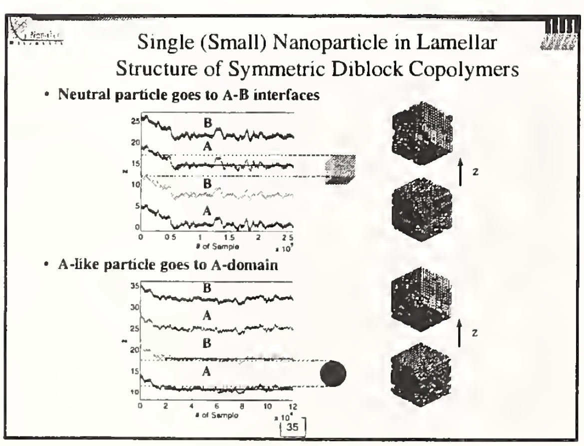
Single (Small) Nanoparticle in Lamellar Structure of Symmetric Diblock Copolymers
• Neutral particle goes to A-B interfaces
B
A
B
A
# of Sample
z
• A-like particle goes to A-domain
B
A
B
A
# of Sample
z
35

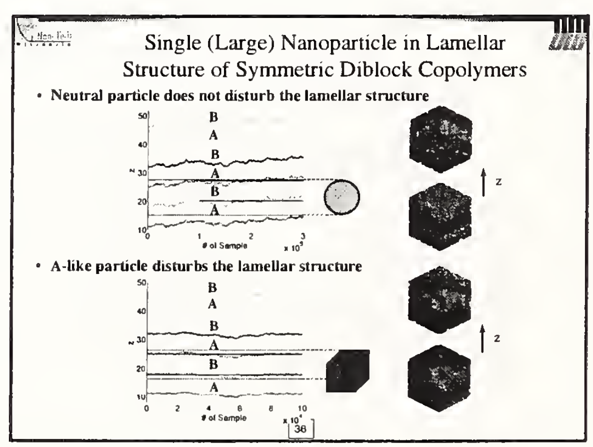
Single (Large) Nanoparticle in Lamellar Structure of Symmetric Diblock Copolymers
• Neutral particle does not disturb the lamellar structure
B
A
B
A
B
A
# of Sample
z
• A-like particle disturbs the lamellar structure
B
A
B
A
B
A
# of Sample
z
36

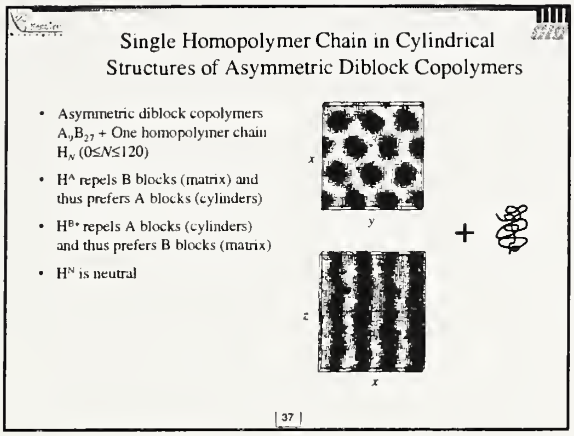
Single Homopolymer Chain in Cylindrical Structures of Asymmetric Diblock Copolymers
• Asymmetric diblock copolymers A_9B_{27} + One homopolymer chain H_N ($0 \le N \le 120$)
• H^A repels B blocks (matrix) and thus prefers A blocks (cylinders)
• H^{B+} repels A blocks (cylinders) and thus prefers B blocks (matrix)
• H^N is neutral
+
37

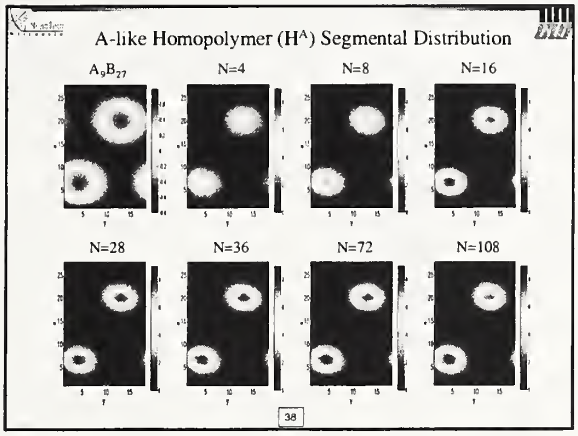
A-like Homopolymer (H^A) Segmental Distribution
A_9B_{27}
N=4
N=8
N=16
N=28
N=36
N=72
N=108
38

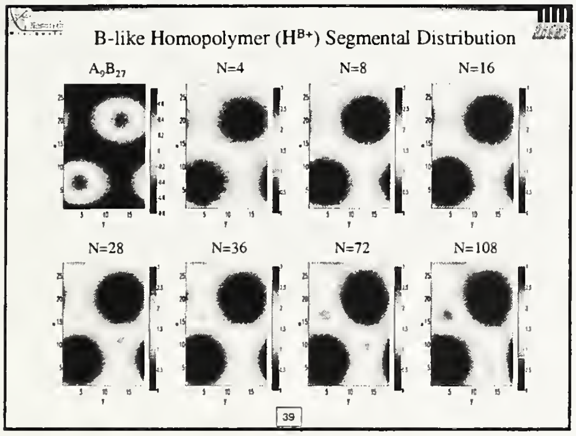
B-like Homopolymer (H^{B+}) Segmental Distribution
A_9B_{27}
N=4
N=8
N=16
N=28
N=36
N=72
N=108
39

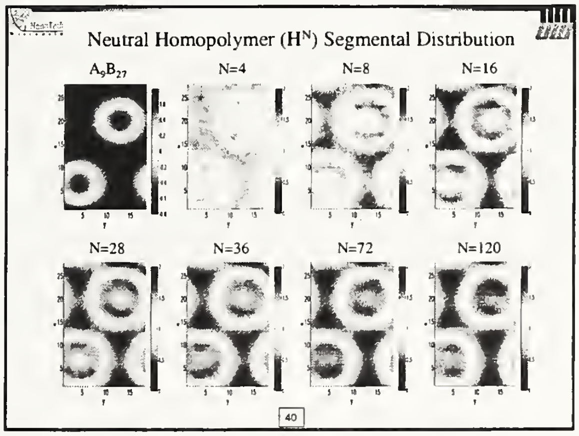
Neutral Homopolymer (H^N) Segmental Distribution
A_9B_{27}
N=4
N=8
N=16
N=28
N=36
N=72
N=120
40

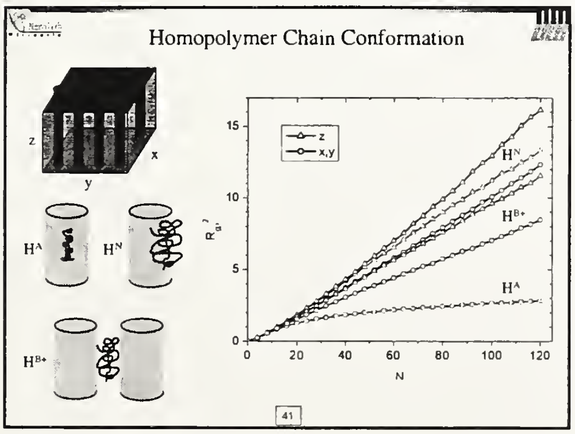
Homopolymer Chain Conformation
z
x
y
H^A
H^N
H^{B+}
z
x,y
R_g^2
N
0
20
40
60
80
100
120
5
10
15
41

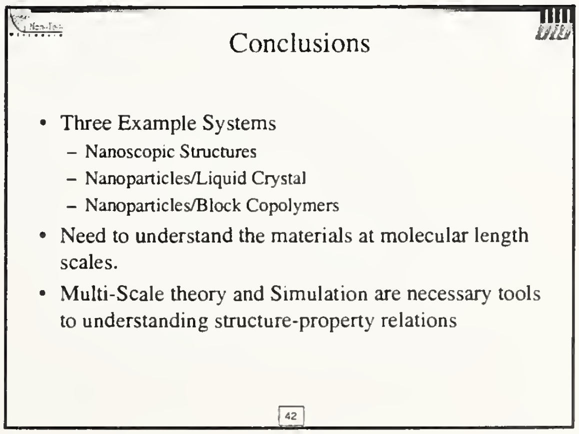
Conclusions
• Three Example Systems
– Nanoscopic Structures
– Nanoparticles/Liquid Crystal
– Nanoparticles/Block Copolymers
• Need to understand the materials at molecular length scales.
• Multi-Scale theory and Simulation are necessary tools to understanding structure-property relations
42

Acknowledgements

Contributors:

- Qang Wang – Diblock Copolymers
- Evelyn Kim – Liquid Crystals

Group Members:

- Roland Faller
- Tushar Jain

Advisors:

- Juan J. de Pablo
- Paul F. Nealey

43

10) Guoqiang Qian, **"Applications of Plastic Nanocomposites"** [PowerPoint] [PDF]

The main purpose of this talk was to provide ample evidence of the growing commercial importance of clay-filled polymer materials. Dr. Qian summarized numerous Nanocor products and the desirable property changes achieved by these products in the area of control of gas permeation, food packaging. The promise of these materials in the area of fire suppression and anti-sagging agents for fiberglass processing was also noted. The development of pre-dispersed pellets enlarges the number of users of these products.

APPLICATIONS OF PLASTIC NANOCOMPOSITES

Guoqiang Qian and Tie Lan

Nanocor

OUTLINE

- **NANOCOR PRODUCT INTRODUCTION**
- **Nano-NYLON 6**
- **Nano-MXD6: ULTRA-HIGH BARRIER**
- **Nano-POLYOLEFIN**
- **Nano-UNSATURATED POLYESTER**
- **SUMMARY**

Nanocor
WWW.NANOCOR.COM

PRODUCTS

- NANOMER® POWDERS
  - I.24TL, I.34TCN, I.42TC for Nylons
  - I.30P, I.44PA for Polyolefins
  - I.30E, I.28E for Thermoset Epoxy
  - Rhoespan® AS for UPE
- NANOMER® CONCENTRATES
  - C.30P, C.44PA, C.30PE, and C.44TPO for Polyolefins
- IMPERM™ NANOCOMPOSITES
  - High Barrier Packaging Applications

Nanocor
WWW.NANOCOR.COM

TARGET SEGMENTS

FIRE RETARDANCY

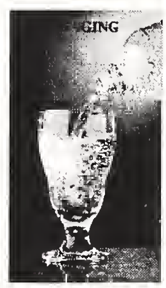

TRANSPORTATION

Nanocor
WWW.NANOCOR.COM

NYLON 6 NANOCOMPOSITES

- **Nanomer I.24 TL**

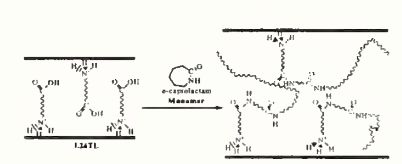

Nanocor
WWW.NANOCOR.COM

NYLON 6 NANOCOMPOSITES

- **COMMERCIAL SOURCES:**
  - Bayer AG and Honeywell Eng. Polymers and Solutions
- **COMMERICAL PRODUCTS:**
  - 2-4% Nanomer® loading
- **FEATURES:**
  - 2-3X improvement in gas barrier
  - FDA Approval for food direct contact
  - Enhanced mechanicals
  - Processes similar to neat nylon

Nanocor
WWW.NANOCOR.COM

BARRIER PROPERTIES OF NANO-PA6

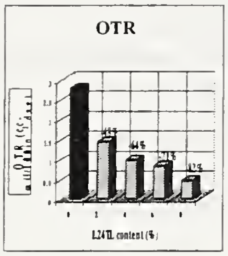

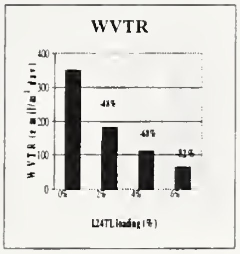

Nanocor
WWW.NANOCOR.COM

REDUCED SENSITIVITY TO HUMIDITY

Percent Improvement Nano-PA6 Versus Neat Nylon 6

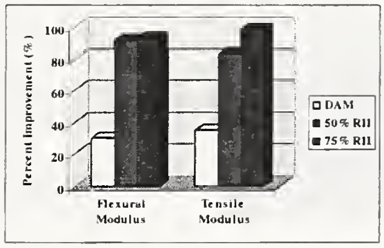

Nanocor
WWW.NANOCOR.COM

FILM APPLICATIONS

- **Mono and multilayer**
- **Thin-wall structures**
- **Stiffness ideal for stand-up pouches**
- **Barrier/strength combo permits down-gauging**

Nanocor
WWW.NANOCOR.COM

FILM APPLICATIONS

End Products	Fabrication Method	Property Enhancements	Benefits

Nanocor
WWW.NANOCOR.COM

Imperm™ ULTRA-HIGH BARRIER NANOCOMPOSITES

- **Nylon MXD6 based nanocomposite**
- **Easy processing for multi-layer and blend applications**

Nanocor
WWW.NANOCOR.COM

Imperm™ ULTRA-HIGH BARRIER NANOCOMPOSITES

- **COMMERCIAL SOURCE:**
  Nanocor
- **FEATURES:**
  3-5X improvement in oxygen barrier vs MXD6
  Low haze
  Rigid and flexible packaging
  Multi-layer or blends with PET and PA6

Nanocor
WWW.NANOCOR.COM

Imperm™ ULTRA-HIGH BARRIER NANOCOMPOSITES

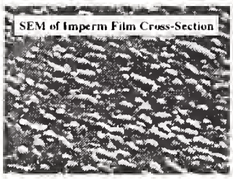

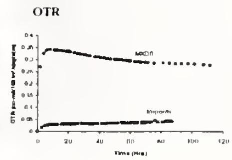

Nanocor
WWW.NANOCOR.COM

Imperm™ BEER BOTTLE

- 16 oz. non-pasteurized
- Multilayer design with 5-10% Imperm™ layer
- OTR
  - 1-1.5 micro-L/day
  - 100X versus PET
- CO_2 shelflife is 28 weeks

Nanocor
WWW.NANOCOR.COM

Imperm™ MULTILAYER PACKAGING

- Juice and other beverage package
- Paper coating/laminate
- PP/Imperm/PP Thermoform package
- PE/Imperm/PE Co-extrusion film
- PET/Imperm/PET film
- PA6/Imperm/PA6 film

Nanocor
WWW.NANOCOR.COM

POLYOLEFIN NANOCOMPOSITES

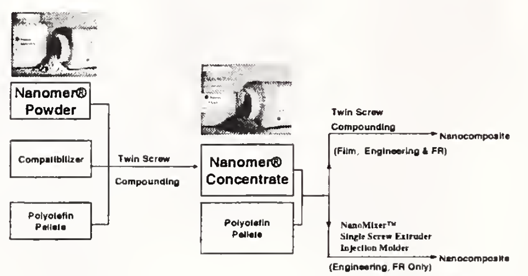

Nanocor
WWW.NANOCOR.COM

POLYOLEFIN NANOCOMPOSITES

- COMMERCIAL SOURCES:
  - Nanocor, PolyOne, and Clariant Corporation
- COMMERCIAL PRODUCTS:
  - Nanomer, Nanomer Concentrates and Nanocomposites
- FEATURES:
  - Enhanced mechanicals
  - Enhanced barrier
  - Synergy with FRs for flame retardancy

Nanocor
WWW.NANOCOR.COM

POLYOLEFIN NANOCOMPOSITES

Masterbatch	Polyolefin Type	Nanomer Loading (%)	Tensile Strength (MPa)	Flexural Modulus (MPa)	Notched IZOD (ft-lb/in)	HDT (C)
	Homo PP	0	32.0	1148	0.7	86.0
C.30P	Homo PP	6	38.0 (+19%)	2043 (+78%)	0.8	114 (+33%)
	TPO	0	19.5	780	9.8	71.0
C.44TPO	TPO	6	21.8 (+12%)	1228 (+57%)	9.8	84.7 (+19%)

Nanocor
WWW.NANOCOR.COM

3

POLYOLEFIN NANOCOMPOSITES

Barrier Properties

FR APPLICATION OF NANOCOMPOSITE

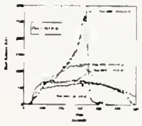

Fundamental Study

Performance Screening

FR-Rating

Nanocor
WWW.NANOCOR.COM

FR APPLICATION OF NANOCOMPOSITE

Reduction of Traditional FR Agents

Reduction of Dripping

Anti-Blooming

Good Mechanical Properties

Easy Processing

Regulation Favorable

Nanocor
WWW.NANOCOR.COM

FR APPLICATION OF NANOCOMPOSITE

Nanomer Synergy with Br-FRs

Components						
Homo-PP (wt%)	73.3	80	77	74	74	68
DBDPO (wt%)	20	15	15	15	15	15
Sb_2O_3 (wt%)	6.7	5.0	5.0	5.0	5.0	5.0
Nanomer I.44PA (wt%)	0	0	3.0	6.0	(3.0)	(6.0)
Nanomer C.44PA (wt%)	0	0	0	0	6	12
UL-94 Rating	V-0	Fail	V-2	V-0	V-2	V-0

- **Nanomer can be added in powder or concentrate forms**
- **6wt% Nanomer can replace at least 6 wt% Br-FR**
- **Reduction of Blooming**

Nanocor
WWW.NANOCOR.COM

FR APPLICATION OF NANOCOMPOSITE

Nanomer Synergy with $Mg(OH)_2$

Components				
EVA (wt%)	40	45	42	47
$Mg(OH)_2$ (wt%)	60	55	55	50
Nanomer I.30P (wt%)	0	0	3	3
UL-94 rating	V-0	Fail	V-0	V-0

- **Nanomer can be added in powder or concentrate forms**
- **3 wt% Nanomer can replace at least 10 wt% Mg(OH)2**
- **Easy Processing**

Nanocor
WWW.NANOCOR.COM

FR APPLICATION OF NANOCOMPOSITE

Mechanical Properties of Nano-FR Formulations

Properties	UL-94	Tensile Modules (MPa)	Elongation @ Break	Specific Gravity
Regular FR EVA $Mg(OH)_2$	V-0	533	30-40%	1.42
Nano-FR EVA $Mg(OH)_2$	V-0	569	30-40%	1.34
Regular Br-FR PP DBDPO/ATO	V-0	2018	20-30%	
Nano-Br-FR PP DBDPO/ATO	V-0	2055	20-30%	

Nanocor
WWW.NANOCOR.COM

4

FR APPLICATION OF NANOCOMPOSITE

- Heavy duty PP electrical enclosure
- SG reduction from 1.35 to 1.16
- Flex modulus increased by 25%
- Maintain UL94 V-0 rating

Nanocor
WWW.NANOCOR.COM

UPE NANOCOMPOSITES

- Rheospan® AS
  - Montmorillonite based anti-sag agent
  - Easy processing and nano benefits

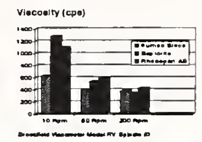

Nanocor
WWW.NANOCOR.COM

SAG CONTROL

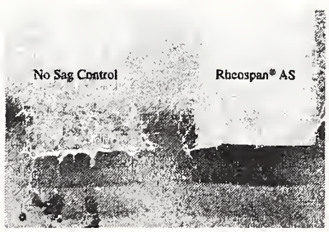

Nanocor
WWW.NANOCOR.COM

UPE NANOCOMPOSITES

- COMMERCIAL SOURCE:
  - Nanocor and Polymeric Supply Inc.
- COMMERCIAL PRODUCTS:
  - Formulations containing 1-2% loading
- FEATURES:
  - Enhanced chemical resistance
  - Char formation for flame retardancy
  - Sag control

Nanocor
WWW.NANOCOR.COM

BOAT ACCESSORIES

- UPE/fiberglass construction
- Reduced microcracking
- Reduced color fading
- Elimination of fumed silica

Nanocor
WWW.NANOCOR.COM

SUMMARY

- Nanocomposite plastics are commercial
- Barrier, reinforcement and flame retardancy drive most applications
- More applications are emerging

Nanocor
WWW.NANOCOR.COM

Acknowledgment

NIST

Amcol/Nanocor Management

Nanocor Technology Group

Nanocor
WWW.NANOCOR.COM

6

11) Eric A. Grulke, "**Production, Dispersion and Applications of Multiwalled Carbon Nanotubes**" [PowerPoint] [PDF]

Dr. Grulke provides an overview of the many activities of the Advanced Carbon Materials center at the University of Kentucky, which specializes in the production characterization, and development of applications of multi-walled carbon nanotubes. The first part of the talk provided a contrast between the morphologies of the single and multi-walled nanotubes. It was made clear that these materials exhibit a variety of hierarchal structures, depending on the conditions of their formation and that dispersion is a matter of degree because of these superstructures. The synthesis procedure for the mass production of multi-walled tubes was then discussed along with economic factors relevant to developing these materials. TEM images showed that these tube layers grow as a 'turf' from the substrate on which they are grown where the iron catalyst particles tend to concentrate near the tips of the growing tubes. The mechanism of the tip growth was identified as a fundamental problem in understanding and controlling the structure of these materials. The further essential problem of tube dispersal makes the functionalization of the tubes another essential problem. Progress on functionalization and the characterization of this functionalization was then summarized. Some essential properties of polymer materials filled with multi-walled tubes are considered. The viscosity depends strongly on shear in these non-Newtonian fluids and large changes in the conductive properties are found. Finally, a variety of processing techniques for forming nanotube filled polymers are reviewed and dispersion and property changes resulting from these various methods are characterized. Preliminary observations indicate that the concentration of the tubes has a large impact on the tendency of the particles to cluster and the resulting properties.

MWNTs Dispersed in Various Media

Bridging the Gap NIST 1

Example of MWNT Dispersion

Nanotubes quickly settle without use of a proper dispersant; b. The very stable nanotube nanofluid produced by this method is thus suitable for thermal conductivity measurements and future heat transfer applications Poly(alpha-olefin)

Bridging the Gap NIST 2

Dispersion with High Thermal Conductivity

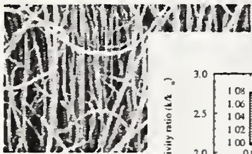

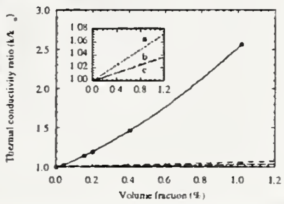

Bridging the Gap NIST 3

2.5 wt % MWNTs in Poly(α-olefin).

High shear dispersion This sample has high thermal conductivity.

Bridging the Gap NIST 4

Dispersion during Melt Blending

- MWNTs in polystyrene
- Haake rheometer, 180 C, Dow 666, 30 min, constant torque @ 30 min, 50 rpm
- Consistent flow properties, physical properties (tensile, resistivity) in bulk tests
- *What is the dispersion quality?*

Bridging the Gap NIST 5

SEM Analysis

A possible dispersion challenge due to mechanical entanglements between MWNTs

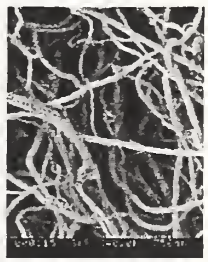

Bridging the Gap NIST 6

PS Melt Blending. 15 min.

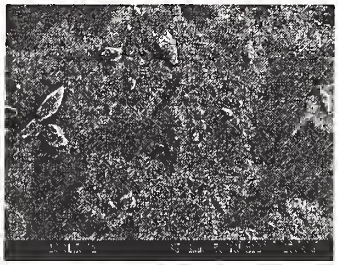

Bridging the Gap... NIST 7

PS Melt Blending. 15 min.

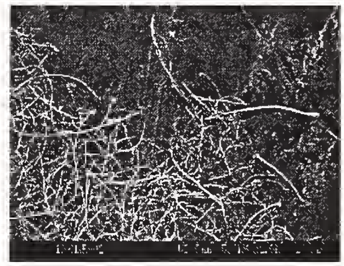

Bridging the Gap... NIST 8

PS Melt Blending. 30 min.

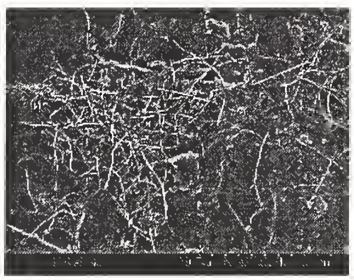

Bridging the Gap... NIST 9

Optical Microscopy

Bridging the Gap... NIST 10

Melt Blending. MWNTs in PS.

5 minute sample. Large fragments of the MWNT "mat" are not dispersed. Toluene suspension. Logo is 50 μ wide.

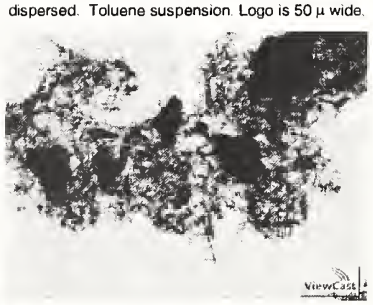

Bridging the Gap... NIST 11

Melt Blending.

10 minute sample. MWNTs in PS.
Toluene suspension. Completely dispersed material. Logo is 20 μ wide.

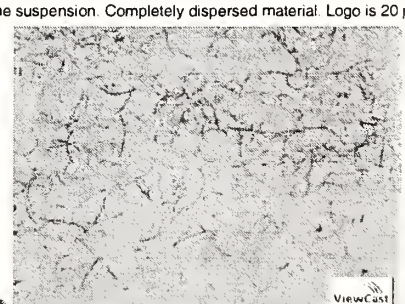

Bridging the Gap... NIST 12

2

Melt Blending.

10 minute sample. MWNTs in PS.
Toluene has evaporated. Logo is 50 μ wide.

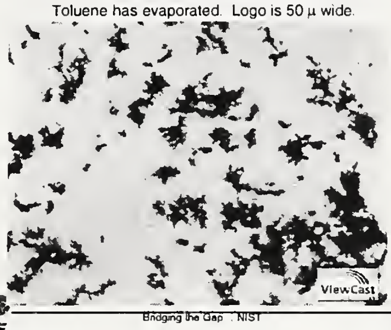

Bridging the Gap . NIST 13

Melt Blending.

30 minute sample MWNTs in PS.
THF has evaporated. Logo is 50 μ wide

Bridging the Gap NIST 14

Melt Blending.

30 minute sample MWNTs in PS.
Toluene suspension. Logo is 50 μ wide.

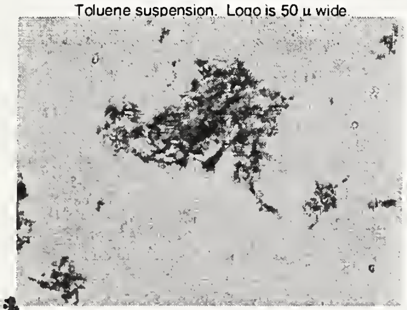

Bridging the Gap.. NIST 15

Melt Blending Dispersion Summary

- The MWNTs are dispersed with respect to bulk properties
- Multiple step dispersion: fragmentation of "Astroturf", expansion, individual tubes
- Evidence that some agglomerates exist that are mechanically entangled
- Potential problems in fiber spinning, high surface gloss

Bridging the Gap NIST 16

Surface Chemistry

- Distinct differences on solvent removal from MWNT solutions
- Drying from toluene gave agglomerates of 25 microns in size, while drying from THF gave much smaller agglomerates
- Surface chemistry (with control by solvent, polymer, surfactants, etc) may be useful in developing aggregate structures

Bridging the Gap NIST 17

Solution Rheology Samples.

VGB 78 (B). 0.1 wt% MWNTs in 20% PS in toluene
Undiluted. A. Karicherla.

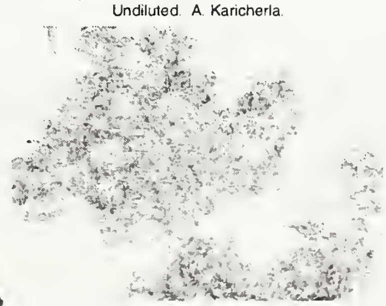

Bridging the Gap NIST 18

Solution Rheology Sample.

VGB 78 (B). Diluted 1:5 20wt% PS. A. Karicherla

Bridging the Gap . NIST 19

Solution Rheology Sample.

VGB 63 (C). Diluted 5.1. 20 wt% PS. A. Karicherla

Bridging the Gap . NIST 20

Re-entanglement (Mechanical)

- Agglomerates that appeared to be physically entangled will redisperse when the MWNT concentration is reduced
- Consistent with statistical approach to percolation, i.e., as the concentration increases, a distribution of particle agglomerates form

Bridging the Gap . NIST 21

Conclusions. Melt Blending.

- MWNT mat fractures to dense fragments, which then "expand" and can disperse
- 30 min. melt blending samples show few dense fragments, but do have "expanded" structures that are mechanically intact
- There is a MWNT length distribution
- Continuous phase affects particle-particle associations, particularly when an air-fluid interface is present

Bridging the Gap.. NIST 22

Conclusions. Ultrasonic Dispersion

- Distribution of MWNT lengths
- Few expanded structures, but long dispersion times used to attain constant viscosities
- Dilutions show that most of the MWNTs can be individually separated

Bridging the Gap. NIST 23

Particle Comminution

- Ultrasonics
- Melt blending
- High shear mixing
- High shear nozzle
- mechanical

Bridging the Gap . NIST 24

As-Produced MWNTs

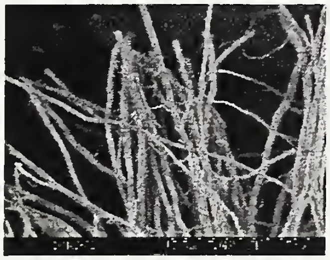

Bridging the Gap NIST 25

As-Produced MWNTs.

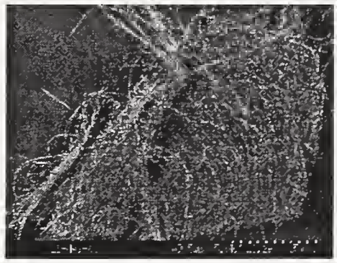

Bridging the Gap . NIST 26

As-Produced MWNTs

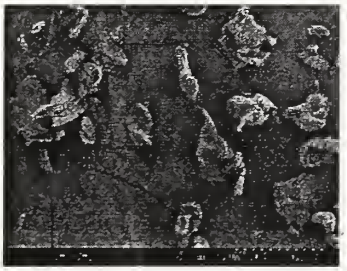

Bridging the Gap NIST 27

Mechanical grinding

Bridging the Gap.. NIST 28

Ground MWNTs

Bridging the Gap NIST 29

Length Reduction via Ultrasonics

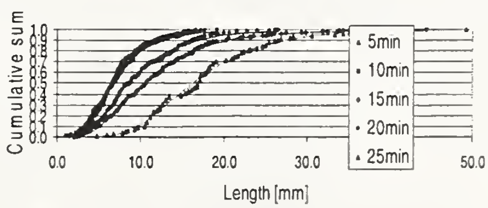

Bridging the Gap NIST 30

Power law comminution model

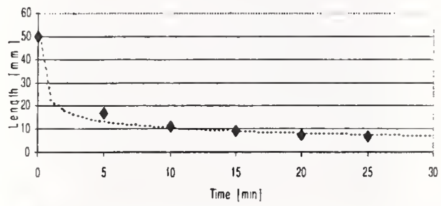

Conclusions. High Shear Dispersions.

- Very efficient dispersion, but lengths are < 10 microns
- Still achieve “percolation” limits, but these should be based on different lengths from the starting material

Composites and Solutions Processing

Carbon Composite Materials

Composites with Nanotube Fibers

Typical composite materials issues:
Fatigue, high temperature, chemical resistance, weathering

Typical composite materials failure mechanisms:
Fiber pullout, stress concentration at fiber ends

Typical composite processing issues:
Dispersion, orientation, conventional processing

Accomplishments

- Dispersion via ultrasonics and polymer melt processing techniques
- Orientation in shear fields, leading to 2-D, 3-D structures
- Adhesion between matrix and MWNTs is an issue: functionalization should help

Commercial Forming Methods for Nanotube Composites

• Pultrusion:	applicable for yarns
• Filament winding:	MWNT-containing fibers (2)
• Compression molding:	extrusion and pelletizing (3)
• Hand lay-up:	thin films fabricated (2)
• Hand spray-up:	spray coatings (3)
• Reactive RIM:	suspending agents (2)

0=science fiction, 2=demonstrated, 4=ready for market

Demonstrated Nanotube Orientation Methods

Uniaxial: fibers, films (Tek-Pak)

Angle Ply: shear flows (thin disks)

Cross Ply: fiber layup expected

Random-in-the-Plane: hot pressing

Random in 3D: bulk solids

Composites: New Work

- Functionalization: improved dispersion in liquids, tethered chains for improved interfacial adhesion, *in situ* end group functionalization
- Mechanical testing of improved nanotube composites
- Engineering science models of processing methods

Solution Processing

- Ultrasonic mixing
- Individual dispersion
- Surfactants for simple fluids
- Neat MWNTs for viscous polymer solutions

- MWNTs in film spun from PS solution. 30 microns diameter

Tensile strength and modulus

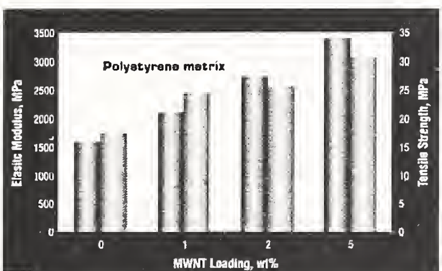

Melt Processing

- Mixing and dispersion into pitch and polymer melts
  - Polystyrene, High Impact PS, Polypropylene, ABS
  - Petroleum Pitch, Coal-derived Pitch
  - Furfural Resins
- Thin polymer film and fiber formation
- Nanotube alignment in shear field
- Use of traditional polymer processing equipment
  - Industrially viable processing techniques

Shear Mixing of MWNTs

- Haake Polylab Shear Mixer
  - 50 gram charge
  - 0 - 25 wt% fiber
- Mixing Energy

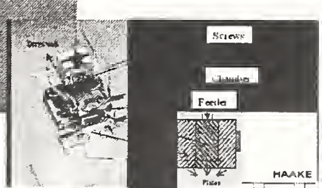

Dispersion of MWNTs

- Determination
  - Optical microscopy
  - SEM and TEM
  - 0 - 10 rating

- Polypropylene matrix
- 2.5 vol% MWNT

2

Mixing Energy for Dispersion

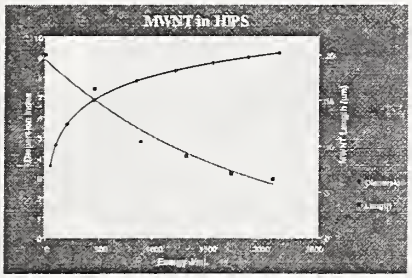

Possible Route to Functionalization!

Bridging the Gap.. 13

Melt Processing

Thin Polymer Films

Bridging the Gap.. 14

Tensile Properties of Films. PP

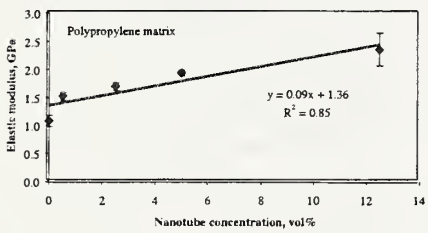

Bridging the Gap.. 15

Surface Resistivity

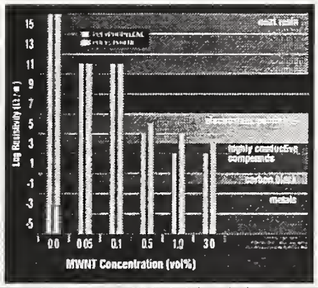

Bridging the Gap.. 16

Conductive Plastics

- Current technology
  - carbon blacks
  - 10-15% loadings
  - loss of mechanical properties
- MWNT Composites
  - 0.1 - 1 wt% loadings
  - low percolation threshold

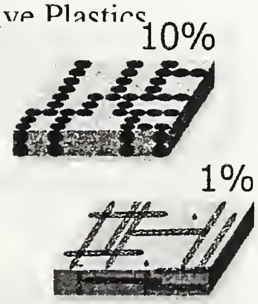

Bridging the Gap.. 17

Melt Processing

Polymer and Pitch Fibers

Bridging the Gap.. 18

3

Polymer Fibers with Aligned MWNTs

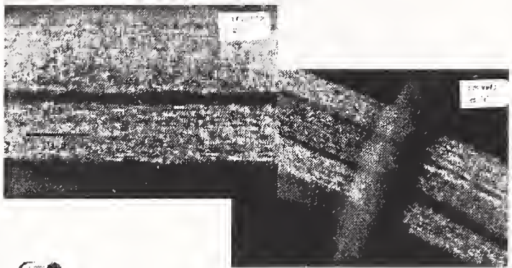

Carbon Fiber with 1wt% MWNT

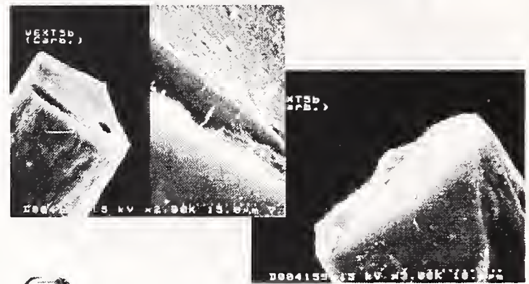

Carbon Fiber with 2wt% MWNT

Benzyne Functionalization of MWNT

- Benzyne addition
  - on sidewall of MWNT
- Composite polystyrene films
  - Improved dispersion
  - Improved matrix-nanotube adhesion
- Results
  - Good dispersion
  - Reduction in film brittleness
  - Improved flexibility over blank films and unfunctionalized MWNT composites

Computational Studies of the Mechanical and Tribological Properties of Carbon Nanotubes. (Sinnott)

- Results for indentation of multi-walled nanotubes on surfaces:
  - Mechanism is the same as for the single-walled nanotubes
  - MWNTs are stiffer than comparably sized SWNTs
- Shearing of Carbon Nanotube Buodles Between Sliding Surfaces
  - Movement of the nanotubes is sliding; no rolling is predicted
- Horizontal bundles of single-walled nanotubes
  - little change in frictional forces with sliding
  - forces do not vary with changes in pressure
- Vertical bundles of single-walled oanotubes:
  - Strong dependence of frictional forces on applied pressure for capped nanotubes
  - little dependence for attached nanotubes

NT-Composite Failure

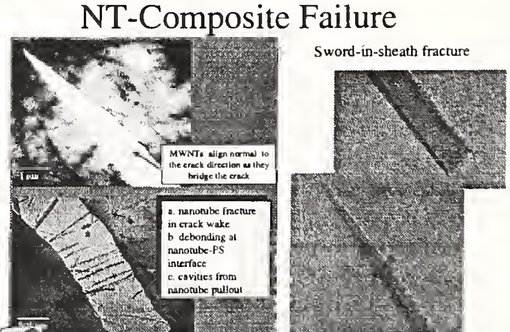

4

Failure modes of MWNT Composites

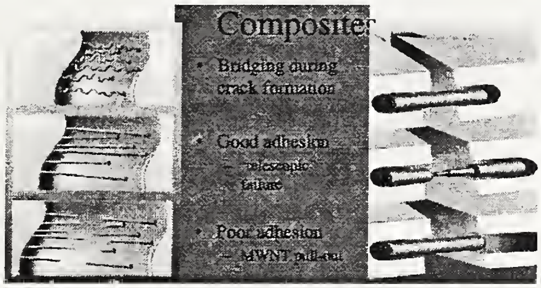

Sizing

- Commercial graphite fibers having sizings that improve fiber/matrix adhesion
- We have been developing sizings for MWNTs in various commodity polymers

Production, Dispersion and Applications of Multiwalled Carbon Nanotubes

Eric A. Grulke
University of Kentucky
egrulke@engr.uky.edu

NSF MRSEC Advanced Carbon Materials Center

- Eric Grulke
- Mark Meier
- Robert Haddon
- Rodney Andrews
- John Anthony
- Jack Selegue
- Madhu Menon
- Janet Lumpp
- Zhi Chen
- Marit Jagtoyen
- Susan Sinnott, U of Fl
- Kozo Saito
- Bruce Hinds
- Leonidas Bachas

Nanoparticle Morphology and Polymer Applications

Theme: nanoparticle morphology has scientific and economic value [this is not a new concept]

- Manipulate the production process to develop different morphologies
- Manipulate dispersion, orientation and interphase region

Outline

- Synthesis of ordered carbons: emphasis on MWNTs
- Functionalization of MWNTs
- MWNTs applications in polymer systems and fluids

Synthesis of Ordered Carbons

1. What can we make?

Single Wall CNTs

1 nm diameter, 1-10 microns long

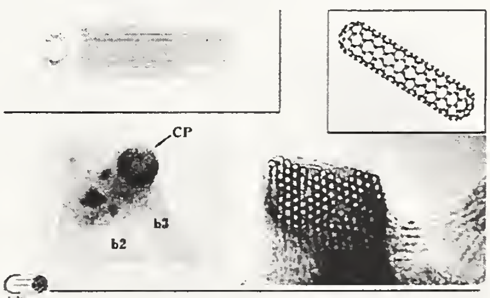

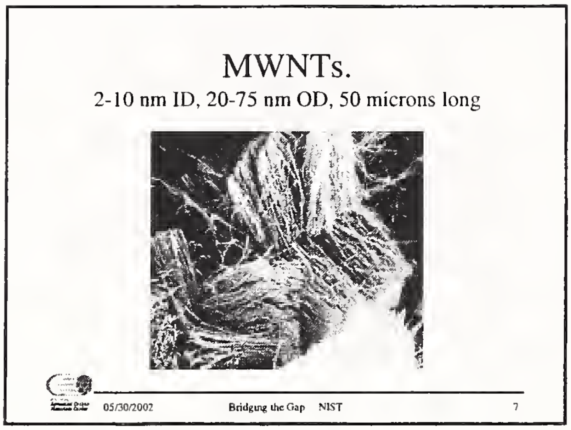
MWNTs.
2-10 nm ID, 20-75 nm OD, 50 microns long
05/30/2002
Bridging the Gap NIST
7

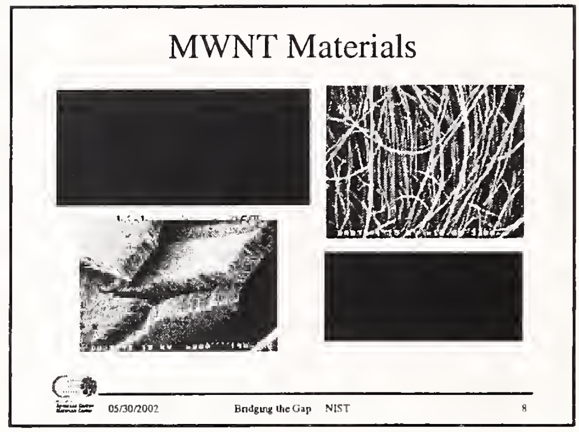
MWNT Materials
05/30/2002
Bridging the Gap NIST
8

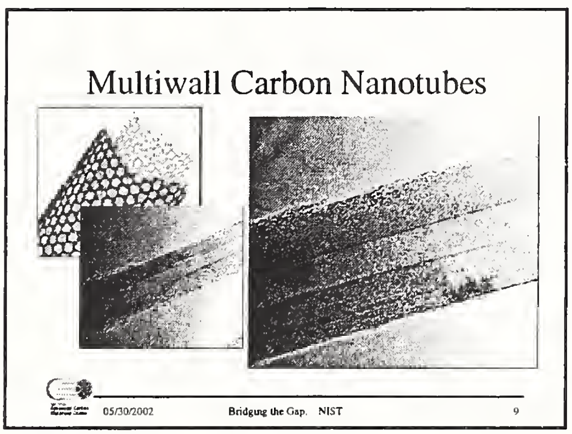
Multiwall Carbon Nanotubes
05/30/2002
Bridging the Gap. NIST
9

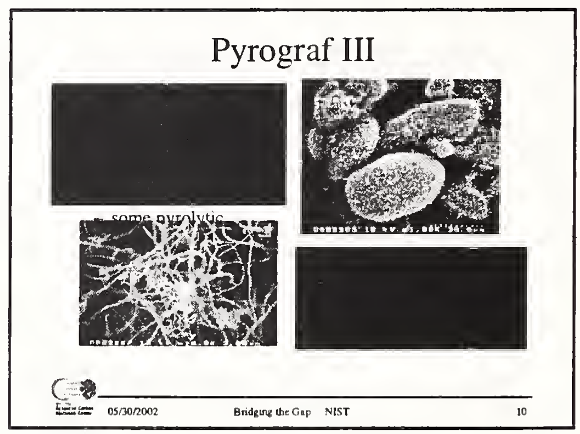
Pyrograf III
05/30/2002
Bridging the Gap NIST
10

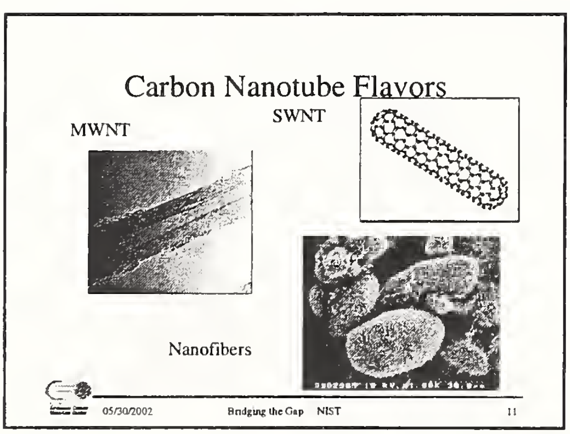
Carbon Nanotube Flavors
MWNT
SWNT
Nanofibers
05/30/2002
Bridging the Gap NIST
11

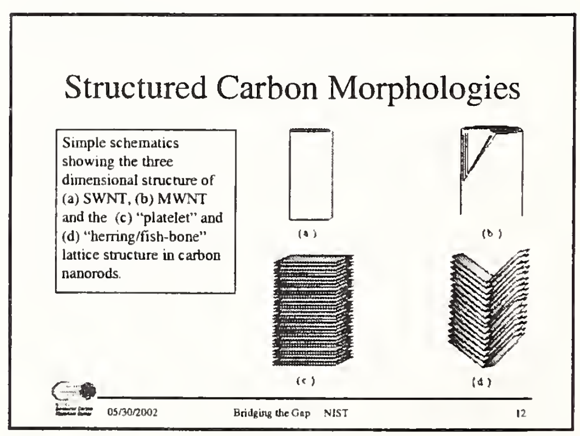
Structured Carbon Morphologies
Simple schematics showing the three dimensional structure of (a) SWNT, (b) MWNT and the (c) "platelet" and (d) "herring/fish-bone" lattice structure in carbon nanorods.
(a)
(b)
(c)
(d)
05/30/2002
Bridging the Gap NIST
12

Platelet Structure: catalyst support?

TEM images of the filamentous carbon growth from Ni/Ta_2O_5. M. A. Keane

Synthesis of Ordered Carbons

- SWNTs, MWNTs and other ordered carbons
- Promote comparison of different carbon materials
- Determine growth mechanisms, rate-limiting steps for synthesis

Synthesis of Ordered Carbons

- What can we make?
- What will it cost?

Production Methods

- SWNTs: arc process (Carbolex), laser/graphite target, gas phase (HIPCO/Rice)
- MWNTs: CVD process, high quality tubes, scalable process, reproducible morphology (ACMC/CAER and others)
- Diffusion flame: MWNTs grown from methane on metal screen (Saito)
- Platelets: heterogeneous catalysis (Keane)

CVD Process Economics

Study by Gene Harlacher, Conoco, CAER visiting scientist, 12/99.

- MWNT cost is sensitive to labor, energy, catalyst cost and efficiency, HC cost and yield
- Fe is a low cost catalyst now
- 10^6 kg/year gives cost of $20/kg MWNT
- **Conclusion: ferrocene-based CVD process is a reasonable choice for extensive research**

CVD Process Economics-Details

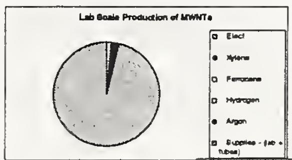

Batch: labor is a major portion of the cost

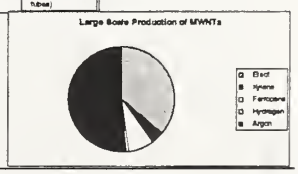

Continuous: raw materials and energy dominate costs

Synthesis of Ordered Carbons

- What can we make?
- What will it cost?
- How do we make more?

Scale-up of Carbon Nanotube Production Systems

- Quantity & Quality
- Bench scale, pilot plant, commercial plant
- Morphology control
- Recycle of gases, conversion and yield, choice of carbon source, catalyst recycle, solids recovery, solids post processing

CVD Methods for Nanotube Synthesis

- Transition metals and their alloys: Fe, Co, Ni
- Prepared nanoscale metal oxide particles Fe_2O_3, NiO-CoO on supports
- Catalyst thin films on silica

Floating catalyst – organometallic precursors form metal nanoparticles *in situ*

Two Step Synthesis

- Gas flow into quartz tube: carbon source, H_2, Ar
- Sublime ferrocene into reaction zone and prepare *in situ* catalyst on reactor surfaces
- Xylene feedstock decomposes over Fe nanoparticles to produce CNTs
- Vary T, C:H ratio to evaluate effect of MWNT growth over rxn. time

Two-Step Synthesis Reactor

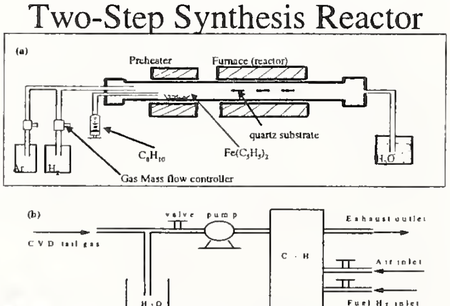

Analytical

- Reactor tailgas: HP 5980 ac, Series 2) on 2 l gas bag for C_mH_n, Rosemount 400A Hydrocarbon Analyzer for total carbon (CH_4-He for calibration)
- TEM: JEOL 2000FX TEM (LaB_6 at 200 kV)
- SEM: Hitachi SN-3200 at 5 kV

4

Results

- Growth mechanism
- Effects of reactor temperature and time on MWNT production

- Effect of C:H ratio
- Chemistry of xylene degradation over Fe nanoparticles

Step 1. Floating Catalyst Production

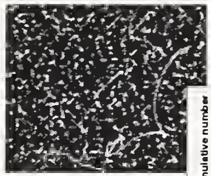

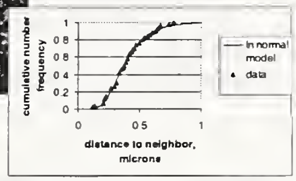

Typical MWNT Growth

Some variation in MWNT mass on various reactor surfaces

Tip Growth

Root ends show no Fe nanoparticles at fracture surface

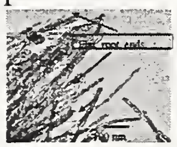

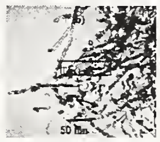

Tip ends are capped with Fe nanoparticles

Tapered MWNTs

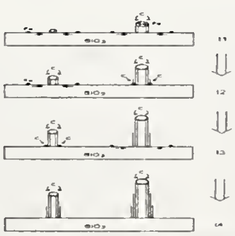

MWNTs taper from the root end (~ 30 nm) to the tip end (~15 nm). Fe may diffuse on surface to MWNT base.

Temperature vs. MWNT Diameter and Length

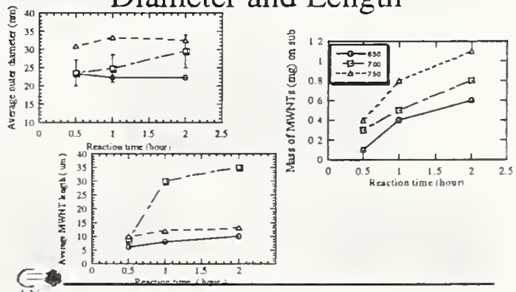

Effects of Temperature

- Tube coarsening is occurring increasing with time at 700 C, while 650 C, 750 C samples have nearly constant tube diameters
- MWNT mass increases with temperature

Effects of C:H Ratio

- Decreasing the C:H ratio results in
- Higher purity MWNTs
- Lower external diameters, and
- Lower standard deviations of the diameter distributions
- H_2:Ar ratio of 0.25:1 gives 8% of MWNTs with D < 10 nm, and some double wall tubes

Effect of C:H Ratio

Gas mixture	C:H ratio	Length (μm)	Average OD (nm)	Purity
0 % H_2 - Ar	1: 1.25	2 (1)	18.2 (12.3)	< 50 % NT
5 % H_2 - Ar	1: 4.3	10 (3.0)	14.1 (6.86)	~ 70 % NT
10 % H_2 - Ar	1: 7.4	35 (31)	24.4 (8.83)	~ 90 % NT
25 % H_2 - Ar	1: 16.6	6 (1.8)	14.4 (7.09)	~ 95 % NT

MWNT Distributions

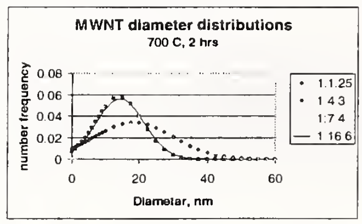

Some distributions may be multimodal, i.e., 1:16.6

Xylene Degradation.

Simplified kinetics, dilute carbon source, no mass transfer limitations

$$C_8H_{10} + H_2 \rightarrow C_7H_8 + CH_4 \qquad (1)$$

$$C_7H_8 + H_2 \rightarrow C_6H_6 + CH_4 \qquad (2)$$

$$C_6H_6 \rightarrow MWNT + 3H_2 \qquad (3)$$

Few hydrocarbons with C < 6 are observed in the tailgas

Hydrocarbons in the Tailgas

Feed has 3750 ppm xylene, 0.1 H2:Ar, 700 C

C_mH_n Fraction (%) (Concentration, ppm)	$C_1H_n + C_2H_n$	C_3H_n	C_6H_6	C_7H_8	C_8H_{10}
5 min	3.47 (5 ppm)	0.00 (0)	0.54 (1)	7.98 (12)	87.45 (135)
15 min	5.38 (11 ppm)	0.00 (0)	0.00 (0)	7.99 (17)	86.63 (182)
30 min	4.49 (21 ppm)	0.20 (1)	0.45 (2)	15.28 (73)	79.58 (379)
60 min	2.93 (23 ppm)	0.09 (1)	0.29 (2)	12.53 (99)	83.39 (657)
90 min	2.90 (42 ppm)	0.07 (1)	0.27 (4)	11.13 (161)	85.63 (1240)
120 min	2.59 (38 ppm)	0.08 (1)	0.26 (4)	11.88 (172)	85.02 (1234)

Catalyst Deactivation

30,000 ppm xylene in feed

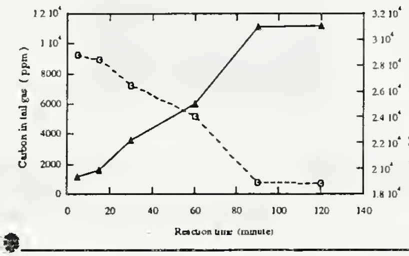

Conclusions

- Tip growth is critical mechanism
- Temperature is important for catalyst coarsening, deactivation
- Xylene, toluene conversions may be rate-limiting; benzene and smaller molecules are present in low mass fractions

Computational Fluid Dynamics

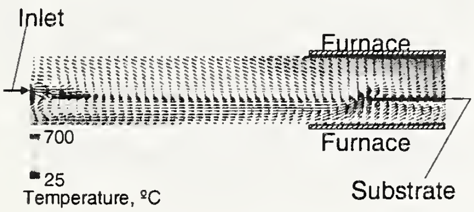

Mass Transfer of C through Fe Nanoparticle

Left: Concentration levels of C.

Right: Flux of C on nanosphere surface.

CVD Process Summary

- Practical experience: scaled from 1 cm to 10 cm tube in 2 steps; from 2 to 6 g/2hr run over one year
- Computational fluid mechanics: gas flows and concentrations
- Overall and component balances: conversion, yield, mechanism(s)
- Catalyst particle model: NT growth, limiting rates
- **Needs/Directions**: multiple scale model, metal nanoparticle detection/control, "morphology" meter

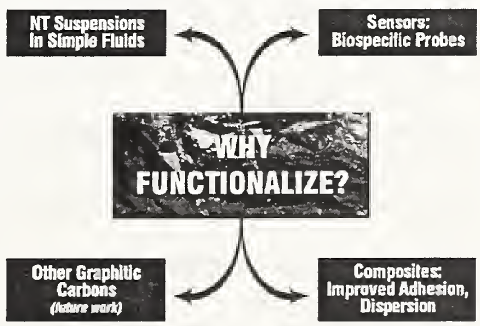

Functionalization: MWNTs

1. What can we make?

Functionalization Methods

Tube Ends

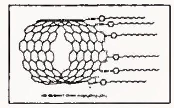

Tube Sides: dichlorocarbene, benzynes, ion bombardment

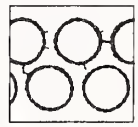

Functionalization via ion bombardment, Ni and Sinnott

Functionalization: New Work

Haddon, Meier, Anthony

- Transfer dichlorocarbene method from SWNTs to MWNTs; benzyne method from fullerenes to MWNTs
- Attach oligomer and polymer chains to MWNTs
- Attach conductive links and ion-specific sites

Functionalization

- Fullerene work shows that "defect sites" are more reactive to functionalization
- Feedstocks used in CVD synthesis control defects
- MWNTs have been functionalized and incorporated into composites

Current Research Directions

Functionalized Carbon Materials

- Additions: halogenation, halomethylation,cycloaddition, Grignard
- Cleaning: CO_2, steam, graphitization
- Novel Carbons: fulleroids, baskets and test tubes
- Functionalized Soluble Graphenes
- Characterization: FFF

MWNTs in Polymer Systems

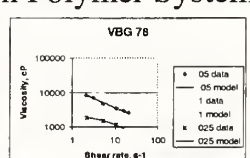

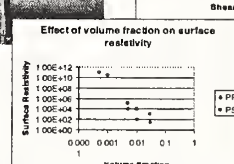

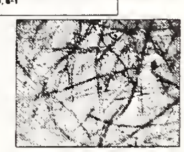

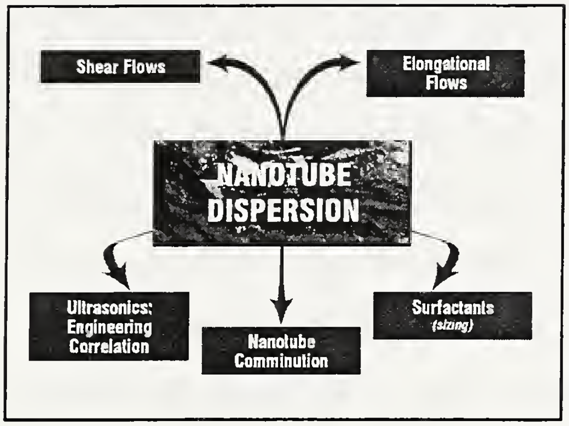
Shear Flows
Elongational Flows
NANOTUBE DISPERSION
Ultrasonics: Engineering Correlation
Nanotube Comminution
Surfactants (sizing)

9

12) Ken McElrath and Tom Tiano, **"Achieving Conductive Polycarbonate with Single Wall Carbon Nanotubes"** [McElrath Powerpoint] [McElrath PDF] [Tiano PowerPoint] [Tiano PDF]

Dr. McElrath and Dr. Tiano give an emphasis on the single-walled carbon nanotubes that is complementary to the presentation of Dr. Grulke that emphasized the multi-walled tubes. The single wall materials should have remarkable strength, electrical conductivity and electrical conductivity and are characterized by a rather precise molecular structure. The realization of this potential is limited by the tendency to form rope like structures and thus there is a great need to improve the dispensability to fully realize the potential of this type of material. Progress on the development of single wall tubes as commercial materials were summarized along with the intense scientific interest generated in the course of the development of this exceptional material.

After the introductory material, the presenters focused specifically on the problem of nanotube dispersal and which solvents were favorable for this. The importance of ultrasonic processing in effective dispersion was also emphasized. The most dramatic success in dispersion was found and characterized for single wall tubes dispersed in polycarbonate. Substantial improvements in electrical and thermal conductivity were found for polar polymer matrices where appreciable dispersion of the tubes was possible. The presentation was concluded with a summary of the many areas where single walled nanotubes have promising commercial applications.

Carbon Nanotechnologies, Inc.

Achieving Conductive Polycarbonate with Single Wall Carbon Nanotubes

Ken McElrath

NIST Workshop; Bridging the Gap Between Structure and Properties In Nanoparticle-Filled Polymers
Gaithersburg, Maryland

1

30-May-02

Agenda

- What are single wall carbon nanotubes?
- Why are they useful?
- CNI plans for SWNT commercialization
- Presentation by Tom Tiano, Research Partner with Foster-Miller

2

Forms of Carbon

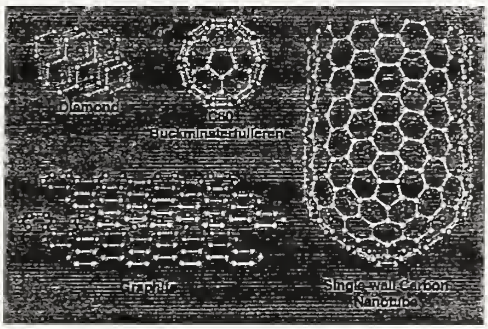

3

Types of Nanotubes

- Defined by the number of walls they are made of

Single-wall (SWNT)

Multi-wall (MWNT)

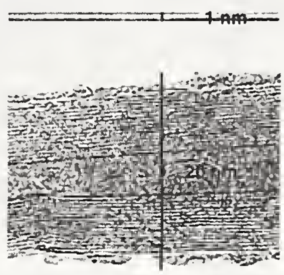

4

SWNTs have Tremendous Accessible Surface Area

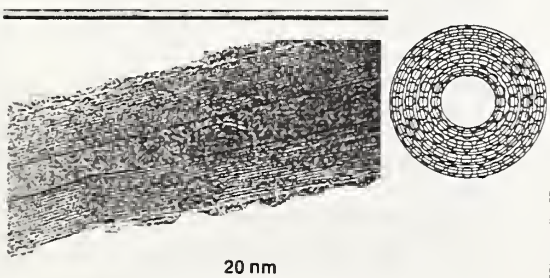

5

SWNTs: The Perfect Material

- Single-wall Carbon Nanotubes (SWNTs) are unique:
  - Fullerene molecules
  - Perfect structures
  - Polymers of pure carbon
- SWNTs have extraordinary properties:
  - Strength (~100x steel)
  - Electrical conductivity (~Copper)
  - Thermal conductivity (~3x Diamond)
  - Combination of the above

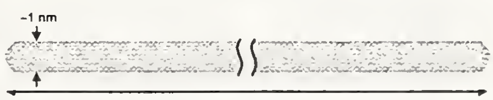

6

1

SWNTs are Perfect: Each Atom in its Place

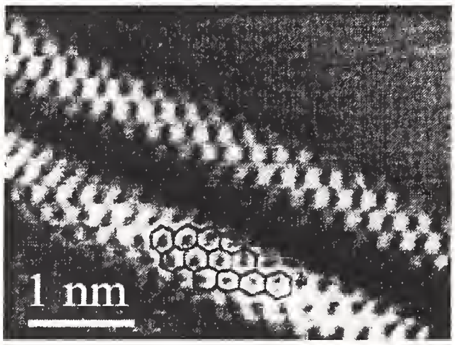

7

CNI Copyright 2002

Ropes of Single-Wall Carbon Nanotubes

- Caused by strong Van der Waals forces between sidewalls
- Enables self-assembly...but makes dispersion challenging

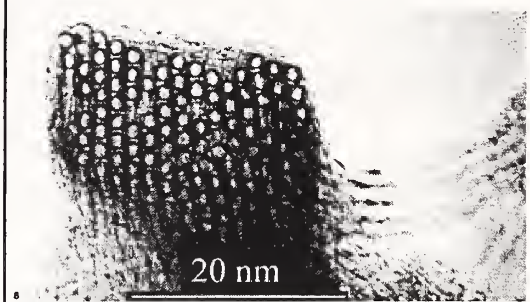

8

CNI Copyright 2002

SWNTs can be Customized

- In most applications, raw SWNTs will need to be customized
- This customization can be precisely controlled using everyday organic chemistry
  - Open ends
  - Closed ends
  - Sidewalls

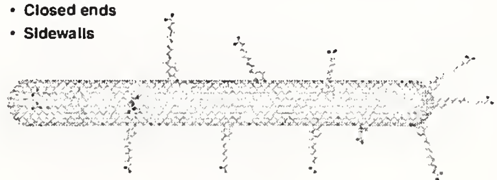

9

CNI Copyright 2002

Dramatic Proof of SWNT-Polymer Interaction

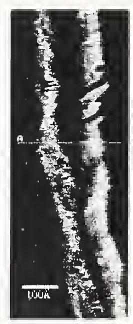

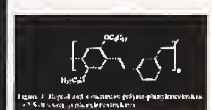

Polyphenylenevinylene

10

Ajayan, Blau, Carroll, Daton, et al. 2001

CNI Copyright 2002

Conductive Polymer Applications

- ABS, PVC, PC, PE, PP, etc. loaded with conductive fillers and inherently conductive polymers
- Total market for conductive polymers is $3.6 billion/year and growing
- A broad range of applications:
  - Electrostatic dissipation (ESD)
  - Electromagnetic shielding (EMI)
- A broad range of potential benefits
  - Lighter
  - Easier to manufacture
  - Cheaper
- Nanotubes should enable new applications that carbon black, carbon fiber, graphite and metal fillers cannot achieve

11

CNI Copyright 2002

Fast Track to Commercialization

- Scaling up from milligrams to kilotonnes
  - Bench unit - g
  - Pilot plant - kg
  - Commercial unit - kt
- Creating commercial products
  - Joint development
  - End-use alliances
- Exploding IP portfolio
  - CNI research
  - Joint research with corporations
  - Ongoing relationship with Rice
  - Research support at other universities

12

CNI Copyright 2002

2

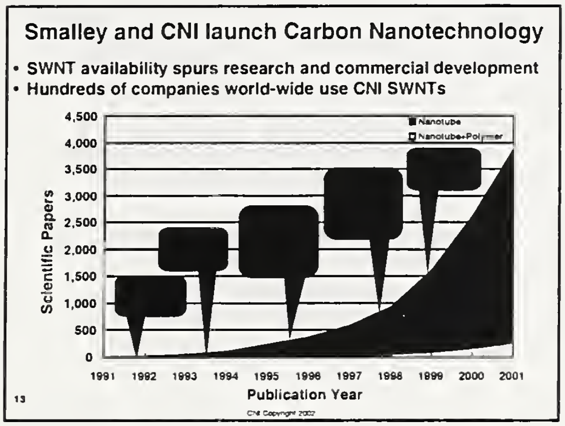
Smalley and CNI launch Carbon Nanotechnology
• SWNT availability spurs research and commercial development
• Hundreds of companies world-wide use CNI SWNTs
Nanotube
Nanotube+Polymer
Scientific Papers
4,500
4,000
3,500
3,000
2,500
2,000
1,500
1,000
500
0
1991 1992 1993 1994 1995 1996 1997 1998 1999 2000 2001
Publication Year
13
CNI Copyright 2002

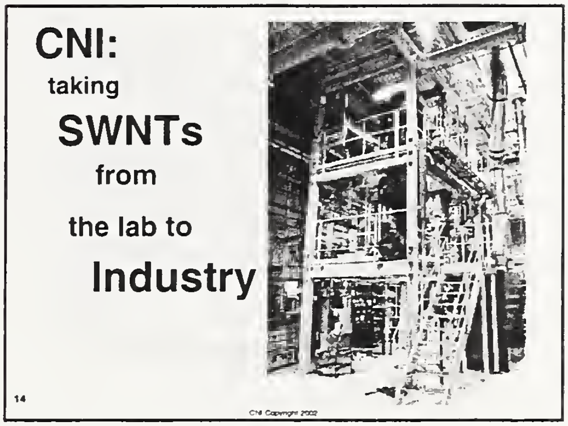
CNI:
taking
SWNTs
from
the lab to
Industry
14
CNI Copyright 2002

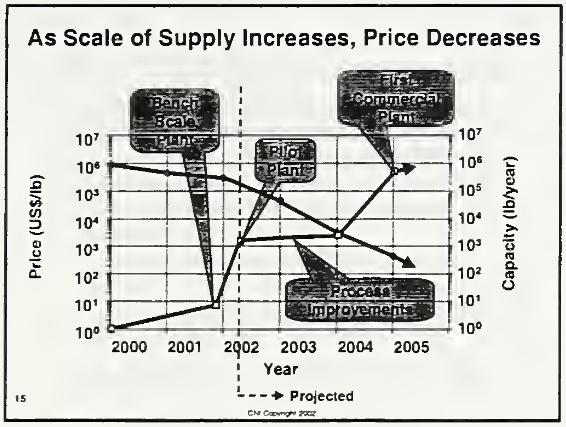
As Scale of Supply Increases, Price Decreases
Bench Scale Plant
Pilot Plant
First Commercial Plant
Process Improvements
Price (US$/lb)
Capacity (lb/year)
2000 2001 2002 2003 2004 2005
Year
Projected
15
CNI Copyright 2002

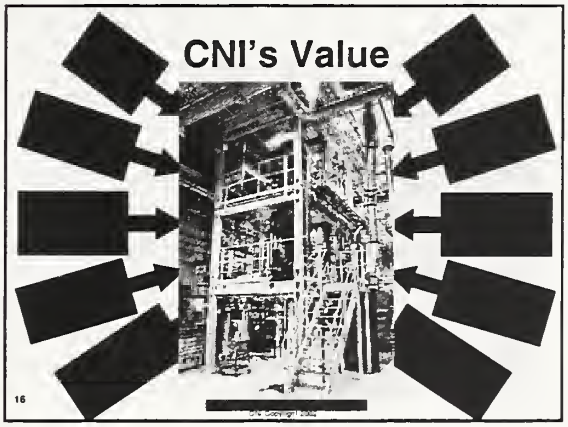
CNI's Value
16

Foster-Miller

Dispersing Single-Wall Carbon Nanotubes in Polycarbonate to Achieve Electrical Conductivity

Thomas Tiano - Foster-Miller, Inc.

Ken McElrath and Ken Smith - Carbon Nanotechnologies, Inc.

Presented to

National Institute of Standards and Technology

May 29 & 30, 2002

Foster-Miller

Objective

- Develop processes for preparing single wall carbon nanotube (SWNT) composites in which the SWNTs are highly dispersed in the polymer matrix.
- Assess electrical and thermal conductivity and mechanical properties.
- Target applications in the electronics industry.

Foster-Miller

Single Wall Nanotubes Properties

Aspect Ratio	1000:1
Specific Gravity	1.3
Electrical Res.	10^{-4} Ω·cm
Therm. Cond.	1750-5800 W/m·K
Young's Modulus	650 GPa - 1 TPa
Tensile Strength	65 - 300 GPa
Tensile Elong.	20%

Adequate dispersion is required to take advantage of these properties in multi-phase systems.

Foster-Miller

Electrical Critical Composition

- Critical composition is the filler volume loading at which a conductive network is created (see schematic).
- Critical composition is highly dependent on aspect ratio (see schematic).

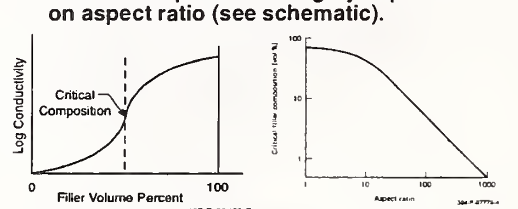

Foster-Miller

Impediments to Dispersion of SWNTs in Nanotube Composites

- Strong Van der Waals interactions
  - SWNTs form ropes (bundles of tubes) ranging from 10 to 100 nm in diameter
  - Ropes are very difficult to de-bundle
- Low surface energy
  - Low affinity for organic solvents and matrices
  - Extremely high critical length

Foster-Miller

Processing Steps

- Disperse SWNT into polar polymer (assisted by polar solvent)
- Remove and recover solvent
- Process composite into parts and specimens
- Perform electrical, thermal and mechanical assessment
- Perform "let-down" studies for processability

Foster-Miller

SWNT Dispersion
Polymer and Solvent Selection

- Solvent Requirements
  - Good dispersant for SWNTs
  - Good solvent for polycarbonate
  - Low boiling point
- Polycarbonate grades
  - Lexan 101-112 (multi-purpose)
  - Lexan HF1110 (high-flow)

7

Foster-Miller

"Solubility" for SWNTs in Organic Solvents

Solvent	"Solubility" (mg/L)	Solvent density (g/cc)	Solubility (wt percent)	Boiling Point °C
1,2 dichlorobenzene	95	1.306	0 0073	180
chloroform	31	1.492	0.0021	61.5
1-methylnaphthalene	25	1 001	0.0025	243
1-bromo-2-methylnaphthalene	23	1 418	0.0016	296
n-methylpyrrolidinone	10	1.028	0.0010	202
dimethylformamide	7.2	0.944	0 00080	153
tetrahydrofuran	4 9	0.889	0.00055	67
1,2-dimethylbenzene (o-xylene)	4 7	0 870	0.00054	145
pyridine	4 3	0 978	0.00044	115
Carbon disulfide	2.6	1.266	0.00021	46
1,3,5-trimethylbenzene	2 3	0 864	0.00027	164

Bahr, Mickelson, Bronikowski, Smalley, Tour; Chem. Comm.,2001;193-194

8

Foster-Miller

SWNT Dispersion
Ultrasonic Processing

- Dissolve polymer into solvent
- Add SWNT to solvent and insonify for 30 minutes
- High amplitude insonification induces cavitation
- Cavitation bubbles nucleate on nanotube clusters
- De-agglomeration occurs when cavitation bubbles collapse on SWNT bundles
- Implosion of voids is driven by reversal of pressure in the sound wave

9

Foster-Miller

SWNT Dispersion
Ultrasonic Processing

- Branson titanium wedge tip ultrasonic welding horn
- 40 kHz frequency
- 2:1 amplitude gain
- Branson 940B power supply
- 700W continuous power
- Adjust amplitude to 45%

10

Foster-Miller

SWNT Solvent Removal

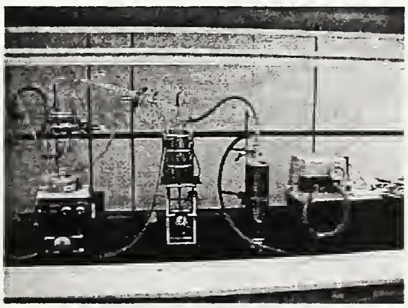

11

Foster-Miller

SWNT composite processing

- Develop conditions for processing composite feedstock into useful parts
- Injection molding and compression molding
  - both require relative high pressure (120 psi & 2000 psi respectively)

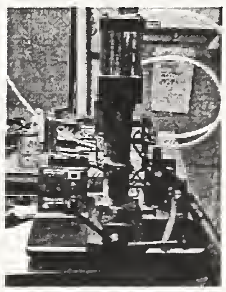

12

Foster-Miller

SWNTs Dispersed in Polymer Matrix

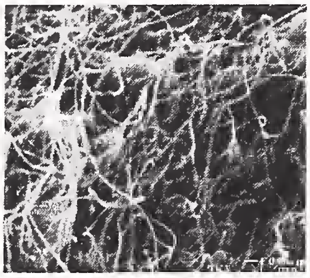

10% SWNTs dispersed in polycarbonate

13

Foster-Miller

AC Electrical Conductivity Measurement

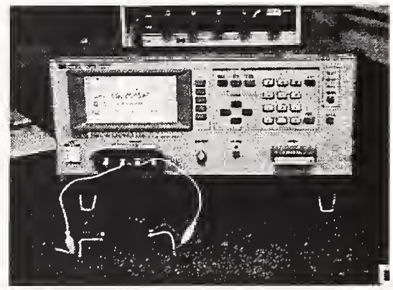

- Specimens fractured to expose surface

14

Foster-Miller

AC Electrical Conductivity (1MHz) SWNT in Lexan 101-112 (In-plane)

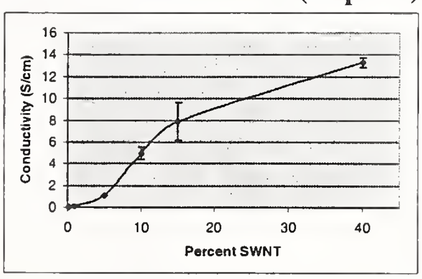

15

Foster-Miller

AC Electrical Conductivity (1MHz) SWNT in Lexan 101-112 (In-plane)

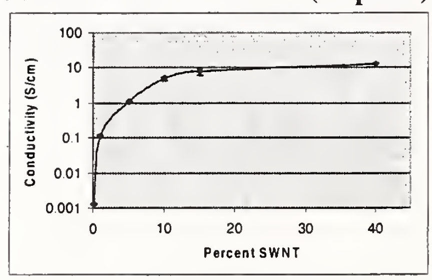

16

Foster-Miller

AC Electrical Conductivity (1MHz) SWNT in Lexan 101-112 (In-plane)

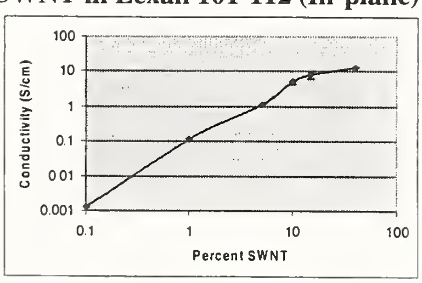

17

Foster-Miller

Thermal Conductivity Measurements

- Samples mounted in vacuum chamber with diffusion pump (10^{-7} torr).
- Thermocouples mounted to side of sample.
- Radiation shield placed over sample.

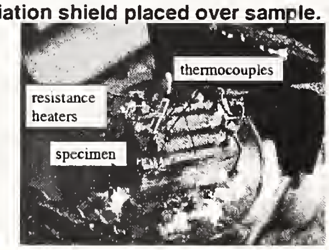

18

3

Foster-Miller

Room Temp. Thermal Conductivity SWNT in Lexan 101-112 (In-Plane)

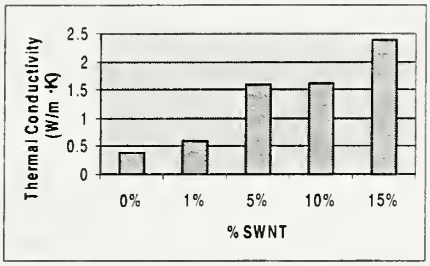

19

Foster-Miller Proprietary

Further Research in Thermoplastics

- Continue to investigate SWNT dispersion techniques to increase conductivity
- Obtain more data for electrical and thermal conductivity and mechanical properties
- Further develop composite processing techniques
- Investigate polymer "let-down" procedures
- Investigate different thermoplastic polymers

20

Foster-Miller

Potential Applications of SWNT-Filled Thermoplastics

- Electromagnetic interference protection
- Electrostatic discharge materials
- Electrostatic paint substrates
- Lightweight thermal management materials
- Thermoplastic die attach

21

FinalParticipants' List

Bridging the Gap between Structure & Properties in Nanoparticle-Filled Polymers

May 29-30, 2002
National Institute of Standards and Technology (NIST), Gaithersburg, MD

Fred Allen
Engelhard Corp.
101 Wood Ave.
Iselin, NJ 08550 USA
Telephone: 732/205-6042
Fax: 732/205-5300
Email: fred.allen@engelhard.com

Eric Amis
NIST
100 Bureau Dr., Mail Stop 8540
Gaithersburg, MD 20899-8540 USA
Telephone: 301/975-6681
Email: eric.amis@nist.gov

Larry Anderson
PPG Industries
4325 Rossanna Dr.
Allison Park, PA 15101 USA
Telephone: 412/492-5210
Email: lyanderson@ppg.com

Tony Andrady
Research Triangle Institute
3040 Cornwallis Rd.
Durham, NC 27709 USA
Telephone: 919/541-6713
Email: andrady@rti.org

Joe Antonucci
NIST
100 Bureau Dr., Mail Stop 8545
Gaithersburg, MD 20899-8545 USA
Telephone: 301/975-6794
Email: joe.antonucci@nist.gov

George Baran
Temple Univ.
1947 N. 12th St.
Philadelphia, PA 19122 USA
Telephone: 215/204-8824
Fax: 215/204-4956
Email: grbaran@astro.templ.edu

Gary Beall
Southwest Texas State Univ.
601 University Dr.
San Marcos, TX 78666 USA
Telephone: 512/245-8796
Fax: 512/245-2374
Email: gb11@swt.edu

Charles Beatty
Univ. of Florida
Dept. of Ma'tl. Sci. & Eng.
Gainesville, FL 32611 USA
Telephone: 352/846-3786
Fax: 352/846-3355
Email: cbeat@mse.ufl.edu

Phillip Britt
Oak Ridge National Laboratory
P.O. Box 2008
Bldg 4500N, C-26, MS
Oak Ridge, TN 37922 USA
Telephone: 865/574-5029
Fax: 865/576-7956
Email: brittpf@ornl.gov

Geoff Broadhurst
GWB Consultants LLC
26 Cottontail Lane
Irvington, NY 10533 USA
Telephone: 914/591-7356
Fax: 914/591-4630
Email: g.broadhurst@worldnet.att.net

Tony Bur
NIST
100 Bureau Dr., Mail Stop 8544
Gaithersburg, MD 20899 USA
Telephone: 301/975-6748
Email: abur@nist.gov

Anthony Carignano
ITC Minerals & Chemicals
6 North Park Dr., Ste. 105
Hunt Valley, MD 21030 USA
Telephone: 410/512-4108
Fax: 815/333-2997
Email: awcarignano@itcglobal.com

John Coulter
Lehigh Univ.
19 Memorial Dr. West
Bethlehem, PA 18015 USA
Telephone: 610/758-5148
Fax: 610/758-5623
Email: john.coulter@lehigh.edu

Mark Dadmun
Univ. of Tennessee
321 Buehler Hall
Knoxville, TN 37996 USA
Telephone: 865/974-6582
Fax: 865/974-3454
Email: Dad@utk.edu

Vinay Dayal
Iowa State Univ.
2271 Howe Hall
AEEM Dept., Rm. 1200
Ames, IA 50011 USA
Telephone: 515/294-0720
Fax: 515/294-3262
Email: vdayal@iastate.edu

Hugh De Long
Air Force Ofc. of Scie. Research
801 N. Randolph St., Rm. 732
Arlington, VA 22203 USA
Telephone: 703/696-7722
Fax: 703/696-8449
Email: hugh.delong@afosr.af.mil

Jack Douglas
NIST
100 Bureau Dr., Mail Stop 8542
Gaithersburg, MD 20899-8542 USA
Telephone: 301/975-6779
Email: jack.douglas@nist.gov

Fangming Du
M.S.E. of UPenn
3231 Walnut St., Rm. 324
Philadelphia, PA 19104 USA
Telephone: 215/898-2700
Email: fangming@seas.upenn.edu

Peter Ferraro
Specialty Minerals, Inc.
640 Noth 13th St.
Easton, PA 18042 USA
Telephone: 610/250-3202
Fax: 610/258-1203
Email: peter.ferraro@mineralstech.com

William Finch
Rohm & Haas Co.
727 Norristown Rd.
P.O. Box 904
Spring House, PA 19477 USA
Telephone: 215/619-1547
Fax: 215/619-1648
Email: WFinch@rohmhaas.com

Jeffrey Gilman
NIST
100 Bureau Dr., Mail Stop 8665
Gaithersburg, MD 20899-8665 USA
Telephone: 301/975-6573
Email: jeffrey.gilman@nist.gov

Harris Goldberg
InMat LLC
216 Route 206, Ste. 7
Hillsborough, NJ 08844 USA
Telephone: 908/874-7788
Fax: 908/874-7672
Email: hagoldberg@inmat.com

Caiguo Gong
ExxonMobil Chemical
5200 Bayway Dr.
Baytown, TX 77520 USA
Telephone: 281/834-1326
Fax: 281/834-2480
Email: caiguo.gong@exxonmobil.com

Eric Grulke
Univ. of Kentucky
Chemical & Materials Engineering
Lexington, KY 40506 USA
Telephone: 859/257-2300
Fax: 859/323-1929
Email: egrulke@engr.uky.edu

Reto Haggenmueller
Univ. of Pennsylvania
3231 Walnut St.
LRSM
Philadelphia, PA 19104 USA
Telephone: 215/898-2700
Fax: 215/573-2128
Email: retohagg@seas.upenn.edu

Charles Han
NIST
100 Bureau Dr., Mail Stop 8543
Gaithersburg, MD 20899-8543 USA
Telephone: 301/975-6772
Email: charles.han@nist.gov

Christopher Harrison
NIST
100 Bureau Dr., Mail Stop 8542
Gaithersburg, MD 20899-8542 USA
Telephone: 301/975-3586
Email: christopher.harrison@nist.gov

Erik Hobbie
NIST
100 Bureau Dr., Mail Stop 8543
Gaithersburg, MD 20899-8543 USA
Telephone: 301/975-6774
Fax: 301/975-4977
Email: erik.hobbie@nist.gov

Douglas Hunter
Southern Clay Products

Tadahiro Ishii
Tokyo University of Science
1-3 Kaguraska
Shinjuku-ku
Tokyo 162-8601, JAPAN
Telephone: 81/3 5228 8257
Fax: 81/3 3235 2214
Email: taishii@ch.kagu.sat.ac.jp

Jack Johnson
ExxonMobil Research & Engineering
1545 Route 22 East
Annandale, NJ 08801 USA
Telephone: 908/730-2895
Fax: 908/730-3198
Email: jack.w.johnson@exxonmobil.com

Karl Kamena
Omni Tech. International
2715 Ashman St.
Midland, MI 48640 USA
Telephone: 989/631-3377
Fax: 989/631-7360
Email: kkamena@omnitechintl.com

Alamgir Karim
NIST
100 Bureau Dr., Mail Stop 8542
Gaithersburg, MD 20899-8542 USA
Telephone: 301/975-6588
Email: karim@nist.gov

Takashi Kashiwagi
NIST
100 Bureau Dr., Mail Stop 8665
Gaithersburg, MD 20899-8665 USA
Telephone: 301/975-6699
Email: takashi.kashiwagi@nist.gov

Hubert King
ExxonMobil Research & Engineering
1546 Route 22 East
Annandale, NJ 08822 USA
Telephone: 908/730-2888
Fax: 908/730-2536
Email: hubert.e.king@exxonmobil.com

Satish Kumar
Georgia Institute of Technology
School of Textile & Fiber Eng.
Atlanta, GA 30332-0295 USA
Telephone: 404/894-7550
Fax: 404/894-8780
Email: satish.kumar@textiles.gatech.edu

Steve Lawrence
Naval Research Lab
Code 6134
Washington, DC 20375 USA
Telephone: 202/767-3310
Fax: 202/767-4642
Email: Steven.Lawrence@nrl.navy.mil

Marshall Ledbetter
Mitsubishi Polyester Film
P.O. Box 1400
2001 Hood Rd.
Greer, SC 29652 USA
Telephone: 864/879-5352
Fax: 864/879-5940

Charles Lee
AFOSR/NL
801 N. Randolph St., Ste. 732
Arlington, VA 22203 USA
Telephone: 703/696-7779
Email: charles.lee@afosr.af.mil

Andre Lee
Michigan State Univ.
Dept. of Chemical Eng. & Mat'l. Scie.
East Lansing, MI 48824 USA
Telephone: 517/355-5112
Fax: 517/432-1105
Email: leea@msu.edu

Wendy Lin
GE Global Research
1 Research Circle
K-1 4B5
Niskayuna, NY 12309 USA
Telephone: 518/387-4081
Fax: 518/387-7403
Email: Wendy.Lin@crd.ge.com

Eric Lundquist
Rohm & Haas Co.
727 Norristown Rd.
Spring House, PA 19477 USA
Telephone: 215/619-5335
Email: wlundquist@rohmhaas.com

Michael Mackay
Michigan State Univ.
Dept. Chem. Eng. Mat. Sci.
East Lansing, MI 48824 USA
Telephone: 517/432-4495
Fax: 517/432-1105
Email: mackay@msu.edu

Michael McBrearty
Chemical ElectroPhysics Co., Inc.
705 Yorklyn Rd.
Hockessin, DE 19707 USA
Telephone: 302/234-8206
Fax: 302/239-4677
Email: cep@cep-corp.com

Kenneth McElrath
Carbon Nanotechnologies, Inc.
16200 Park Row
Houston, TX 77084 USA
Telephone: 281/492-5883
Fax: 281/492-5810
Email: kmcelrath@cnanotech.com

Alexander Morgan
Dow Chemical Company
1776 Bldg, Door A
Midland, MI 48674 USA
Telephone: 989/638-1774
Fax: 989/638-9716
Email: abmorgan@dow.com

Tinh Nguyen
NIST
100 Bureau Dr., Mail Stop 8621
Gaithersburg, MD 20899-8621 USA
Telephone: 301/975-6718
Email: tinh.nguyen.nist.gov

Marc Nyden
NIST
100 Bureau Dr., Mail Stop 8665
Gaithersburg, MD 20899-8665 USA
Telephone: 301/975-6692
Email: marc.nyden@nist.gov

Byoungkyeu Park
Cornell Univ.
Bard Hall
Ithaca, NY 14853 USA
Telephone: 607/255-4557
Fax: 607/255-2365
Email: bkp@cornell.edu

Ray Pearson
Lehigh Univ.
5 East Packer Ave.
Bethlehem, PA 18015 USA
Telephone: 610/758-3857
Fax: 610/758-4244
Email: rp02@lehigh.edu

Giampaolo Pellegatti
Basell USA, Inc.
912 Appleton Rd.
Elkton, MD 21921 USA
Telephone: 410/996-1677
Fax: 410/996-1811
Email: giampaolo.pellegatti@basell.com

Louis Pilato
Pilato Consulting
598 Watchung Rd.
Bound Brook, NJ 08805 USA
Telephone: 732/469-4057
Fax: 732/764-9747
Email: pilato-consulting@worldnet.att.ne

Srinivasa Raghavan
Univ. of Maryland
Dept. of Chem Engineering, Bldg. 090
College Park, MD 20742 USA
Telephone: 301/405-8164
Email: sraghava@eng.umd.edu

Asif Rasheed
Univ. of Tennessee
Dept. of Chemistry
Knoxville, TN 37996 USA
Telephone: 865/974-6596
Email: arasheed@utk.edu

Kim Rasmussen
Los Alamos National Laboratory
Theoretical Div.
MS-B262
Los Alamos, NM 87545 USA
Telephone: 505/665-3851
Fax: 505/665-4063
Email: kor@lanl.gov

Robert Reitz
Dupont Co.
Experimental Station, Bldg. 310
Wilmington, DE 19880 USA
Telephone: 302/695-2182
Fax: 302/675-1513
Email: robert.r.reitz@usa.dupont.com

Paul Rice
NIST
325 Broadway
Boulder, CO 80305-3328 USA
Telephone: 303/497-7601
Fax: 303/497-5030
Email: paulrice@boulder.nist.gov

Stephanie Scierka
NIST
100 Bureau Dr., Mail Stop 8621
Gaithersburg, MD 20899-8621 USA
Telephone: 301/975-6448
Fax: 301/990-6891
Email: stephanie.scierka@nist.gov

John Shost
Congoleum Corp.
861 Sloan Ave.
P.O. Box 3127
Trenton, NJ 08619 USA
Telephone: 609/584-3347
Fax: 609/584-3333
Email: jshost@congoleum.com

Andrew Slifka
NIST
325 Broadway
Boulder, CO 80305 USA
Telephone: 303/497-3744
Fax: 303/497-5030
Email: slifka@boulder.nist.gov

James Smith
Univ. of Utah
12 S. Central Campu,. MSE Dept.
EMRO 304
Salt Lake City, UT 84112 USA
Telephone: 801/585-6131
Fax: 801/581-4816
Email: jsmith@bede.coe.utah.edu

Chad Snyder
NIST
100 Bureau Dr., Mail Stop 8541
Gaithersburg, MD 20899-8541 USA
Telephone: 301/975-4526
Fax: 301/975-3928
Email: chad.snyder@nist.gov

Francis Starr
NIST
100 Bureau Dr., Mail Stop 8540
Gaithersburg, MD 20899-8540 USA
Telephone: 301/975-8359
Email: francis.starr@nist.gov

Li-Piin Sung
NIST
100 Bureau Dr., Mail Stop 8621
Gaithersburg, MD 20899-8621 USA
Telephone: 301/975-6737
Fax: 301/990-6891
Email: lipiin@nist.gov

Atsushi Takahara
Kyushu University
Hokozaki, Higashikm
Fukuoka, 812-8581 JAPAN
Telephone: 81/92 642 2721
Fax: 81/92 642 2715
Email: takahara@cstf.kyushu-u.ac.jp

Russell Thompson
Los Alamos National Laboratory
Theoretical Div.
MS B262
Los Alamos, NM 87545 USA
Telephone: 505/665-9283
Fax: 505/665-4063
Email: rthompson@lanl.gov

Richard Vaia
Air Force Research Laboratory
2941 P St.
AFRL/MLBP
WPAFB, OH 45433 USA
Telephone: 937/255-9184
Fax: 937/255-9158
Email: richard.vaia@wpafb.af.mil

Kevin Van Workum
Univ. of Wisconsin

Mark VanLandingham
NIST
100 Bureau Dr., Mail Stop 8621
Gaithersburg, MD 20899-8621 USA
Telephone: 301/975-4686
Fax: 301/990-6891
Email: mack.vanlandingham@nist.gov

Noel Vanier
PPG Industries, Inc.
4325 Rosanna Dr.
Allison Park, PA 15101 USA
Telephone: 412/492-5640
Fax: 412/492-5522
Email: vanier@ppg.com

Vedagiri Velpari
PPG Ind., Inc.
Guys Run Rd.
Pittsburgh, PA 15238 USA
Telephone: 412/820-4946
Fax: 412/820-4952
Email: velpari@ppg.com

Daike Wang
Milliken Research Corp.
920 Milliken Rd.
Spartanburg, SC 29334 USA
Telephone: 864/503-2793
Fax: 864/503-2793
Email: daike.wang@millliken.com

Howard Wang
NIST
100 Bureau Dr., Mail Stop 8543
Gaithersburg, MD 20899-8543 USA
Telephone: 301/975-6781
Email: wangh@nist.gov

J.B. Wright
U.S. Army SBCCOM
Kansas St.
Natick, MA 01760 USA
Telephone: 508/233-6313
Fax: 508/233-5521
Email: jeffery.wright@natick.army.mil

Jusong Xia
Milliken Chemical
920 Milliken Rd., M-401
Spartanburg, SC 29304 USA
Telephone: 864/503-6055
Fax: 864/503-1365
Email: jusong.xia@milliken.com

Langqiu Xu
PPG Industries, Inc.
Glass Technology Ctr.
P.O. Box 2844
Pittsburgh, PA 15230-2844 USA
Telephone: 412/820-4953
Fax: 412/820-4952
Email: lqxu@ppg.com

Xiaoping Yang
Goodyear Tire & Rubber Co.
142 Goodyear Blvd.
Akron, OH 44305 USA
Telephone: 330/796-1325
Fax: 330/796-7060
Email: Xiaoping_Yang@goodyear.com

William Znidarsic
Univ. of Pennsylvania
4045 Baltimore Ave.
Apt C-1
Philadelphia, PA 19104 USA
Telephone: 215/662-7523
Email: williamz@seas.upenn.edu